Polyphenylene-Based Materials for Organic Photovoltaics

Chen Li,[†] Miaoyin Liu,[†] Neil G. Pschirer,[‡] Martin Baumgarten,[†] and Klaus Müllen*,[†]

Max Planck Institute for Polymer Research, Ackermannweg 10, D-55128 Mainz, Germany, and BASF SE, Research Specialty Chemicals, D-67056 Ludwigshafen, Germany

Received February 17, 2010

Contents

Chen Li studied chemistry and completed his Master's thesis under the supervision of Professor He Tian at the East China University of Science and Technology in 2003. In 2004, he joined the group of Professor Klaus Müllen at the Max Planck Institute for Polymer Research to work on functional rylene dyes for dye-sensitized solar cells. He received his Ph.D. in 2008 from the Johannes Gutenberg University of Mainz. Presently he works in the same group as a project leader, and his research interests are functional dyes and pigments as well as their applications.

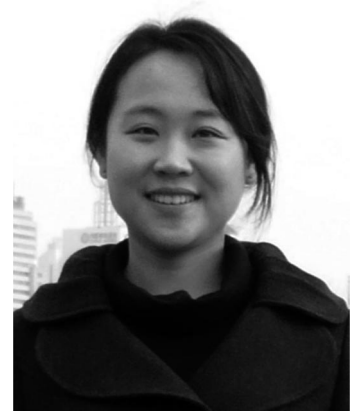

Miaoyin Liu received her Master's degree from the East China University of Science and Technology. In 2010, she earned her Ph.D. degree from the Johannes Gutenberg University of Mainz under the supervision of Professor Klaus Müllen. Her research interest is the investigation of new materials for organic thin-film photovoltaics.

1. Introduction

1.1. Prologue

Energy will be one of the most important factors to influence human society in the 21st century.[1,2] Cost, availability, and sustainability of energy have a significant impact on the quality of our lives, development of global economies, relationships between nations, and the stability of our environment. Scientists are now focusing on the development of renewable energies[3] generated from natural resources such as sunlight, wind, rain, tides, and geothermal heat. Among these, the sun has the potential to make the largest energy contribution: only one hour of sunshine (3.8×10^{23} kW) is more than enough to satisfy the highest human demand for energy for an entire year (1.6×10^{10} kW in 2005).[4−7]

Solar cells, also called photovoltaics,[8] are devices based on solar technology which convert sunlight directly into electricity under the photovoltaic effect. Becquerel was the first to recognize this effect in 1839, when he shined light

* To whom correspondence should be addressed. E-mail: muellen@mpip-mainz.mpg.de.
[†] Max Planck Institute for Polymer Research.
[‡] BASF SE.

10.1021/cr100052z
Published on Web 06/29/2010

Neil Pschirer was born in Pittsburgh, Pennsylvania, in 1974. He received his Ph.D. in 2001 from the University of South Carolina on the topic of emissive polymers for OLEDs via alkyne metathesis under the advisement of Professor Uwe Bunz. Between 2002 and 2004 he performed postdoctoral research at the Max Planck Institute for Polymer Research in Mainz, Germany, in the group of Professor Klaus Müllen on the subjects of novel rylene-based near-infrared absorbing dyes and organic solar cells. In 2004 he joined BASF SE in Ludwigshafen, Germany, where his current focus is on the further development of organic solar cells toward market implementation.

Martin Baumgarten received his Ph.D. in organic chemistry at the Freie Universität Berlin in 1988. From 1988 to 1990 he held a postdoctoral position and a DFG fellowship at Princeton University with Prof. G. C. Dismukes studying Photosystem II, the water splitting enzyme, and Mn model complexes. In 1990 he joined the Max Planck Institute for Polymer Research in Mainz as a project leader. In 1996/97 he achieved his habilitation and was appointed Privatdozent at the University of Mainz. For two semesters in 2001/2002 he was guest professor at the Universität des Saarlandes, Saarbrücken, teaching organic chemistry. In 2004 he was appointed visiting professor of northeast normal university in Changchun, China. His primary interests focus on the synthesis of novel conjugated oligomers, polymers, and dendrimers, organic high spin molecules, and molecular magnets as well as organic and hybrid spin networks.

onto an AgCl electrode in an electrolyte solution and a light-induced voltage was discovered.[9] Forty-four years later, Fritts created the first device made from Se wafers with a power conversion efficiency (PCE) of approximately 1%.[10] Since 1946, when modern junction semiconductor solar cells were patented by Ohl,[11] an intensive search for highly efficient photovoltaics has been ongoing. In 1954, Chapin, Fuller, and Pearson at Bell Laboratories improved the efficiency of a Si cell to 6%.[12] Today standard solar panels based on multicrystalline silicon have power conversion efficiencies around 15%. However, the expensive investment in semiconductor processing technologies of the silicon-based solar cells has limited their popularization. Therefore, it became increasingly

Klaus Müllen is one of the directors at the Max Planck Institute for Polymer Research in Mainz, Germany, a post he has held since 1989. His research interests range from new polymer-forming reactions, including methods of organometallic chemistry, multidimensional polymers with complex shape-persistent architectures, and molecular materials with liquid crystalline properties for electronic and optoelectronic devices, to the chemistry and physics of single molecules, nanocomposites, and biosynthetic hybrids. He is Past President of the German Chemical Society and serves as a member of many editorial advisory boards and as an associate editor of the *Journal of the American Chemical Society*. His work has led to the publication of over 1300 papers, and he is one of the most cited authors in his field. He holds numerous honorary degrees and has received, among many others, the Max-Planck-Research-Prize, the Philip-Morris-Research-Prize, the Elhuyar Goldschmitt Award of the Spanish Chemical Society, and the International Award of the Society of Polymer Science Japan.

important to find a new technology which utilizes inexpensive materials as well as fabrication methods to collect solar energy. In 1986, the first organic thin-film solar cell with reasonable efficiency (approximately 1%) was created and reported by Tang.[13] Since then, there has been great interest within the scientific and industrial communities in the advantages of using organic materials in the solar cell field: namely, low costs, various synthetic methods, sustainability, and plastic processing ability. For years, the number of publications and new patents in the field of photovoltaics has been increasing (Figure 1). Publications regarding solar cells have soared over the last 10 years as it became clear that the organic solar cell also has the potential for high power efficiency and stability.[6] A number of high-tech companies came into being. With a theoretical efficiency just as high as the one of conventional semiconductor devices, organic solar cells are one of the most promising approaches toward significant cost reduction.[6] When distinguished by

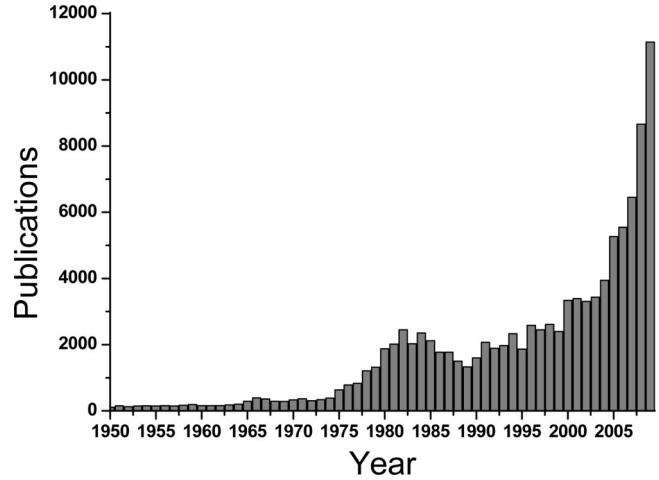

Figure 1. Solar cells publications by year (Via SciFinder).

device structures, organic photovoltaics (OPVs) can be divided into three main categories: flat-heterojunction,[14] bulk-heterojunction,[15] and dye-sensitized solar cells.[16,17] The applied materials in the devices can be categorized into three main types: small molecules,[18] polymers,[19] and hybrid organic−inorganic materials (for example, the combination of organic dyes or polymers with inorganic semiconductors, such as TiO_2 and ZnO).[20] The key to accomplishing high power conversion efficiencies with organic solar cell technologies is the investigation of new materials which fulfill the multiple parameters necessary for the OPV purpose, such as light harvesting, charge transfer, and charge transport. Material scientists, therefore, are still absorbed in the search for favorable novel organic compounds for solar cells.

In organic chemistry, benzene is a natural constituent of crude oil and may also be synthesized from other compounds present in petroleum.[21] By using benzene as a building block, polyphenylene-based materials can be synthesized, extendable in one, two, or three dimensions.[22] The benzene moiety thereby provides a reliable platform for the design of functionality and demanding structural architectures.[23,24] As one-dimensional systems, linear conjugated polyphenylenes are considered to play a very important role in the field of organic electronics.[25] As two-dimensional compounds, extended planar graphene molecules and their derivatives possess some unique properties, such as strong $\pi-\pi$ interaction and self-organizable behavior.[26−28] In the three-dimensional realm, polyphenylene dendrimers[29] provide many possibilities to obtain multifunctional materials, such as multichromophores,[30,31] which can more efficiently harvest light from the sun. Due to the presence of different functionalizations of these materials, e.g. electron-rich and electron-poor moieties or solubilizing alkyl chains with different lengths, it is possible to fine-tune the photophysical and electrochemical properties, solubility, and, consequently, the formation of perfectly self-organizable arrangements. All of these aspects are significantly important for the improvement of device performance.

In considering the uniqueness of polyphenylene-based materials, the present article focuses on organic semiconductors and sensitizers obtained when using benzene as a regular building block. This review is divided into three parts.

The first part provides a general introduction to different cell structures and their practical characterizations, including flat-heterojunction, bulk-heterojunction, and dye-sensitized solar cells.

In the second part, the focus is on polyphenylene-based materials. It first describes one-dimensional polyphenylenes or oligophenylene rod-type compounds, then 2D polyphenylenes (especially perylenes and their derivatives), and finally polyphenylene dendrimers. Moreover, this section includes the application and performance of these materials in photovoltaics. The conjugated polyphenylenes are mainly applicable to bulk-heterojunction polymer solar cells, while the conjugated oligomers with donor−acceptor end groups are primarily employed in dye-sensitized solar cells. With their facile functionalization, extraordinary absorption, as well as photostability, the application of perylenes and their derivatives covers all types of solar cells. Finally this second section concludes with a description of multichromophoric dendrimers and the concept of single-molecular level light-harvest systems.

The third part of the paper provides a conclusion as well as an outlook.

1.2. Organic Photovoltaic Devices

In photovoltaics, one of the most critical issues, besides achieving adequate efficiencies and lifetimes, is to reduce the costs associated with achieving economies of scale. Organic solar cells, which can be processed from solution, have great potential to reach the goal of a photovoltaic technology that is economically viable for large-scale power generation, where the organic materials are the key elements for converting light into electricity.[32] Organic photovoltaic materials have many advantages compared to inorganic semiconductors:

(1) Organic materials can be made via various synthetic pathways, which make them inexhaustible in supply and always available for use.

(2) Via structure tuning and different functionalizations, organic compounds can fulfill the requirements of an efficient photovoltaic device, for example, broad absorption spectra, suitable redox energies, and self-organization abilities facilitating efficient exciton and charge transport.

(3) Most organic compounds can be dissolved in common organic solvents. They can, hence, be processed not only via vacuum evaporation/sublimation but also by means of other low-cost manufacturing technologies, such as roll-to-roll or inkjet printing, drop-casting, spin- or dip-coating, doctor-blading, and other solution casts.[5] These printing techniques render organic solar cells potentially manufacturable in a continuous printing process with large area coating.

(4) In solutions or in thin films, organic materials often show high absorption coefficients, which allow organic solar cells to still be efficient in very thin films and under low sunlight irradiation. In such thin films (around 100 nm), organic materials can absorb almost all incoming light (within their absorption range).[33] In comparison, a standard silicon wafer would need a thickness of around 300 μm to absorb the same amount of photons.[34]

(5) Solar cells based on organic materials can be structurally flexible, and most of them are semitransparent. Organic solar cells, therefore, have a much larger application potential than conventional solar cells. They can be used not only as electricity providers on roof tops, like common inorganic solar cells, but can also be used for decoration in fashion, windows, toys, and mobile applications, e.g. charging for mobile phones or laptops.

These features make organic materials attractive for commercialization. When it comes to creating these organic materials, however, a careful molecular design is required to synthesize organic compounds which are valuable for the photovoltaics. Regarding the structural variation of polyphenylene-based materials, 1D-to-3D structure architectures can be built up via the six-functionalizable positions of benzene. They can be applied in all types of organic solar cells: flat-heterojunction solar cells, bulk-heterojunction solar cells, and dye-sensitized solar cells. The typical structures of these three kinds of organic solar cells are shown below.

1.2.1. Flat-Heterojunction Solar Cells (FHJs)

Some 2D polyphenylene-based materials are slightly soluble and/or sublimable, making them candidates for light-harvesting materials in flat-heterojunction solar cells (FHJs). In such devices, the materials are normally deposited on the surface under vacuum to obtain layer-by-layer cell structures. This technology has been applied since the first efficient

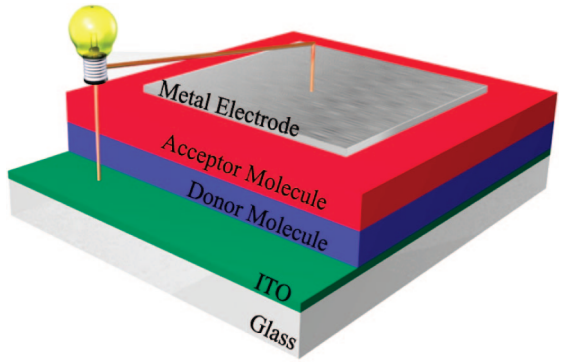

Figure 2. Flat-heterojunction configuration in small molecule solar cells: the charges are generated in the donor and acceptor molecule layers (active layer). In the device, electrons flow from the active layer to the metal electrode (Al, Ag, etc.) and then transport the electricity to the external circuit before moving to the ITO anode.

organic photovoltaic cell from Tang, which was based on a two-active-layer structure of perylenedibenzimidazole and copper phthalocyanine (CuPc).[13] Due to special requirements for the sublimation, the flat-heterojunction photovoltaics are mainly molecular solar cells in which small organic compounds are used. Generally, FHJs are fabricated in the sandwich structure. The active organic layers are located between the indium tin oxide (ITO, or tin-doped indium oxide) and the metal electrode. As shown in Figure 2, the donor and the acceptor compounds are deposited on the ITO-coated glass substrate layer by layer. On top of the acceptor layer, the metal electrode is deposited under vacuum. The most common materials for this metal electrode are silver or aluminum. When light shines on the device, photons absorbed by donor and acceptor materials (the active layer) lead to the formation of electronic excited states, where the electrons and holes are bound by Coulombic forces. These Coulomb-correlated electron−hole pairs are properly described as excitons. Subsequently, the excitons diffuse to the interface of donor−acceptor materials where charge separation occurs. There the excitons dissociate into electrons and holes. Finally, the free charge carriers move to their corresponding electrodes (holes to ITO and electrons to metal electrode) with the help of the internal electric field.

In FHJs, the separated layer structure of donor and acceptor has a small interfacial area limiting the amount of absorbers which can actually contribute to the photocurrent. Here, only those excitons generated in an extremely thin layer near to the interface of the donor and acceptor junction will be able to dissociate prior to dissipative recombination. Unfortunately, the exciton diffusion length is generally much less than the optical absorption length, which limits the quantum efficiency of such devices.

1.2.2. Bulk-Heterojunction Solar Cells (BHJs)

To improve the efficiency of FHJ devices, one possibility is to enlarge the donor−acceptor interface area, where excitons are dissociated.[35,36] In the so-called bulk-heterojunction formation, where the donor phase is intimately intermixed with the acceptor phase, the excitons can more easily access the donor−acceptor interface and subsequently dissociate to holes and electrons at the donor−acceptor interface. The free charge carriers will then move to the corresponding electrodes by following the continuous route of either donors or acceptors. The electrons, after reaching the metal electrode, move to the electrical load and then transmit to the ITO layer. Obviously, if the network in the active layers is bicontinuous, the charge collection efficiency can be quite high.

To achieve a bulk-heterojunction layer with insoluble small molecules, it is necessary to cosublime two materials (donor and acceptor compounds). The cosublimation complicates the cell structure and raises the costs of manufacturing, however, much improving the efficiency. A mixed layer of donor and acceptor molecules sandwiched between homogeneous donor and acceptor layers can have significantly improved device performance compared to a simple donor−acceptor flat-heterojunction solar cell. Additionally, a transparent organic exciton-blocking layer (EBL) can be inserted between the photoactive region and the metal electrode, in order to eliminate parasitic exciton quenching at the electron acceptor/cathode interface as well as to prevent damage due to cathode evaporation.[37] Using the same organic semiconductors as Tang in the first efficient organic solar cells and, additionally, an EBL from bathocuproine (BCP), Peumans et al. demonstrated the effectiveness of the bulk heterojunction architecture, which improved the device power efficiency from 1.0% to 2.7%.[38]

Replacing perylenedibenzimidazole with C_{60}, a power conversion efficiency of 5% was reported by Forrest et al. in 2005.[39] Quite recently, a new world record using the same technology in a tandem solar cell with an active area size of 2 cm^2 was achieved by Heliatek GmbH with an efficiency as high as 6.07%.[40]

In order to avoid the high cost of sublimation, a mixture of soluble donor−acceptor materials can be used. As most conjugated polymers can be dissolved in organic solvents, scientists have been using polymers in bulk-heterojunction organic solar cells (BHJs) since the 1990s.[41−48] Independently, Morita et al.[43] and Heeger et al.[15] carried out research on the blend of conjugated polymers and C_{60} for the photovoltaic purpose. In the film of the mixture, an ultrafast, reversible, metastable, photoinduced electron transfer from conjugated polymers to C_{60} was observed. This discovery stimulated investigation of BHJs with soluble organic materials. Donor and acceptor materials should generally have self-assembling ability to form separated donor and acceptor phases, which enhances the continuous path construction for the electron/hole collection to the respective electrodes.

To date, BHJs are still mainly polymer solar cells fabricated using conjugated polymers as donors and fullerene derivatives as acceptors. Such solar cells have efficiencies approaching 6−7%.[49−51] Even a 7.9% efficency was reported by Solarmer Energy Inc. in the end of 2009.[52] By using plastic substrates, coated with a transparent conducting electrode, polymer solar cells can be produced flexibly in an easily scalable and high-speed printing process. A typical bulk-heterojunction solar cell contains an ITO-coated glass substrate, covered by a transparent, conductive polymer, most often poly(3,4-ethylenedioxythiophene):polystyrene-sulfonate (PEDOT:PSS).[53,54] In BHJs, the PEDOT:PSS layer provides an improved interface between the active layer and the electrode and, consequently, improves the performance of the devices. PEDOT:PSS is generally applied as a dispersion of gelled particles in water. The highly conductive PEDOT:PSS layer can be obtained by spreading the dispersion on the ITO surface, usually by spin-coating and driving out the water by heat. The mixture of the conjugated polymer with fullerene can be printed on top of PEDOT:PSS. Via vacuum

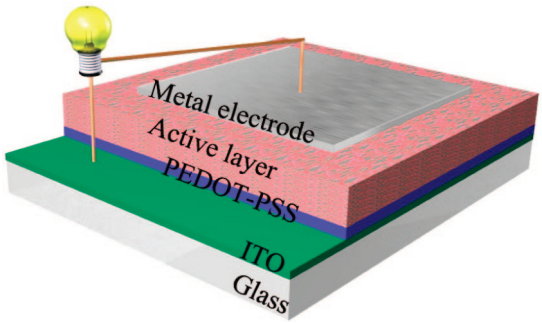

Figure 3. Bulk-heterojunction architecture in polymer solar cells: the PEDOT:PSS layer improves the interface between the active layer and the ITO. A photoinduced charge generation occurs in the active layer, and the exciton dissociates into an electron and a hole at the donor−acceptor interface.

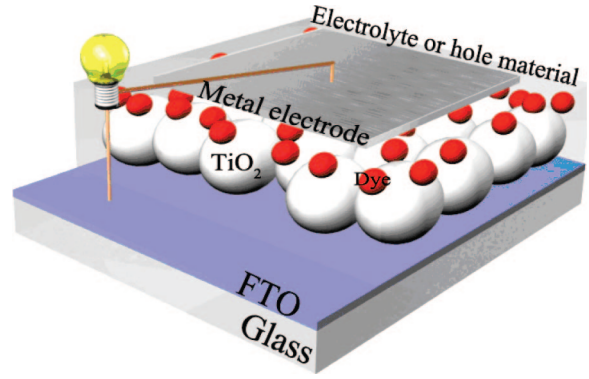

Figure 4. Dye-sensitized solar cell: an FTO-coated glass substrate is covered by TiO_2 nanoparticles, to which a single layer of dye is attached. Electrolyte or hole-transport materials are filled onto the surface of the dye-TiO_2 layer. The metal electrode finally completes the cell.

deposition, a silver or aluminum film as counter electrode covers the active layer (Figure 3).

1.2.3. Inverted-Heterojunction Solar Cells (ISCs)

In both FHJs and BHJs, holes typically flow from the donor material toward the ITO electrode and the electrons from the acceptor to the metal electrode: for example, a flat-heterojunction solar cell with a device structure of ITO/donor molecule/acceptor molecule/Al, or a polymer bulk-heterojunction solar cell with a device structure of ITO/PEDOT:PSS/polymer:fullerene/Al. However, in principle, ITO is capable of collecting either holes or electrons, since the work function of ITO is about 4.5−4.7 eV, which lies between the typical highest occupied molecular orbital (HOMO) and lowest unoccupied molecular orbital (LUMO) values of common organic semiconductors for solar cells. The polarity of the ITO electrode depends mainly on the contact properties, that is, the modification of the ITO surface. For hole extraction, ITO can be coated with a high-work-function layer (such as PEDOT:PSS) or covered by donor materials (such as polymers or metal phthalocyanine). However, if an ITO electrode is coated by hole blocking materials such as ZnO, TiO_x, or Cs_2CO_3, an inverted solar cell can be processed and ITO can collect electrons.[55−60] Another way to build an inverted solar cell is coating acceptor materials directly on ITO[57] and inserting a p-type (and/or electron blocking) semiconductor (such as PEDOT:PSS, V_2O_5, or MoO_3) between metal electrodes and active layers.[55] The organic semiconductors for inverted solar cells are typically the same as in noninverted cells, and the advantages include suspected improvements in active layer morphology as well as device stability.

1.2.4. Dye-Sensitized Solar Cells

In addition to FHJs and BHJs, there is another type of organic solar cell, namely dye-sensitized solar cells (DSCs), also known as Grätzel cells, invented by Grätzel and O'Regan at École Polytechnique Fédérale de Lausanne (EPFL) in 1991.[16] Due to their high efficiency and stability, DSCs were the first organic photovoltaic products to reach the market. G24 Innovations Limited (G24i), a U.K. company founded in 2006, uses DSCs technology to manufacture and design solar modules. Their cells and products are extremely lightweight and ideal for integration or embedding into a wide array of products, such as mobile electronic devices, tents, and building materials. Unlike FHJs and BHJs, a DSC (Figure 4) contains a fluorine-doped tin oxide (SnO_2:F, FTO) covered glass as anode, a thin, wide-band-gap oxide semiconductor mesoporous film, such as TiO_2, a dye monolayer which is deposited on the surface of the TiO_2 layer from solution, an electrolyte or hole transport material which fully covers the TiO_2/dye surface, and a counter electrode (such as platinum on glass for electrolyte-containing DSCs or a silver or gold electrode for cells using organic hole conducting materials).[61,62] The monolayer of dye serves to harvest solar energy. Under light irradiation, an electron is injected from an excited dye into the conduction band (CB) of the TiO_2. The electrons migrate across the inorganic semiconductor nanoparticle network to the current collector (FTO). After traversing the electrical load, the electrons proceed to the counter electrode (metal electrode). The electrolyte or the organic hole conductor serves to regenerate the sensitizer and transport the positive charges to the counter electrode, where they recombine with the electrons. Liquid-electrolyte DSCs, with an iodide/triiodide redox couple as the electrolyte, are the most efficient organic solar cells (up to 11%) up to now.[63,64] Outstanding TiO_2 pore-filling properties can be achieved due to the fluidity of the electrolyte. However, due to disadvantages of solvent-based electrolytes, such as solvent evaporation, leakage, and toxicity, to make liquid-electrolyte free, long-term stable, reliable, solid-state dye-sensitized solar cells (sDSCs) is more attractive for industry.[65−67] In 1998, Grätzel reported the first efficient sDSC based on 2,2′,7,7′-tetrakis(*N*,*N*′-di-*p*-methoxyphenylamine)-9,9′-spirobifluorene (spiro-MeOTAD) as a hole transport material together with a thinner (4.2 μm thick compared to ~10 μm of TiO_2 in the first liquid electrolyte-based DSCs) mesoporous TiO_2 sensitized with a ruthenium dye.[17] Up to now, the spiro-MeOTAD containing sDSCs have reached a record power conversion efficiency of 5.1%.[68]

However, these records are still held by cells based on expensive and environmentally unfriendly ruthenium complexes. The various organic synthetic methods provide us opportunities to develop organic metal-free dyes. Their optical and electrochemical properties can be easily tuned through suitable molecular design. In these dyes, anchoring groups such as the carboxylic acid or phosphoric acid of the sensitizers help the dyes to attach stably to the surface of TiO_2. Among polyphenylene-based materials, functionalized 1D oligophenylenes, derivatives of 2D polycyclic aromatic hydrocarbons, and 3D multichromophores are all candidates for DSC sensitizers.

Like FHJs and BHJs, which can also be structured so as to operate in an inverse mode, a dye-sensitized solar cell, where a nanoporous p-type metal oxide semiconductor is used, can also operate in an inverse mode, where dye-excitation is followed by rapid electron transfer from the valence band of the semiconductor to the dye (dye hole injection). Until now, research on p-type DSCs is mainly based on NiO as a photocathode, which provides an entry toward the preparation of a tandem solar cell.[69−79] With only one photoactive inorganic semiconductor electrode, the theoretical upper limit for a cell is around 30%, which is similar to the case for solid-state devices with one active material. Correspondingly, the limit for a tandem device with two photoactive electrodes is around 43%.[71] Therefore, a simple way to improve a tandem dye-sensitized solar cell is combine high-band-gap n-type semiconductors (such as TiO_2 or ZnO) and low-band-gap p-type semiconductors (such as CdSe, CdTe, or InP). However, most of these p-type semiconductors are not stable with most electrolytes. Some polyphenylene-based sensitizers for p-type DSCs with NiO will be described in this review.

1.3. Determination of Photovoltaic Performance

Besides the insight into the overall photon-to-current conversion efficiency η (or power conversion efficiency, PCE), there are many other parameters to characterize the above-mentioned organic solar cell devices, for example, the incident photon-to-current conversion efficiency (IPCE), the short circuit current (I_{sc}), the open circuit voltage (V_{oc}), and the fill factor (FF).

1.3.1. Incident Photon-to-Current Conversion Efficiency (IPCE)

The photocurrent action spectrum of solar cells is very informative for the characterization of new materials in a device. It represents the ratio of the observed photocurrent divided by the incident photon flux as a function of the excitation wavelength and is referred to as the incident photon-to-current conversion efficiency (IPCE). The photocurrent which is normally measured is obtained outside the solar cell device; therefore, IPCE can also be named as external quantum efficiency (EQE), e.g. the current obtained outside the photovoltaic device per incoming photon:

$$\mathrm{IPCE}(\lambda) = \frac{n_{\mathrm{electrons}}}{n_{\mathrm{photons}}} = \frac{I/e}{P/h\nu} = \frac{I}{P} \times \frac{hc}{e\lambda} = \frac{I}{P} \times \frac{1240}{\lambda\ (\mathrm{nm})}$$

where I is the photocurrent in A m^{-2} and P is the incident light power in W m^{-2}.

By recording the photocurrent response while continuously varying the wavelength of the incident light, the conversion efficiency of photons to electrons, namely IPCE, can be determined. The IPCE value is expressed as a product of three factors:

$$\mathrm{IPCE}(\lambda) = \mathrm{LHE}(\lambda) \times \Phi_{\mathrm{inj}} \times \Phi_{\mathrm{col}}$$

where $\mathrm{LHE}(\lambda)$ is the light-harvesting efficiency of active materials, Φ_{inj} is the charge injection efficiency between the active materials (in the case of FHJs and BHJs, the charge injection is mainly from the donor to the acceptor while, in the case of DSCs, the charge injects via the sensitizers into the semiconductors), and Φ_{col} is the charge collection efficiency at the external electrodes.

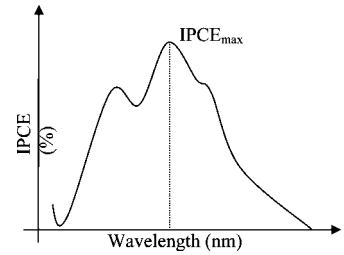

Figure 5. IPCE curve measured at monochromatic incident light.

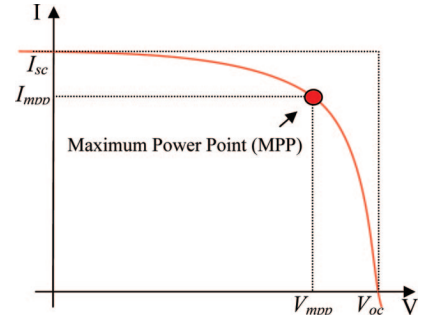

Figure 6. Typical $I-V$ curve of solar cells.

The maximum IPCE value ($\mathrm{IPCE}_{\mathrm{max}}$) is a key parameter for describing the device and correlating the performance to the dye absorption and thereby its molecular structure. The higher the $\mathrm{IPCE}_{\mathrm{max}}$ and the broader the spectrum, the higher the photocurrent will be (I_{sc} corresponds to the integral IPCE curve). A typical example of a photoaction spectrum is shown in Figure 5.

1.3.2. Power Conversion Efficiency (I−V Curve)

The photocurrent action spectrum inspects the ability of the solar cells to convert photons to electrons under the irradiation of light with various wavelengths or intensities, which gives the reference of the photon to electron transfer capability of solar cells. However, to decide whether a solar cell has the potential to be commercialized or not, the most efficient method is to measure the photocurrent and photovoltage under the simulated AM 1.5 solar light. A typical solar cell $I-V$ curve is shown in Figure 6.

The overall power conversion efficiency (PCE), η, is calculated according to the following equation:

$$\eta = \frac{P_{\mathrm{out}}}{P_{\mathrm{in}}} = \mathrm{FF}\frac{V_{\mathrm{oc}}I_{\mathrm{sc}}}{P_{\mathrm{in}}}$$

where P_{out} is the maximum output electrical power (in W m^{-2}) of the device under illumination, P_{in} (in W m^{-2}) is the light intensity incident on the device, V_{oc} is the open circuit voltage, and I_{sc} is the short circuit current in A m^{-2}.

The parameter FF is known as the fill factor, which is defined as

$$\mathrm{FF} = \frac{V_{\mathrm{mpp}}I_{\mathrm{mpp}}}{V_{\mathrm{oc}}I_{\mathrm{sc}}}$$

where V_{mpp} and I_{mpp} are the voltage and current at the maximum power point in the $I-V$ curve, respectively.

The maximum rectangular area ($V_{mpp} \times I_{mpp}$) under the $I-V$ curve corresponds to the maximal output power of the device. An ideal device would have a rectangular shaped $I-V$ curve and therefore a fill factor FF $\approx$ 1. The overall efficiency is an important parameter for evaluating the performance of the device and is the default efficiency value mentioned in the literature.

Besides experimentally characterizing the performance of the organic solar cells, some parameters can also be calculated based on the redox potentials of materials in the active layers. In heterojunction solar cells, the open circuit voltage is most often simply estimated to be the difference between the donor HOMO level and the acceptor LUMO level. For example, in the case of polymer:fullerene-based solar cells, the V_{oc} value can be estimated by the following equation:

$$V_{oc} \approx E_{LUMO,Acceptor} - E_{HOMO,Donor} - 0.3\ V$$

where the constant 0.3 V represents the lost energy during the photoinduced charge-generation process. Based on this, Scharber et al. found a relationship among (1) the LUMO level of the donors, (2) the band gap of the donors, and (3) the power conversion efficiency of the devices.[80] From the calculation, the highest power conversion efficiency could be over 10% for single polymer:fullerene bulk-heterojunction solar cells.

Similar to multilayer or bulk-junction solar cells, dye-sensitized solar cells have similar V_{oc} values, corresponding to the difference between the Fermi level[81,82] of the n-type material (i.e., TiO_2) and the work function[83] of the electrolyte or hole-transporting materials.[84−86] Interestingly in DSC, the dye's energy levels are only indirectly responsible for the cell's V_{oc}. However, a dye which can transfer electrons to inorganic semiconductors and obtain electrons from the hole-transport materials must have a higher LUMO level than the Fermi level of TiO_2 and a lower HOMO level than the work function of the hole materials.

In brief, to achieve an organic solar cell with a reasonable power conversion efficiency and stability, the materials have to be designed carefully in order to fulfill the parameters, such as redox energies, absorption, and self-organization ability. In this review, we give an overview of all the polyphenylene-based materials which have been used as key components for organic solar cells. 1D conjugated polymers can be applied for bulk-heterojunction polymer solar cells. 2D perylene pigments have been intensively applied in small molecular flat-heterojunction solar cells, while 2D perylenes with electron-donating moiety-based copolymers have been widely used in polymer solar cells.[87] Furthermore, donor−acceptor groups functionalized perylenes, and their derivatives are applicable for dye-sensitized solar cells.[87] The 3D multichromophores offer an excellent opportunity for their implementation in organic solar cells due to their strong light-harvesting ability. To understand the relationship between the molecular structures and their photovoltaic performance, the following part of this paper will begin with the color control principle of the polyphenylene-based materials.

2. Polyphenylene-Based Materials for Organic Photovoltaics

When choosing suitable materials for solar cells, certain properties have to be taken into account, such as broad absorption bands and high absorption coefficients for efficient light harvesting, favorable HOMO and LUMO energies for efficient charge transfer, self-assembling ability to form the ideal layer morphology for efficient charge transport, and reasonable stability for durable devices. The first two requirements correspond to the color of the compounds. The color of a molecule can be changed by tuning the ground state energy, the excited state energy, and the energy gap (ΔE) between the ground state energy and the excited state energy. In order to reduce the ΔE of a given chromophore, thereby shifting the λ_{max} to longer wavelengths, the following major approaches can be adopted (Figure 7): (i) enlargement of the π systems, (ii) transition from aromatic to quinoidal structures, (iii) introduction of donor−acceptor substituents, and (iv) polymerization.

As the epitome of aromatic compounds, polyphenylenes are compounds which contain benzene as unique building blocks. Benzene can undergo electrophilic or nucleophilic aromatic substitutions. Polymerization yields polyphenylene compounds, which can be further functionalized by donor or acceptor groups. In certain conditions, with strong donor−donor, donor−acceptor, or acceptor−acceptor interactions, conjugated oligophenylenes can transform to quinoidal compounds. Benzene compounds can be easily extended into two dimensions. One example of such a compound exists abundantly in nature, namely graphite. Due to the facile functionalization, polyphenylene-based materials represent highly versatile species, which provide an interesting playground for creating intricate function as well as demanding structural complexity. They provide possibilities for multi-

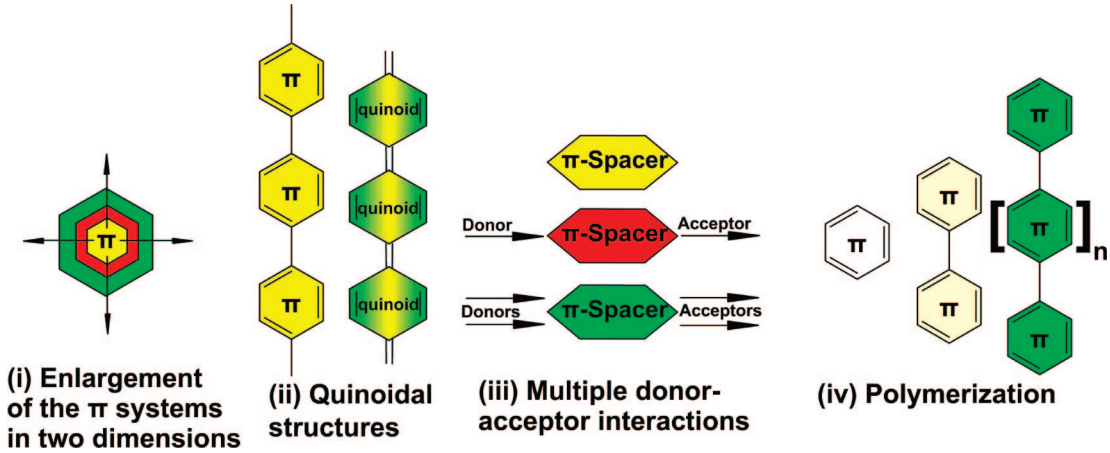

Figure 7. Approaches of color tuning.

dimensional structure architectures to realize materials with different color. Polyphenylene compounds, therefore, are considered one of the most important classes of compounds used in organic electronic applications.

2.1. Conjugated Polyphenylenes

Coupling benzene molecules via their *para* position is the easiest pathway to enhance the conjugation. Since the 1960s, polyphenylenes and their derivatives have been developed and used for many important applications.[88−90] As rodlike materials, linear polyphenylenes such as unsubstituted polyphenylenes (polymer **1**) or oligophenylenes have had limited applications because of their poor solubility. This can easily be improved by introducing solubilizing groups into the main chain, which, however, leads to torsion within the polymer backbone (polymer **2**).[91−93] In order to maintain planarity, the method of introducing heteroatoms (such as N and Si for polymers **4** and **5**, respectively) or carbon bridges (polymer **3**) has been widely used, as the bridge not only restricts the rotation between the monomer units but can also improve the solubility of the polymers via substituents on bridge atoms (Chart 1).[94]

A further modification of polyphenylene compounds is to turn the structure from a stepladder to a full-ladder species (Chart 2).[95−101] This has been shown to be useful for improving the stability as well as the optical and electrochemical properties of polyphenylenes. Additionally, enhancing the electron affinity of polyphenylenes or oligophenylenes can be achieved by altering the bridge atoms. In the last 20 years, ladder-type oligophenylenes and polyphenylenes have been used in many optoelectronic applications.[102,103]

2.1.1. Polyphenylenevinylenes (PPV)

In the family of benzene-based polymers, another class of conjugated polymers containing phenylenes are polyphenylenevinylenes (PPVs), which are one of the most well-known conducting polymers and arose from the discovery of mobile photoinduced charged states in organic semiconductors.[104] Using this property in conjunction with a molecular electron acceptor, long-lived charge separation based on the stability of photoinduced nonlinear excitations on the conjugated polymer backbone can be achieved. The photophysics of a bilayer of poly[2-methoxy-5-(2′-ethylhexyloxy)-1,4-phenylene vinylene] (MEH-PPV, compound **7** (Chart 3)) with C_{60} was first reported in 1992.[105,106] The experiments clearly evidenced an ultrafast, reversible, metastable photoinduced electron transfer from MEH-PPV to C_{60} in solid films. This result accelerated the development of polymer solar cells for many years, and poly[2-methoxy-5-(3,7-dimethyloctyloxy)-1,4-phenylene vinylene] (MDMO-PPV, compound **8**) is still being used in organic solar cells today.[107−113] Combined with 1-[3-(methoxycarbonyl)propyl]-1-phenyl-(6,6)-C_{61} (PCBM), efficiencies of MDMO-PPV-based solar cells of up to 2.9% could be obtained.[114,115]

Chart 2. Ladder-Type Polyphenylene

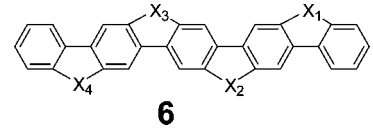

6

Chart 3. Chemical Structures of PPV Derivatives MEH-PPV (7) and MDMO-PPV (8)

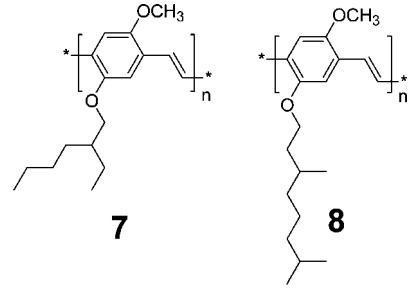

7 **8**

Chart 4. Chemical Structures of Cyano-Containing PPV Polymer 9 and Poly-3-(4-octylphenyl)thiophene (10)

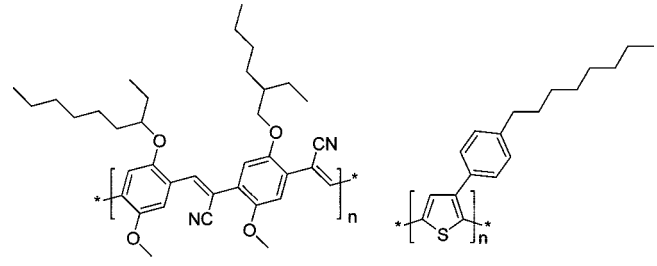

9 **10**

Although PPV is well-known as a donor material in solar cell devices, a cyano derivative of PPV (compound **9**; Chart 4) was used as the first polymer electron acceptor.[116] By using a lamination device processing technique,[117] Friend et al. reported a two-layer polymer cell based on compound **9** and polythiophene **10**.[118,119] The resulting device provided an $IPCE_{max}$ of up to 29% and an overall power conversion efficiency of 1.9% under a simulated solar spectrum.[117]

Most polyphenylenevinylenes can only absorb light around 500 nm, which limits their photovoltaic performance. Additionally, they are not stable in the presence of even small amounts of air. The oxygen radicals will be formed in the presence of water and will attack the structure of polymers, leading to their degradation. Thus, to make a stable photovoltaic device based on PPVs, one must take special precautions to prevent oxygen contamination during processing. Due to these two aspects, using PPVs to make organic solar cells is not often reported. Therefore, to find a new design principle for polyphenylenes better suited for photovoltaics is very important. The easiest way to improve the absorption and stability of polyphenylenes is the introduction of a bridge atom between two linked benzenes, such as fluorene, carbazole, and dibenzosiloles. It has been proven

Chart 1. Polyphenylene and Its Soluble Derivatives

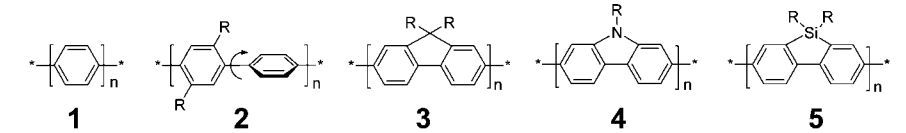

1 poly-p-phenylene
2 substituted poly-p-phenylene
3 poly-2,7-fluorene
4 poly-2,7-carbazole
5 poly-2,7-dibenzosilole

Chart 5. Chemical Structures of Fluorene-Containing PF Copolymers 11 and 12

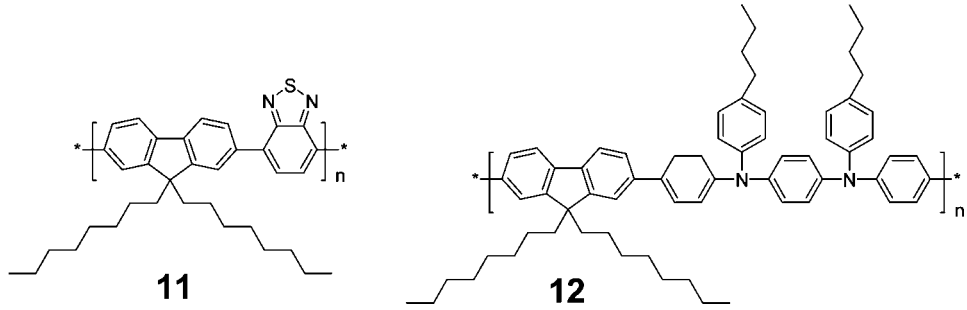

Chart 6. Chemical Structures of Donor−Acceptor-Type Fluorene-Thiophene-Containing PF Copolymers 13−26

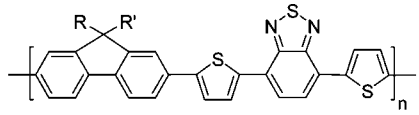

13 R = hexyl, R' = 2-ethylhexyl
14 R = R' = hexyl
15 R = R' = octyl
16 R = R' = dodecyl

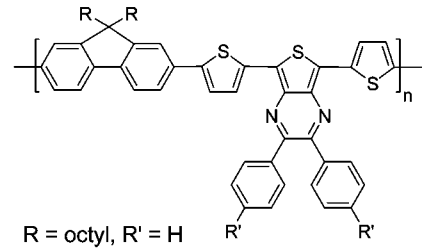

18 R = octyl, R' = H
19 R = octyl, R' = 2-ethylhexyloxy
20 R = octyl, R' = octyl

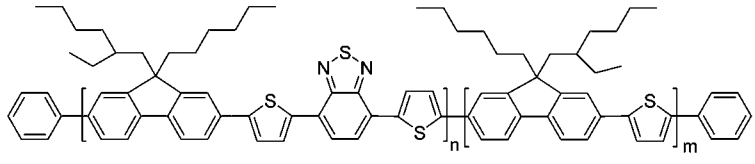

17

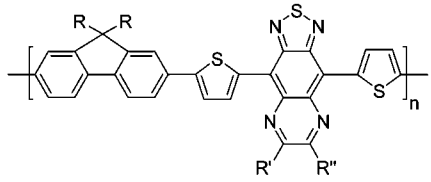

21 R = octyl, R' = R'' = phenyl
22 R = octyl, R' = hexyl, R'' = 2-ethylhexyl
23 R = octyl, R' = R'' = 2-ethylhexyloxyphenyl

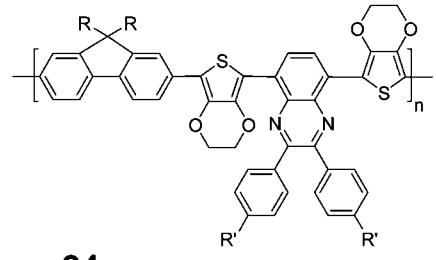

24 R = octyl, R' = 2-ethylhexyloxy

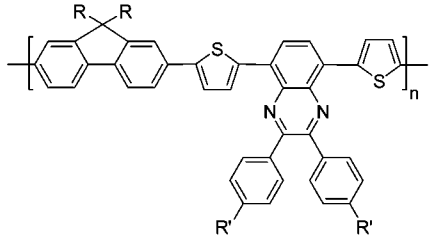

25 R = octyl, R' = octyloxy

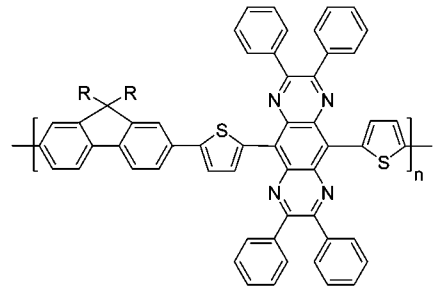

26 R = octyl

that the polymers based on these planarized biphenyl monomers can achieve better performance in solar cells.

2.1.2. Polyfluorenes (PF)

Polyfluorene (PF) is to date the most important blue light-emitting polymer due to its electroluminescence. PF contains the structure of *para*-polymerized benzene, where each adjacent pair of phenylene groups is tied together in a coplanar fashion by methylene bridges to form a fluorene unit. The side chains can be introduced in the 9-position of each fluorene. Because of their weak absorption in the visible region, the homopolyfluorenes are not suitable for the solar conversion purpose. However, fluorene building blocks have been copolymerized with other aromatic compounds, where the fluorene units could improve the solubility and maintain the conjugation in the whole copolymers.

Friend et al. reported a completely polymer solar cell based on two fluorene-containing polymers as donor and acceptor,

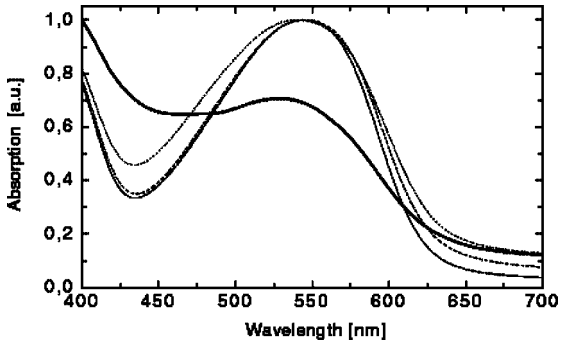

Figure 8. Normailized absorption spectrum of spin-coated films of compound **13** from chloroform (dot-dashed line), xylene (dashed line), and toluene (dotted line) and absorption of a film from a composite of **13**:PCBM (1:4) spin-coated from chloroform (solid line). Adapted with permission from ref 130. Copyright Wiley-VCH Verlag GmbH & Co. KGaA.

respectively, in the device, where polymer **11** (Chart 5) with the benzothiadiazole group serves as the acceptor and polymer **12** with the triphenylamine as the donor.[120,121] Although this combination showed low power efficiency in the device ($IPCE_{max} < 5\%$), polymer **11-** and **12**-based solar cells provide an excellent platform for investigating the interface and electronic structures of donor and acceptor heterojunctions.[122−128]

The first breakthrough in fluorene-based polymer solar cells was demonstrated by Andersson et al.[129,130] They reported an alternating polyfluorene copolymer, poly[2,7-(9-2′-ethylhexyl)-9-hexylfluorene]-*alt*-5,5-(e′,7′-di-2-thienyl-2′,1′,3′-benzothiadiazole] (**13**; Chart 6) with extended absorption.[130] Films of the polymer show the longest wavelength absorption maximum at approximately 545 nm (Figure 8). The films from xylene solution show small grains, and they are not as even as the films processed from chloroform. The authors ascribed this difference to the partial insolubility of **13** in xylene.

In polymer **13**, fluorene groups with two different side chains were introduced in this polymer to enhance its solubility. The two thiophene units together with the benzothiadiazole group formed a donor−acceptor copolymer and improved the optical properties of the target polymer. Blended with PCBM, the polymer solar cell containing ITO/PEDOT:PSS/polymer **13**:PCBM/LiF/Al showed a 2.5% power conversion efficiency. The authors claimed that the combination of benzothiadiazole and thiophene moieties creates a low-band-gap segment which largely improves the light absorption of the whole polymer. Since then, many low-band-gap polymers with benzothiadiazole and thiophene groups have been reported by these authors.

With different side chains in the 9-position of the fluorene moiety, polymers **13**−**16** were compared in terms of photovoltaic performance.[131] The side chains influence the packing of the main chains as well as the morphology of the active layer and consequently produce different photovoltaic properties. Here, the octyl substituted polymer exhibited the best power conversion efficiency of 2.6%.[132,133] A polyfluorene block copolymer **17** which contains a higher amount of fluorene moieties was also investigated. Effects of blend composition and film thickness on the device parameters were examined. The device with a thickness of 200 nm, fabricated from a 1:4 blend of polymer **17**:PCBM, showed a maximum efficiency of 1.7% under simulated solar light illumination (light intensity 100 mW cm^{-2}).[134] The authors have reported additional polyfluorene copolymers **18**−**26** with stronger acceptor or donor moieties in order to enhance the absorption of the polymers.[135−142] The absorption spectrum of polymer **18** shows a broad absorption from 300 to 850 nm with two local maxima at 380 and 615 nm.[135−137] Unlike **18**, compound **19** contains two branched alkoxy side chains on the repeating unit. These chains improve the solubility, resulting in a soluble, high-molecular-weight polymer.[138] The absorption spectrum of **19** demonstrates similar absorption bands to that of **18**, but both peaks are bathochromically shifted. Two broad peaks occur at 430 and 660 nm, respectively. Polymer **20** has two linear octyl side chains, which also increase the solubility of the polymers and induce a bathochromically shifted absorption with an absorption maximum at 660 nm.[141] Devices based on polymers **18**, **19**, and **20**, blended with PCBM, were fabricated and characterized. The solar cells of polymer **19** exhibited a top efficiency of 2.2%.[143]

Wang et al. reported another series of low-band-gap polyfluorene copolymers **21**−**23** that have a fluorene and a donor−acceptor−donor moiety.[138] Electrochemical and optical absorption measurements showed that the optical onset band gaps of these polymers range from 1.2 to 1.5 eV. The polymers were blended with a newly synthesized C_{70}-derivative (3′-(3,5-bis-trifluoromethylphenyl)-1′-(4-nitrophenyl)pyrazolino[70]fullerene, BTPF70) for solar cell fabrication, which showed an onset of the photocurrent spectral response extending up to 1 μm (Figure 9). A photocurrent density of 3.4 mA cm^{-2}, an open circuit voltage of 0.58 V, and a power conversion efficiency of 0.7% under the illumination of AM 1.5G (1000 W m^{-2}) were obtained from polymer **21**-based devices. It can be observed that all polymer **21**−**23**-based solar cell devices exhibited similar IPCE spectra, which have two bands (around 85% for the high energy peak and only 37% for the low energy peak, Figure 9). Because of this, although polymers **21**−**23** have very broad absorption bands, their solar cells did not deliver high currents. The weak IPCE signals in the NIR region are due to the optical absorption of the PEDOT layer, which is 10 times higher in the near-infrared compared to the visible region. Therefore, desirable anode materials that are transparent in both the visible and near-infrared regions and have suitable work functions are required in order to avoid the loss of the absorption in the near-infrared region.

Inganäs and his co-workers reported fluorene-, thiophene-, and quinoxaline-containing copolymers **24** and **25**.[140,141] Both polymers showed broad absorption and emission bands. Solar cells based on blends of **25** and PCBM had a very high efficiency of 3.7%,[139] while **24** exhibited an efficiency of 1.1%[141] when characterized under standard AM 1.5 solar illumination. Moreover, pure **25** thin solid films gave rise to efficient LEDs of red color.[141]

Another fluorene-containing copolymer **26** was reported by Zhang and Andersson et al.[142] where pyrazino[2,3-*g*]-quinoxaline was introduced into the polymer backbone between two thiophene rings. The absorption spectrum of pure **26** displayed two peaks at 400 and 710 nm, extending to 900 nm. Solar cells based on **26** and [6,6]-phenyl-C71-butyric acid methyl ester ([70]PCBM) presented a photoresponse up to 900 nm with an I_{sc} of 6.5 mA cm^{-2}, a V_{oc} of 0.81 V, and a power conversion efficiency of 2.3% under AM 1.5G illumination.

Shortly after Andersson et al. had published the photovoltaic performance of polymer **13**, Cao and his co-workers

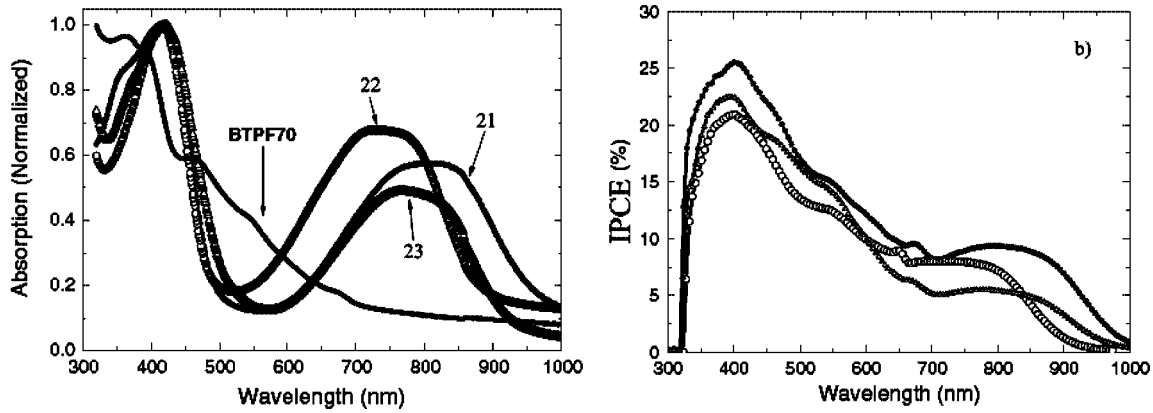

Figure 9. (a) Normalized absorption spectra of compound **21** (line−solid circle), **22** (line−open circle), **23** (line−open triangle), and BTPF70 (solid line). (b) IPCE of solar cells-based on polymer **21**:BTPF70 (line−solid circle), **22**:BTPF70 (line−open circle), and **23**:BTPF70 (line−open triangle). Adapted with permission from ref 138. Copyright 2006 Elsevier.

Chart 7. Chemical Structures of Thiophene-, Silole-, or Selenophene-Containing PF Copolymers 27−31

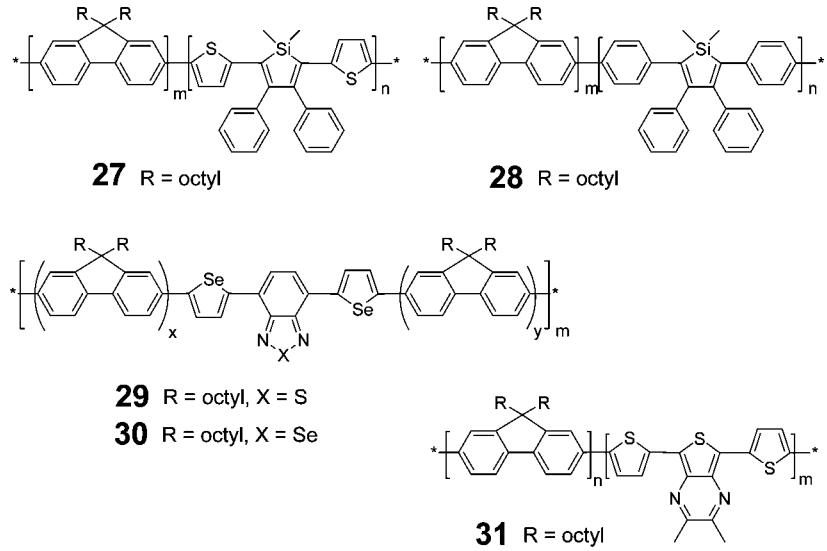

demonstrated polymer solar cells of polymer **15** with a 1.95% power conversion efficiency.[144] One year later, Chen and Cao et al. reported polyfluorene copolymers **27** and **28** with silole moieties (Chart 7).[145,146] Siloles, or silacyclopentadienes, are a group of five-membered silacycles that possess a unique low-lying LUMO level associated with the $\sigma^*-\pi^*$ conjugation arising from the interaction between the σ^* orbital of two exocyclic σ-bonds on the silicon atom and the π^* orbital of the butadiene moiety. Due to their high electron accepting strength and high electron mobility, siloles have been utilized as electron-transporting and light-emitting layers in the fabrication of electroluminescence devices. There have been great efforts to incorporate siloles into polymers. The ratio of fluorene and silole units in these polymers can be tuned to vary the absorption. When the ratio between 9,9′-dioctylfluorene (PFO) and 1,1-dimethyl-3,4-diphenyl-2,5-bis(2′-thienyl)silole (TST) was 1:1, polymer **27** exhibited an absorption maximum at 520 nm in film (Figure 10). The photovoltaic performance of a device based on the blend of **27** and PCBM (1:4) showed a power-conversion efficiency of 2.01% under an AM 1.5 solar simulator.[145] Because of the poor absorption in the visible region, the photovoltaic performance of **28** was not mentioned.

The introduction of selenium-containing heterocycles to the polyfluorene main chain resulted in a significant red shift in comparison with that of sulfur-containing heterocycles. Polymers **29** and **30** have selenophene and benzoselenadiazole groups which could decrease the band gap of the polyfluorene copolymers.[147] Their optical band gaps are quite low, 1.87 eV for **29** and 1.77 eV for **30**. The spectral response is extended to 675 and 750 nm for **29-** and **30-**based OPVs, respectively. Among these devices, the best performance was obtained from polymer **29**:PCBM (1:4), reaching 2.53 mA cm^{-2} of I_{sc}, 1 V of V_{oc}, 37.4 of FF, and a power conversion

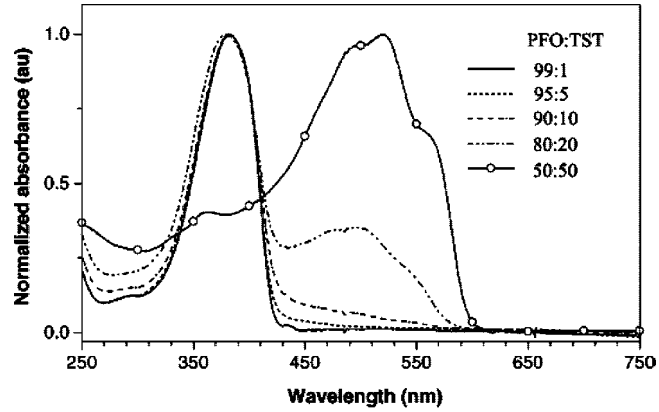

Figure 10. The UV−vis absorption spectra of copolymers **27** in film: the monomer ratio of PFO to TST is 99:1, 95:5, 90:10, 80:20, and 50:50. Adapted with permission from ref 145. Copyright 2005 American Chemical Society.

Chart 8. Chemical Structures of Rigid-π-Moieties-Containing PF Copolymers 32−35

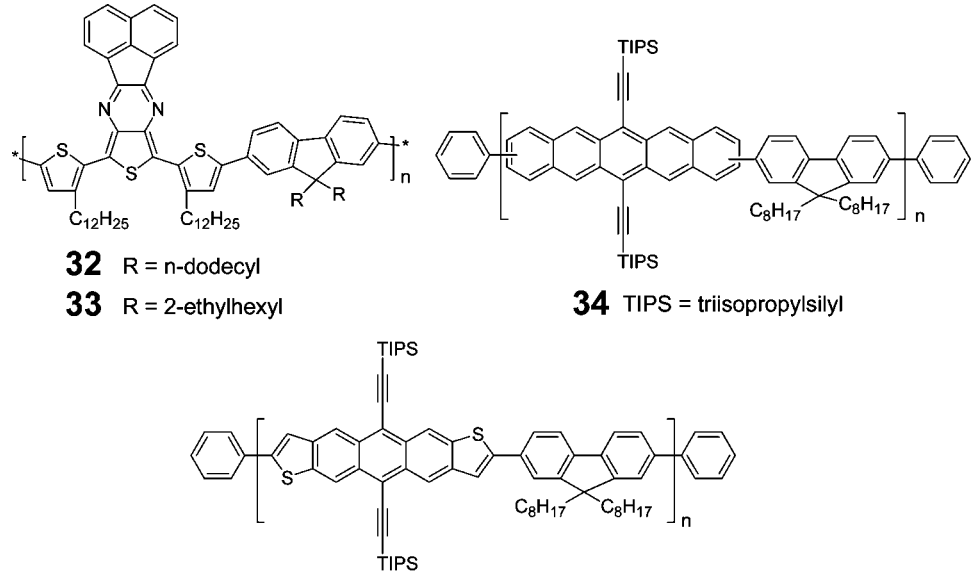

32 R = n-dodecyl
33 R = 2-ethylhexyl

34 TIPS = triisopropylsilyl

35 TIPS = triisopropylsilyl

efficiency of 1.0% under AM 1.5G illumination (78.2 mW cm^{-2}). It can be noted that the device has a promising open circuit voltage; therefore, the low current and fill factor (probably because of the limited charge extraction owing to nonoptimal device thickness) are the main reason for the low PCE.

Similar to the report on the introduction of thienopyrazine into the polyfluorene backbone by Inganäs, Cao and his coworkers described polyfluorene copolymer **31**, which was derived from 2,3-dimethyl-5,7-dithien-2-ylthieno[3,4-*b*]pyrazine groups, the key moiety to lower the band gap of the whole copolymer.[148] Photovoltaic devices based on a composite thin film of polymer **31**/PCBM (1:1) blended as an active layer showed a promising short circuit current (≈4.1 mA cm^{-2}) and a moderate energy conversion efficiency (0.83%) under AM 1.5G solar illumination. The edge of the spectral response was extended to 740 nm.

Recently, Bao et al. presented a rigid naphthalene moiety fused to the 2,3-positions of thienopyrazine which was copolymerized with fluorene.[149] The planar and electron rich π-face of acenaphtho[1,2-*b*]thieno[3,4-*e*]pyrazine promoted $\pi-\pi$ stacking between polymer chains and led to improved charge carrier mobility. Polymers **32** and **33** (Chart 8) showed high p-type mobilities of up to 0.2 $cm^2\ V^{-1}\ s^{-1}$ in organic thin film transistors. Polymer **33**/PCBM-based solar cells exhibited a power conversion efficiency of 1.4% under an AM 1.5 solar simulator. By applying the same strategy, i.e. incorporating rigid π-groups (thienopyrazine for polymer **32** and **33**) into polymer chains to decrease the band gap of the polymer, they also synthesized pentacene and anthradithiophene−fluorene conjugated copolymers **34** and **35**.[150] These two polymers were achieved by Suzuki coupling reactions in good yields and exhibited high molecular weights with band gaps of 1.64 and 1.91 eV, respectively, which correspond to their longest wavelength absorption maxima of 670 and 586 nm in film. The solar cell fabricated from a blend of **35** and PCBM in a 1:3 ratio possessed an open circuit voltage of 750 mV, a short circuit current of 2.35 mA cm^{-2}, and a power conversion efficiency of 0.68%.

In addition to introducing large ribbon-type π-motifs into a polymer backbone, Wong and Djurišić et al. developed

Chart 9. Chemical Structures of Platinum-Containing PF 36−39

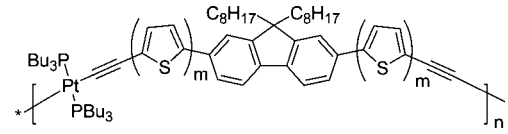

36 m = 0
37 m = 1
38 m = 2
39 m = 3

platinum-containing polymers.[151−153] The incorporation of heavy metals into an organic framework can have a significant influence on its electronic and optical properties.[154] Combined with thiophene and benzothiadiazole units, polyplatinyne-based solar cells achieved overall power conversion efficiency up to 5%.[153] In order to expand the spectral width of absorption appropriate for sunlight harvesting, platinum as well as thiophene fragments have also been incorporated into polyfluorenes. The resulting new polymers **36−39** (Chart 9) exhibit absorption maxima between 399 and 457 nm and energy band gaps of 2.33−2.93 eV (Figure 11).[151] Although **36−39** have shorter absorption maxima and larger band gaps compared to P3HT, their solar cells achieved respectful PCEs of up to 2.9% and peak IPCEs of 83%. More importantly, the narrow absorption bands (the onset values of their absorption spectra are close to 500 nm in solution and 700 nm in film, Figure 11) render them as good candidates for tandem solar cells,[155,156] where these polymers can be the active components in the bottom devices to harvest the short wavelength light.

Summarizing these fluorene-based polymers, it is easy to find that fluorenes act as key moieties to improve the solubility of polymers, since the carbon bridge atom in fluorene can provide solubilizing substituents, normally alkyl chains. However, for the purpose of light-harvesting, fluorene compounds have to be combined with other groups, either acceptor groups (such as benzothiodiazole) or donor units (such as thiophene). Nearly all polyfluorenes with high photovoltaic efficiency have thiophene groups in the polymer

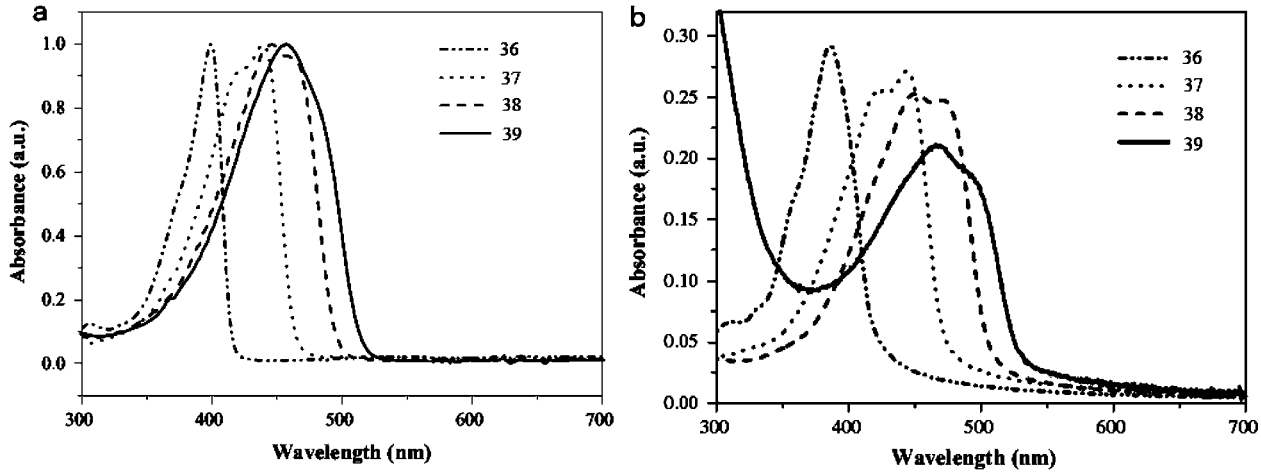

Figure 11. Absorption spectra of polymer **36**−**39**: (a) in CH_2Cl_2 and (b) in film. Adapted with permission from ref 151. Copyright Wiley-VCH Verlag GmbH & Co. KGaA.

backbone. For example, polymer **27**, which contains thiophene, has an absorption maximum at 520 nm in a film, which results in a good power conversion efficiency of 2.01%. However, polymer **28**, a polymer without thiophene units, shows poor results. Besides the introduction of thiophene, the additional acceptors in polymers can further tune the absorption behavior of the whole compounds. According to this structural design, polymer **25**, which has fluorene, thiophene, and quinoxaline groups, gives the best PCE of 3.7% among all the fluorene-based polymers.

2.1.3. Polycarbazoles (PC)

The introduction of nitrogen bridges instead of methylene bridges into the structure of the biphenyl compound results in electron-rich materials called carbazoles. Polycarbazoles (PC) are one of the most widely investigated and applied semiconductors due to their photoconductive properties and ability to form charge transfer complexes arising from the electron-donating character of the carbazole moiety. One could expect an improvement in the mobility of the charge carriers if carbazole groups are covalently incorporated in the main chain to form conjugated backbones. There are two ways to connect carbazole units to one another: the first is to link the repeating units at the 3,6-positions to yield poly(3,6-carbazole)s, and the second is to connect them via the 2,7-positions toward poly(2,7-carbazole)s. Oligo(3,6-carbazole)s were first synthesized in 1968 by Ambrose.[157] In 2004 Siove et al. succeeded in synthesizing a high molecular weight polymer by oxidative polymerization.[158] A field effect transistor (FET) based on poly(*N*-butyl-3,6-carbazole) showed a charge carrier mobility of 10^{-3} cm^2 V^{-1} s^{-1}.[159]

The first photovoltaic cell based on poly(*N*-alkyl-2,7-carbazole)[160−163] was reported by our group in 2006.[162] In order to improve the solubility of polycarbazoles and to obtain easy fabrication of solar cell devices, 2-decyltetradecyl alkyl chains were introduced. It has previously been demonstrated that the introduction of such branched alkyl substituents is an efficient way to increase the solubility of perylene-based dyes[164,165] and 2D polycyclic aromatic hydrocarbons.[166−168] The onset oxidation potential versus ferrocene was 0.8 V, corresponding to a HOMO energy level of −5.6 eV. Using the band gap from the absorption spectrum of the thin film, the LUMO is estimated at −2.6 eV. Therefore, the HOMO energy level of **40** (Chart 10) is

Chart 10. Chemical Structures of Compounds 40−42

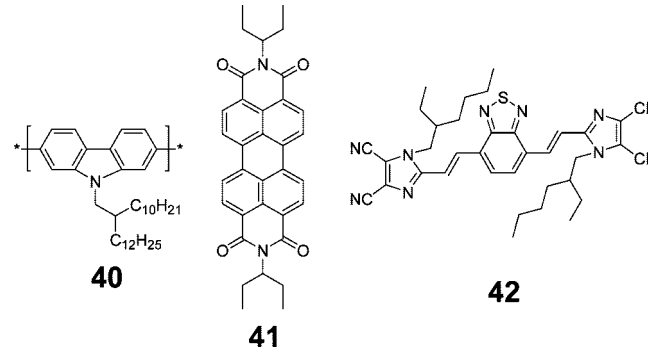

lower than that of poly(3-hexylthiophene)- (P3HT) (e.g., −5.2 eV for P3HT) and PPV-based materials (e.g., −5.3 eV for MDMO-PPV), offering improved chemical stability. In photovoltaic devices, both perylenediimide **41** and PCBM were chosen as acceptors and combined with **40** in the active layer. **41** revealed an absorption maximum at 537 nm in a thin film while PCBM showed an absorption peak only in the blue region with an extended tail to 600 nm. In terms of light absorption, PDI **41** compensates **40** more efficiently than PCBM. The photovoltaic devices were fabricated based on blends of **40**:**41** and **40**:PCBM at a D−A ratio of 1:1. The IPCE spectrum of the device using PCBM exhibited an IPCE maximum at 400 nm with a value of 2.5%.[162] In contrast, the device using PDI **41** revealed a broad IPCE spectrum with two strong peaks showing IPCE values of 3.4% at 420 nm and 3.8% at 500 nm, corresponding to the absorption of **40** and PDI **41**, respectively. The **40**/**41** (1:1) blend solar cells exhibited a power conversion efficiency which is 3-fold of the efficiency of **40**/PCBM-based solar cells under the irradiation of the same light. The blend containing 20 wt % of **40** and 80 wt % of **41** (1:4) gave an overall efficiency of 0.63% (under 10 mW cm^{-2} sunlight intensity) and a maximum IPCE of 15.7% at 495 nm. It is worth mentioning that using **41** as acceptor, in combination with P3HT instead of **40**, showed lower efficiency than **40**-based solar cells. Its power conversion efficiency is only around 0.4%.[162,169] This result indicated that high-band-gap conjugated polymers can also be applied as candidates for efficient solar cells if appropriate electron acceptors are chosen. In **41**-based solar cells, replacing **40** with P3HT led to a drop in V_{oc} from 0.7 to 0.4 V (as expected from the lower HOMO energy level of **40** than that of P3HT), which

points to the main reason for the different PCE values between **40** and P3HT contained solar cells.

As an alternative to **41** as a nonfullerene-type acceptor, Sellinger and co-workers recently reported polycarbazole **40**-based bulk-heterojuncion solar cells with another small molecule acceptor **42**.[170] The photoluminescence (PL) of the **40/42** blend was measured via excitation at the absorption maxima of **40** and **42**, which are 395 and 444 nm, respectively. The intensity of the blend PL was substantially weaker than that of similarly excited films of neat **40** and **42**, indicating efficient exciton dissociation in the blend. The solar cells were fabricated in the structure of ITO/PEDOT:PSS/**40**:**42**/Ca/Ag. The most efficient device was obtained using 70% of **42** upon annealing at 80 °C. This yielded a power conversion efficiency of 0.75%, an I_{sc} of 1.14 mA cm^{-2}, a V_{oc} of 1.36 V, and a FF of 49% under AM 1.5G irradiation (100 mW cm^{-2}). Considering that the absorption of polycarbazole **40** is mainly in the UV region (corresponding to only 5% of the sun's energy), the extraordinary open circuit voltage and reasonable efficiency of **42**-based solar cells suggest the investigation of new acceptor molecules for photovoltaic applications.

Compared to the application of strongly absorbing acceptor materials (such as compound **41** and **42**), improving the light harvesting properties of the donors (polymers) seems more efficient and realizable. Currently, this remains the main method used to improve the efficiency of organic polymer solar cells. Leclerc and co-workers have reported the synthesis of electroactive and photoactive polycarbazole copolymers linked at the 2,7-positions of the carbazole monomer.[171] To enhance the light-harvesting ability of carbazole-containing polymers, oligothiophenes were introduced. In the film, the absorption maxima of polymers **43**−**47** are 426, 462, 487, 491, and 514 nm, respectively. Compared with polycarbazole **40**, all polymers **43**−**47** (Chart 11) showed red-shifted absorptions, depending on the percentage of thiophene units in the polymer chains. This indicates that the band gap of the polymers can easily be tuned upon addition of thiophene units into the polymer backbone. Moreover, the addition of *S*,*S*-dioxide thiophene induces a significant bathochromic shift of the absorption maximum due to the donor−acceptor effect. With the sandwich structure ITO/PEDOT:PSS/polymer:PCBM/Al, the solar cells of polymers **43**−**47** were fabricated. The devices were tested under 90 mW cm^{-2} light intensity. Of all these polymers, **47** exhibited the best photovoltaic performance with a 0.8% power conversion efficiency (I_{sc} is 1.56 mA cm^{-2}, V_{oc} is 0.8 V, and FF is 0.55). The low current values indicated that better efficiencies should be obtained by optimizing the polymer:PCBM ratio, the device configuration, and the morphology of the active layer.

Based on the discovery that including oligothiophenes or *S*,*S*-dioxide thiophene into the polycarbazole backbone can enhance the absorption via the donor−acceptor effect and, hence, the photovoltaic performance, Leclerc et al. developed more polycarbazoles by incorporating other stronger acceptor groups into the polymer chains.[172−175] Polymers **48**−**53** (Chart 12) were synthesized under this concept design and exhibited two broad absorption peaks in the region between 300 and 700 nm.[172] Among all these polymers, polymer **50** showed the highest hole mobility of up to 0.001 cm^2 V^{-1} s^{-1} and an on/off current ratio of 3×10^4 in OFETs.

The best photovoltaic result was presented for polymer **50** with a power conversion efficiency of 4.6%.[173,175] The

Chart 11. Chemical Structures of PC Copolymers 43−47

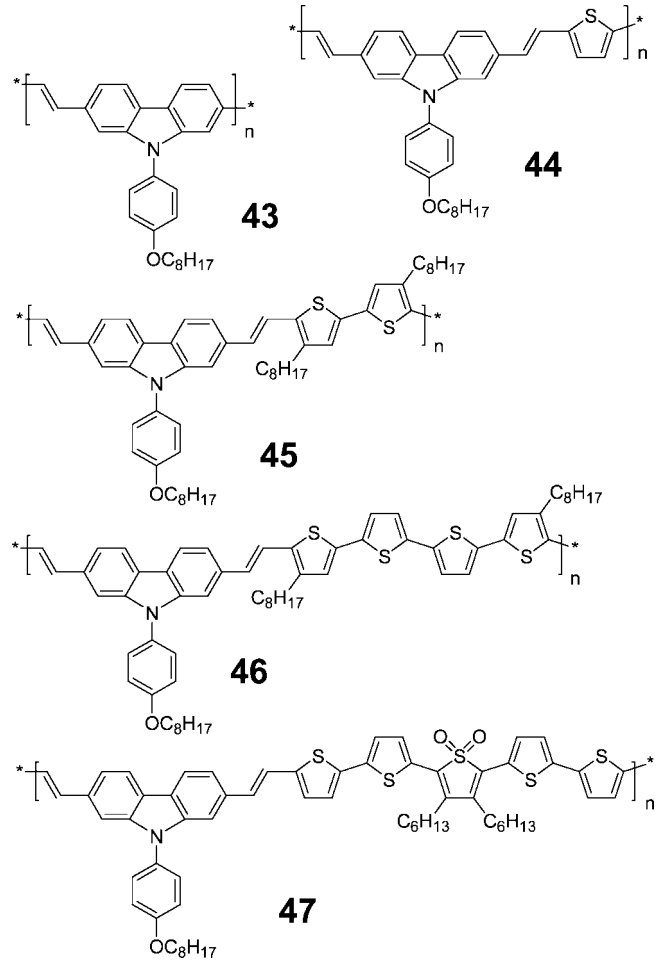

Chart 12. Chemical Structures of Carbazole-Thiophene-Acceptor-Thiophene-Based PC Copolymers 48−53

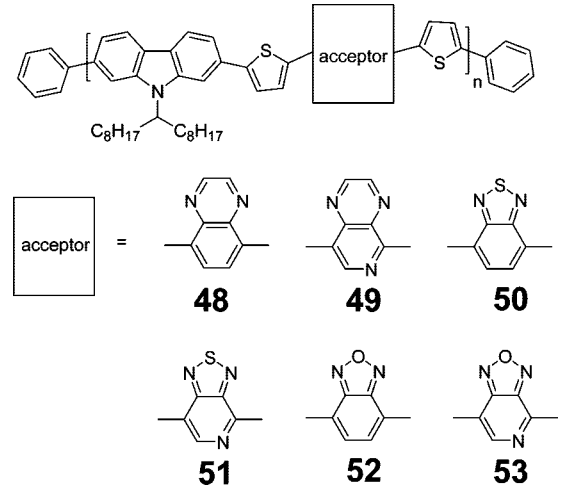

Table 1. Performance Parameters of BHJ Solar Cells Based on 50 under AM 1.5G Illumination

device materials (w:w)	active layer (nm)	V_{oc} (V)	I_{sc} (mA cm^{-2})	FF	PCE (%)
50:[60]PCBM (1:2)	60	0.90	9.42	0.51	4.35
50:[70]PCBM (1:2)	70	0.89	10.22	0.51	4.57

high I_{sc} and FF values (Table 1) in polymer **50**-based solar cells are attributed to the good hole mobility resulting from the higher structural organization. With the solar cell structure of ITO/PEDOT:PSS/**50**:[70]PCBM/TiOx/Al, a new record

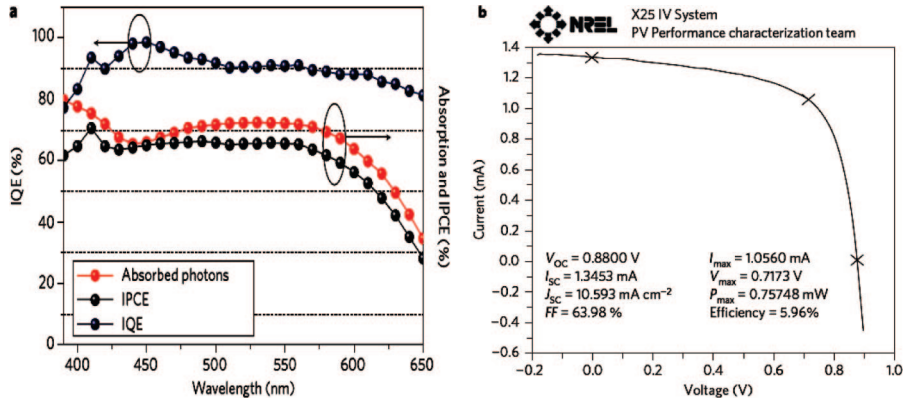

Figure 12. (a) Internal quantum efficiency (IQE) of ITO/PEDOT:PSS/**50**:[70]PCBM/TiO_x/Al-based solar cells. The red line shows the total absorption of the device, and the black line the IPCE. (b) NREL-certified $I-V$ characteristics of a ITO/PEDOT:PSS/**50**:[70]PCBM/TiO_x/Al-based solar cell. Adapted with permission from ref 49. Reprinted by permission from Macmillan Publishers Ltd.: Nature Photonics, Copyright 2009.

power conversion efficiency of 6%, certified by NREL, was achieved under AM 1.5 irradiation (Figure 12).[49] More importantly, the internal quantum efficiency (IQE is the ratio of the number of charge carriers collected by a solar cell to the number of photons of a given energy that shine on the solar cell from outside and are not reflected back by the device, nor penetrate through) of **50**- and [70]PCBM-containing solar cells approaches 100% (Figure 12), implying that every photon absorbed leads to a separated pair of charge carriers and that every photogenerated mobile carrier is collected at the electrodes. It is worth mentioning that this power conversion efficiency value of solar cells based on **50** and PCBM is close to its anticipated maximum (6.5%), according to the empirical efficient calculation diagram[80] via the LUMO (−3.6 eV) and the band-gap (1.9 eV) values of polymer **50**. Besides favorable polymer structure design, the extraordinary efficiency of **50**-based solar cells is also attributed to the additional transparent titanium oxide (TiO_x) layer between the metal electrode and the photoactive diode, which not only serves as an electron transport and collecting layer but also stabilizes the whole device because titanium oxide has the ability to protect the polymers from oxygen, water, and photoexcited electrons. By using the TiO_x layer, Heeger et al. reported organic tandem solar cells fabricated by all-solution processing, showing remarkably high efficiencies of up to 6.7%.[176] This result encourages scientist to prognosticate possible efficiencies of 15% organic tandem cells for an optimized material couple.[155]

To further push the absorption of carbazole-containing copolymers into the near-infrared region, as described for the polyfluorene copolymers, 6,7-diphenyl-4,9-bis(thiophene-2-yl)[1,2,5]thiadiazolo[3,4-*g*]quinoxaline repeat units were also introduced into polycarbazoles.[177] In the film, the absorption maxima of polymers **54**−**56** are 773, 772, and 867 nm, respectively (Chart 13). In particular, polymer **56** absorbs light up to 1200 nm and displays an optical energy gap of 1.1 eV. However, the strong absorption in the visible and near-infrared region of these three polymers did not help them to achieve reasonable photovoltaic performance in solar cell devices. Using a 1:1 blend of **56** and PCBM as the active layer yields devices with a V_{oc} of 0.41 V, an I_{sc} of 5.16 mA cm^{-2}, a FF of 0.29, and a power conversion efficiency of 0.61%. The relatively small energy difference between the HOMO level of polymer **56** (4.8 eV) and the LUMO level of PCBM (3.8−4.3 eV) resulted in the low open circuit voltage. The LUMO values of these three polymers are located at about −3.8 eV, which is very close to the LUMO

Chart 13. Chemical Structures of Thiadiazoloquinoxanline-Containing PC Copolymers 54−56

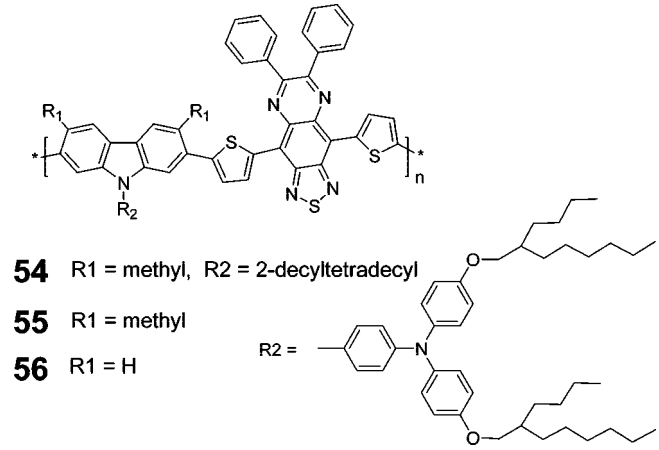

level of PCBM. This suggests a weak driving force for electron transfer from polymers to PCBM; therefore, to obtain a higher power efficiency, another acceptor with a lower lying LUMO level has to be used.

As an alternative to using benzothiadiazole and its derivatives as acceptor motifs in low-band-gap polymers, recently, diketopyrrolopyrrole[178,179] (DPP) was introduced into carbazole-containing copolymers. Winnewisser et al. reported a low-band-gap donor−acceptor copolymer (poly[3,6-bis(4′-dodecyl[2,2′]bithiophenyl-5-yl)-2,5-bis(2-hexyldecyl)-2,5-dihydropyrrolo[3,4]pyrrole-1,4-dione]) containing thiophene (electron-rich unit) and DDP (electron-deficient) units that exhibited excellent ambipolar charge transport properties.[180] Mobilities up to 0.1 cm^2 V^{-1} s^{-1} for holes and up to 0.09 cm^2 V^{-1} s^{-1} for electrons were obtained in OFETs. Meanwhile, Janssen and co-workers used a similar polymer (**57**; Chart 14) for solar cell purposes where the polymer was processed from a mixture of chloroform and *ortho*-dichlorobenzene and blended with [70]PCBM.[181] Under this procedure, the power conversion of the solar cells reached 4%. Based on this promising result, polymer **58** was then designed and synthesized.[182] Polymer **58** shows the combination of a high glass transition temperature, good solubility, relatively high molecular weight, and air stability. Preliminary results on the photovoltaic device based on the **58**:PCBM bulk heterojunction stated a power conversion efficiency of 1.6%. Quite recently, Hashimoto et al. optimized the structure of compound **58** by varying the alkyl

Chart 14. Chemical Structures of Diketopyrrolopyrrole-Containing Poythiophene, Polyfluorene, and Polycarbazole Copolymers 57−61

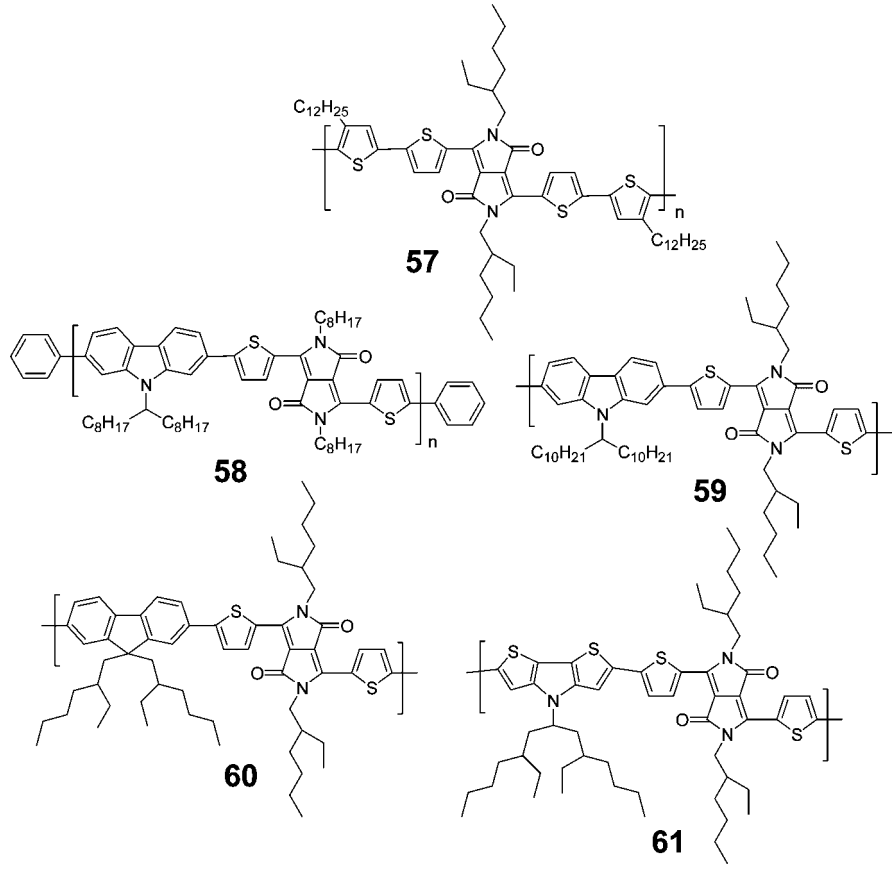

Table 2. Optical, Electrochemical, and Photovoltaic Properties of Polymers 59−61

polymer	λ_{max}[a]	band gap[b]	device materials (w:w)	V_{oc}[c] (V)	I_{sc}[c] (mA cm^{-2})	FF[c]	PCE[c] (%)
59	676 nm	1.69 eV	**59**:PCBM (1:2)	0.76	5.35	0.56	2.26
60	654 nm	1.78 eV	**60**:PCBM (1:2)	0.74	2.51	0.47	0.88
61	852 nm	1.38 eV	**61**:PCBM (1:3)	0.44	4.47	0.57	1.22

[a] Absorption maxima in film. [b] The band gaps are calculated by cyclic voltammetry (CV). [c] The photovoltaic performance is measured under the illumination of AM 1.5G, 100 mW cm^{-2}.

substituents to obtain the new polymer **59**. Together with **59**, they reported two other DPP-based copolymers where the carbazole unit is replaced by fluorene (for **60**) and dithieno[3,2-*b*;2′,3′-*d*]pyrrole (for **61**).[183] From the photovoltaic results of all these three polymers, it is clear that carbazole-based polymer **59** delivers the best performance, which is due to the high current (5.35 mA cm^{-2}) (see Table 2). However, in direct comparison with polymers **59**−**61**, the solar cells based on **57** and PCBM showed the best performance with a short current of 9.4 mA cm^{-2}, an open circuit voltage of 0.63 V, and a fill factor of 0.54, resulting in a power conversion efficiency of 3.2% in this study, when the device is fabricated via the chloroform and *o*-dichlorobenzene solution.[181] Interestingly, the absorption spectrum of **57** in chloroform is dominated by an absorption band at 650 nm. In *o*-dichlorobenzene, however, the polymer has a strong tendency to aggregate (forming a suspension), even at low concentrations. This can be exemplified by a significant shift of the onset of absorption from 720 to 860 nm and the appearance of a vibronic fine structure. Therefore, the photovoltaic performance of **57** can be largely improved by changing the casting solvent from chloroform to *o*-dichlorobenzene and further to the mixture thereof, yielding overall efficiencies of 1.1, 2.9, and 3.2%, respectively. The results indicated that polymers **58**−**61** still have the possibility to show improved device results if a favorable solvent can be found.

Compared to fluorene, carbazole can afford a stronger electron-donating effect; therefore, in combination with strong acceptor groups, the carbazole-based donor−acceptor copolymers can have absorption maxima even in the near-infrared region. Also, the N atom in carbazole can be functionalized by aliphatic or aromatic groups which can improve the solubility of the entire polymer. However, in photovoltaic materials, as seen in the best fluorene-based polymers, the best polycarbazoles also have thiophene units. Polycarbazole copolymer **50**, when compared to the structurally similar polyfluorene copolymer **25** (acceptor is benzothiadiazole for **50** and quinoxaline for **25**), shows a much better photovoltaic performance with power conversion efficiencies up to 6%. The monomer structure of **25** is fluorene−thiophene−acceptor−thiophene, and in the case of **50**, it is carbazole−thiophene−acceptor−thiophene. Although the key units for high photovoltaic performance remain thiophene and the acceptor groups, both fluorene and carbazole improve the polymers' solubility and in the right combination could offer the optimal band offset (for example, compound **50**).

Chart 15. Chemical Structure of Thiophene−Benzothiadiazole−Thiophene-Containing PD Copolymer 62

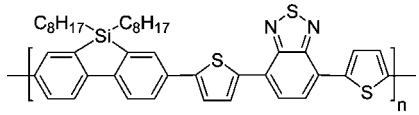

62

2.1.4. Polydibenzosiloles (PD)

The stability of polydibenzosilole has been described as being better than that of polyfluorene in terms of photoluminescence. In the case of polyfluorene, it can form fluorenone due to oxidation and result in a longer wavelength emission (around 530 nm). Additionally, similar to fluorene, two functional groups can be introduced in the 9-position of dibenzosilole, which can largely improve the solubility of polymeric dibenzosilole. Despite these promising features, only a few copolymers that contain silicon atoms have been investigated in organic solar cells. Regarding the outstanding photovoltaic results of the 4,7-dithien-2-yl-2,1,3-benzothiadiazole containing polyfluorene and polycarbazole copolymers, Leclerc, Cao, and their co-workers successfully introduced the polydibenzosilole copolymer **62** (Chart 15) into solar cells.[184,185] A power conversion efficiency of up to 5.4% was observed from solar cells in the structure of ITO/PEDOT:PSS/**62**:PCBM/Al with a V_{oc} of 0.90 V, an I_{sc} of 9.5 mA cm^{-2}, and a FF of 0.51.

Obviously, the structure design of polymer **62** is still the same as that for polymers **25** and **50**. Its monomer is dibenzosiloles−thiophene−acceptor−thiophene, which again supports the effectiveness of the thiophene−acceptor−thiophene block. Various chromophores providing solubilizing groups can be impregnated into this structure, resulting in efficient photovoltaic materials. Meanwhile, for polyphenylenes, the improvement of their absorption is the most promising pathway for reaching high efficiency. Therefore, ladder-type polyphenylene will be an alternative choice for enhancing the light-harvesting of polymers.

2.1.5. Ladder-Type Polyphenylene

Ladder-type oligophenylenes can absorb more radiation in the visible region than normal nonplanar oligophenylenes, obviously important when discussing photovoltaics. A ladder-type polyphenylene homopolymer, where the monomers are ladder-type oligophenylene-containing carbazole or fluorene moieties to enhance the polymer properties, has been reported.[186−190] In order to tune the length of the oligophenylenes and the content of the nitrogen atoms in the monomers, three different ladder-type polymers **63**−**65** (Chart 16) were synthesized and characterized in solar cells.[161,163] Cyclic voltammetry indicated that the redox behavior of polymers **63**−**65** in thin films revealed two oxidation peaks. Polymer **63**, which has the largest density of electron-rich nitrogen in the backbone, shows the highest HOMO level (−5.40 eV) and, hence, is the strongest electron donor among these three compounds, whereas **63**, with the shortest conjugation unit, possesses the lowest HOMO level (−5.54 eV). The band gaps were calculated from the UV spectra, allowing the estimation of the LUMO levels (the LUMO levels of **63**−**65** are −2.82, −2.76, and −2.78 eV, respectively). These values lead to a larger potential difference in HOMO (D)−LUMO (A) than for P3HT, when considering PCBM as the acceptor. Since the difference between the HOMO of the donor and the LUMO of the acceptor can approximately determine the open circuit voltage, a higher V_{oc} is expected for devices based on the ladder-type polymers **63**−**65** than for those based on P3HT and PPV. The typical V_{oc} of these ladder-type polymer:PCBM devices was in the range 0.9−1.0 V, much higher than that reported for P3HT:PCBM (0.6 V) or PPV:PCBM cells (0.8 V). This is in accordance with the HOMO of P3HT (−5.2 eV) or PPV (−5.1 eV), being higher than the HOMO of polymers **63**−**65** (−5.40, −5.46, and −5.54 eV, respectively). However, the photocurrent of devices based on polymers **63**−**65** was lower than that of P3HT-based devices, due to the absorption at longer wavelength of P3HT resulting in higher light-harvesting efficiency. Of these three polymers mentioned above (Figure 13), **65** exhibited the best photovoltaic performance with an I_{sc} of 0.23 mA cm^{-2}, a V_{oc} of 0.95 V, and a FF of 0.54, yielding 0.74% efficiency (under 15 mW cm^{-2} sunlight intensity). The low power efficiency is due to the poor absorption in the visible and IR range of these polymers (the absorption maxima of **63**−**65** are only in the region between 400 and 500 nm). This can also be confirmed by the IPCE spectra of these polymer-based devices, as seen in Figure 13. Additionally, the IPCE value is quite low, 10%, which can either result from poor absorption or poor charge generation. The tuning of the absorption to harvest more of the solar energy without altering the HOMO level is a way to a considerably enhanced the efficiency.

Chart 16. Chemical Structures of Ladder-Type Polyphenylenes 63−65

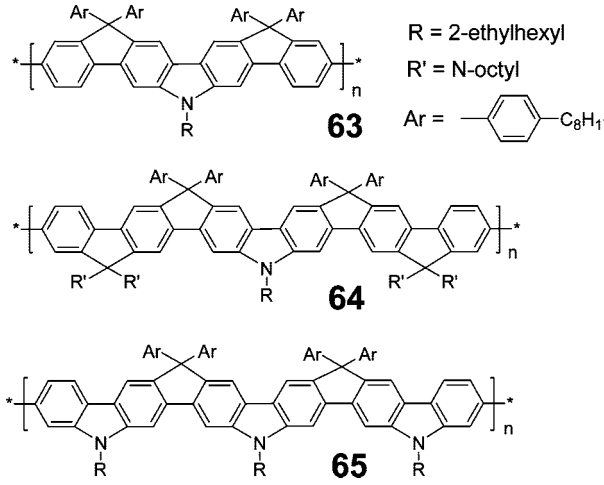

63 **64** **65**

To obtain a broad and bathochromically shifted absorption of ladder-type oligophenylenes, a benzothiadiazole-cored thiophene moiety was introduced into an indolo[3,2-*b*]carbazole unit, which was reported by Tao et al.[191] In the chloroform solution of polymer **66** (Chart 17), a broad and structureless absorption peak at 538 nm, corresponding to the intramolecular charge transfer (ICT) transition, together with a strong absorption band at shorter wavelength (395 nm) could be detected. In comparison to the solution spectrum, **66** showed a significant red shift of about 100 nm of the absorption edge in a thin film. With a device structure of ITO/PEDOT:PSS/**66**:PCBM/LiF/Al, **66**-based solar cells exhibited a 3.6% power conversion efficiency under AM 1.5 simulated solar illumination.

To further simplify the synthesis of ladder-type oligophenylene copolymers, Chen and his co-workers reported a series of donor−acceptor copolymers based on indolo[3,2-*b*]carbazole and thienopyrazine (see **67**, **69**, and **72**), benzothia-

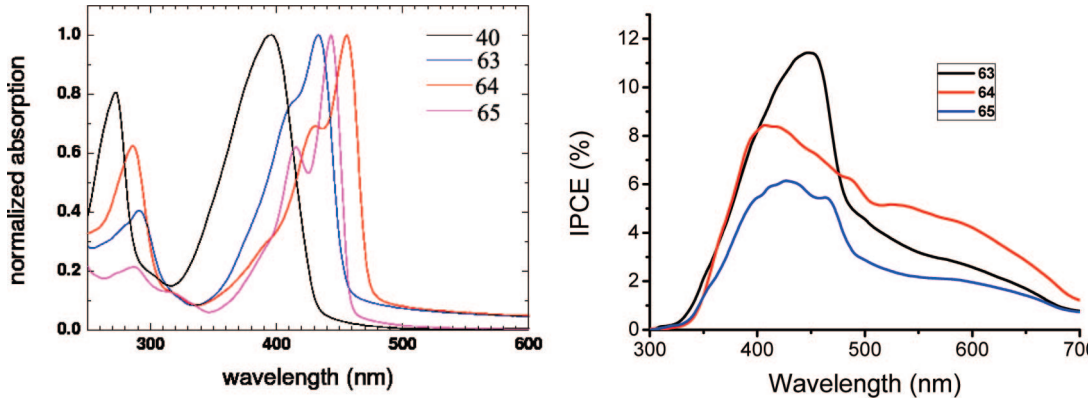

Figure 13. UV−vis spectra of polymers **40** and **63**−**65** in thin films. (left). IPCE spectra of polymer 63−65:PCBM (1:4)-based solar cells (right).

Chart 17. Chemical Structures of Ladder-Type Oligophenylene Copolymers 66−72

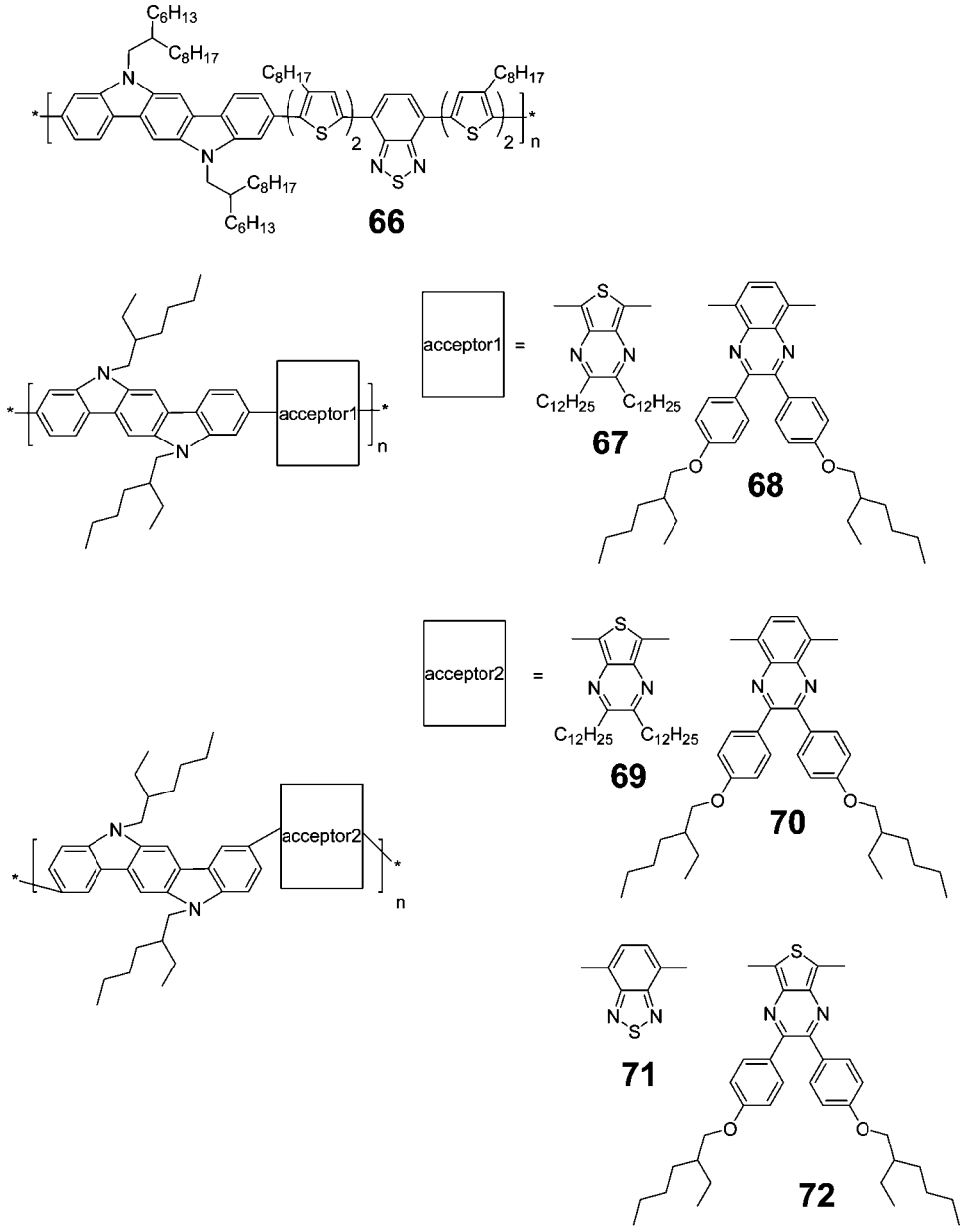

diazole (for polymer **71**), and quinoxaline (for polymers **68** and **70**).[192] The polymers were synthesized by the Suzuki coupling reactions. All absorption spectra of these copolymers have two distinct peaks: one in the wavelength range 420−800 nm and another peak in the wavelength range 320−420 nm. Of these polymers, **72** has the longest absorption maximum at 660 nm in a film, corresponding to the smallest band gap of 1.58 eV. Polymer **68**, on the other

Chart 18. Chemical Structures of *p*-Phenylenevinylene-Containing Sensitizers 73−75

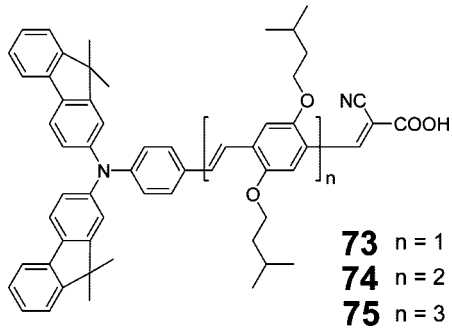

hand, possesses a λ_{max} at only 445 nm and a band gap of 2.34 eV in the film. The bulk heterojunction solar cells based on polymers **67**−**72** were fabricated with a structure of ITO/PEDOT:PSS/polymer **67**−**72**:PCBM/Ca/Al. The power conversion efficiencies of the corresponding polymer:PCBM-based devices were 0.66, 0.32, 0.22, 0.87, 0.49, and 0.14%, respectively. Polymer **66**, which possesses two additional thiophenes in the repeating unit, gives much higher efficiency than these more direct D−A systems. Obviously, the thiophene moieties are very important in conjugated polymers to achieve efficient solar cells.

Ladder-type polyphenylene is the last example listed here which can be used for polymer solar cells. A clear trend can be observed, that the best polyphenylenes, e.g. polyfluorenes, polycarbazoles, and polydibenzosiloles, as well as ladder-type polyphenylenes, all contain thiophene−acceptor−thiophene units. Thiophene has a higher oxidation potential than benzene, which makes thiophene a favorable candidate for tuning the energy levels of polymers. To achieve lower band gap polymers, thiophene groups are very important. Moreover, the band gap of polymers can be further decreased by incorporating additional acceptor groups. In general, phenylene or oligophenylene units in polymers enable a fine-tuning of energy levels and also a significant improvement of polymer solubility.

2.1.6. Oligophenylenes and Ladder-Type Oligophenylenes

Oligophenylene or ladder-type oligophenylene monomers normally have very narrow absorption bands in the blue region.[103,187] In order to tune their color into the red spectral region, the introduction of donor and acceptor groups at either end of oligophenylenes provides an alternative method to polymerization. Donor−π-conjugated bridge−acceptor (D-π-A) compounds have to be considered for dye-sensitized solar cells, since they display broad and intense absorption features and have been developed into a very promising classes of organic sensitizers.[193−196] Obviously, oligophenylenes and ladder-type oligophenylenes can also act as π-spacers. With anchoring groups such as carboxylic acids, donor−acceptor functionalized oligophenylenes are excellent candidates for dye-sensitized solar cells.

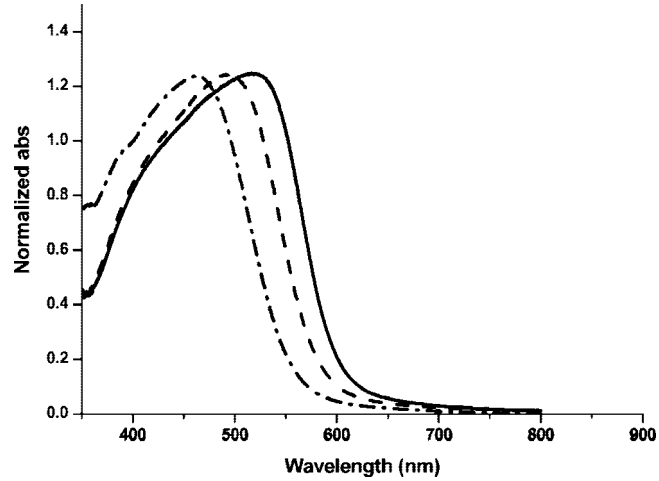

Figure 14. UV−vis absorption spectra of dyes **73** (dash dotted line), **74** (dashed line), and **75** (solid line) adsorbed on TiO_2 film. Adapted with permission from ref 196. Copyright 2008 American Chemical Society.

Regarding the outstanding photovoltaic performance of polyphenylenevinylene and its derivatives shown in polymer solar cells,[114,115] the oligo(*p*-phenylenevinylene)s have also been used as bridges between donor and acceptor groups. Ko and co-workers have reported oligophenylenevinylenes **73**−**75** (Chart 18) which were functionalized with bis(9,9-dimethyl-9H-fluoren-2-yl)amine groups (D) and cyanoacrylic acid units (A).[197] The absorption maxima showed bathochromic shifts in the following order: **75** (λ_{max} = 472 nm) > **74** (λ_{max} = 466 nm) > **73** (λ_{max} = 457 nm). The λ_{max} shifts to longer wavelengths with increasing number of phenylenevinylene components, and the power conversion efficiency was also shown to be sensitive to the length of the bridge (Table 3). PCE values of 5.34 and 6.89% were obtained for devices with **73** and **74** (each single device contained a 4 μm thick TiO_2 scattering layer and a 10 μm thick TiO_2 transparent layer and an electrolyte containing 0.6 M 3-hexyl-1,2-dimethyl imidazolium iodide, 0.05 M I_2, 0.1 M LiI, and 0.5 M *tert*-butylpyridine in acetonitrile). Under the same test conditions, the **75**-sensitized solar cell gave a PCE of 7.02%. The PCE difference among **73**−**75**-based solar cells was mainly due to the difference in current (the I_{sc} values of compounds **73**−**75**-based solar cells were 10.50, 13.26, and 14.26 mA cm^{-2}, respectively). Additionally, these results can be attributed to their different absorption properties on TiO_2 (Figure 14). Compound **75** has the broadest absorption band among all these three dyes, which renders it with the best light-harvesting properties, resulting in the highest power conversion efficiency in DSCs.

Ho and Lin et al. reported D-π-A sensitizers which contained fluorene as a spacer. A DSC based on **76** (Chart 19) showed a PCE value of 5.23% with I_{sc} = 12.9 mA cm^{-2}, V_{oc} = 710 mV, and FF = 0.74.[198] The PCE values of compounds **76**−**80** were 2.86, 3.35, 3.89, and 3.80%, respectively. Interestingly, it was found here that the ef-

Table 3. Optical and Redox Properties as Well as Photovoltaic Performance of Sensitizers 73−75

dye	λ_{max} (nm)[a]	ε (M^{-1} cm^{-1})[a]	E_{ox} (V)[b]	E_{0-0} (V)[c]	I_{sc} (mA cm^{-2})	V_{oc} (V)	FF	PCE (%)[d]
73	457	38650	1.13	2.41	10.50	0.69	0.73	5.34
74	466	70056	1.13	2.38	13.26	0.73	0.71	6.89
75	472	68390	1.09	2.38	14.26	0.70	0.70	7.02

[a] In THF solution. [b] On TiO_2, measured in THF with 0.1 M (n-C_4H_9)$_4$NPF$_6$ with a scan rate of 50 mV s^{-1} (vs NHE). [c] Determined from intersection of absorption and emission spectra in THF. [d] Measured under the illumination of AM 1.5G, 100 mW cm^{-2}.

Chart 19. Chemical Structures of Fluorene-Containing Sensitizers 76−80

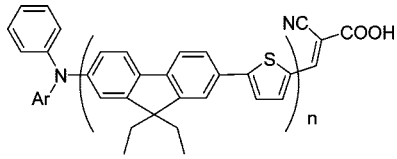

76 Ar = 1-naphthyl, n = 1
77 Ar = 9-anthracenyl, n = 1
78 Ar = 1-pyrenyl, n = 1
79 Ar = 1-naphthyl, n = 2
80 Ar = 1-naphthyl, n = 3

ficiency decreased with increasing spacer length. Additionally, dyes **76**, **79**, and **80** exhibited similar absorption maxima at 421, 423, and 423 nm, respectively, but their emission maxima showed a decreasing trend at 538, 512, and 472 nm, respectively. The longer π-conjugated spacer weakens the interaction between the donor and acceptor groups, resulting in a lower photocurrent of the devices. The short circuit currents of **76**, **79**, and **80** sensitized solar cells were 12.47, 9.83, and 9.81 mA cm^{-2}, respectively. A longer spacer, therefore, does not always equal better performance. In the parent case, the longer π-spacer only improves the dye's absorption coefficient but does not shift the absorption maxima. The change in size most likely alters the dye loading properties on the TiO_2 surface as well as the photovoltaic performance.

Compared to fluorene, the electronic effect of a bridging nitrogen atom makes carbazole a better hole acceptor. The carbazole unit is therefore often used as the donor part in D-π-A-type sensitizers. Many carbazole-based sensitizers have been reported during the last several years.[199−203] Analyzing the structure of these sensitizers **81**−**97** (Chart 20), it can be observed that all compounds possess thiophenes or oligothiophenes as π-spacers. The best photovoltaic performance among them was achieved by the solar cell devices based on compound **88**, which contains three thiophenes. Under AM 1.5G irradiation, a compound **88**-sensitized solar cell exhibited a short current of 16.0 mA cm^{-2}, an open circuit voltage of 0.71 V, a fill factor of 0.71, and an overall power efficiency of 8.1%.[202]

Besides using carbazoles as donor substituents in D-π-A sensitizer systems, Koumura, Hara, and their co-workers also reported indolo[3,2-*b*]carbazole donor groups.[204] Using the same molecular design principle as in carbazole-based sensitizers, they synthesized compounds **98** and **99** (Chart 21), which also have thiophene spacers. Both **98**- and **99**-sensitized solar cells showed good stability under a long time visible-light irradiation as well as high photovoltaic performance with 7.3 and 6.7% overall power conversion efficiencies, respectively, under standard AM 1.5G irradiation. When

Chart 20. Chemical Structures of Carbazole-Containing Sensitizers 81−97

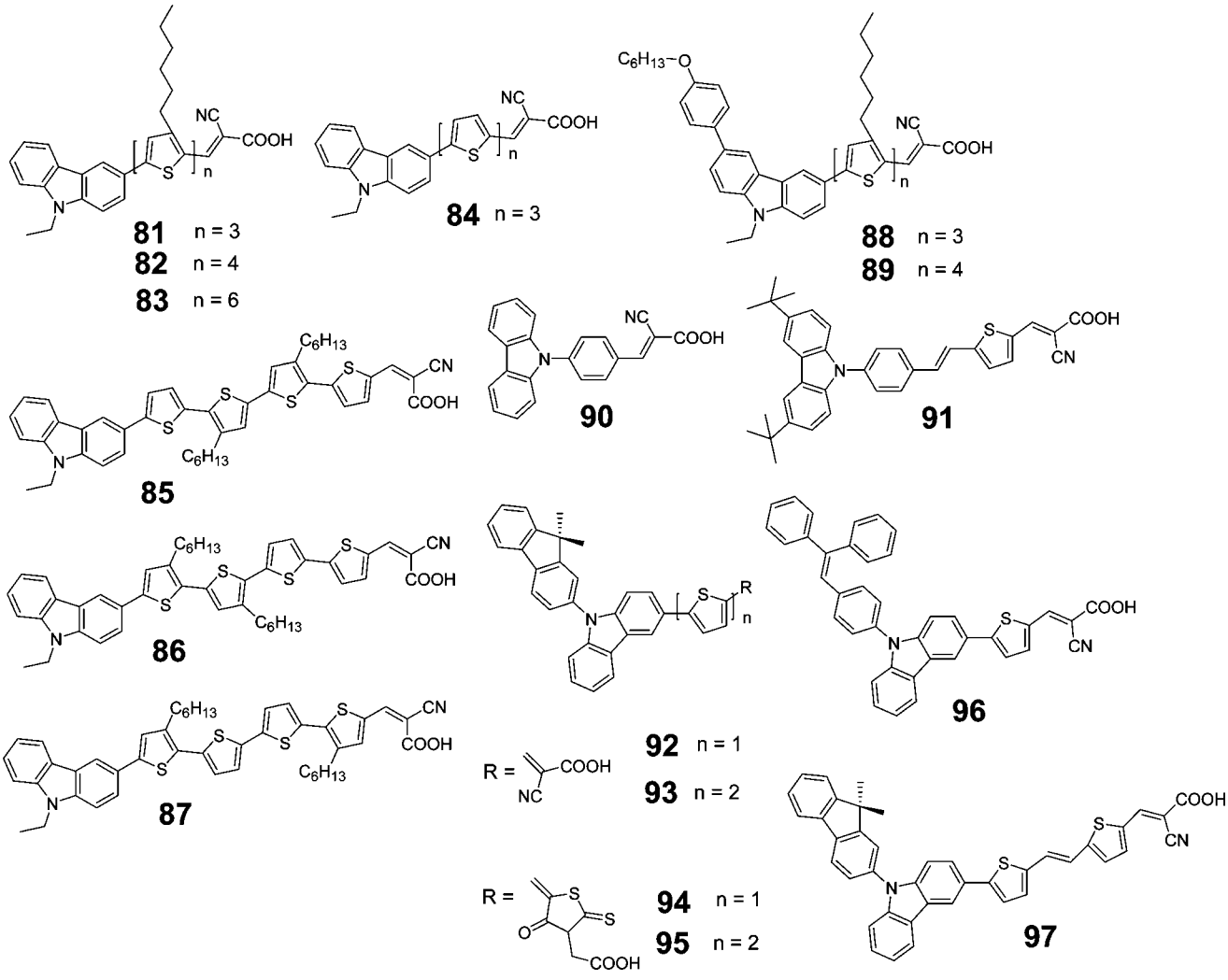

81 n = 3
82 n = 4
83 n = 6
84 n = 3
85
86
87
88 n = 3
89 n = 4
90
91
92 n = 1
93 n = 2
94 n = 1
95 n = 2
96
97

Chart 21. Chemical Structures of Indolocarbazole-Containing Sensitizers 98 and 99

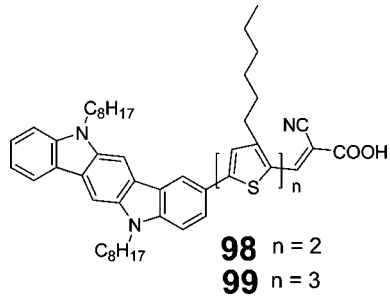

Chart 22. Chemical Structures of Ladder-Type Pentaphenylene-Containing Sensitizers 100−102

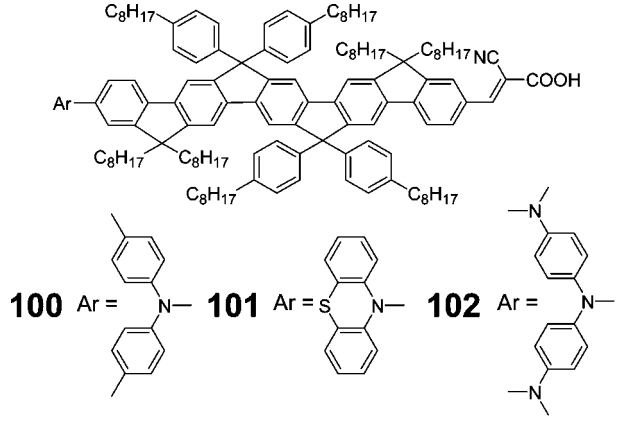

introduced into a similar donor-π-acceptor structure, the electron donating ability of the indolo[3,2-*b*]carbazole unit is stronger than that of carbazole. Increasing the number of thiophene units can further extend the π-conjugation and increase the short circuit photocurrent (15.4 mA cm^{-2} for **98**, 15.5 mA cm^{-2} for **99**), as the result of the red-shifted absorption of the sensitizer loaded TiO_2 film. These results indicate that the application of indolo[3,2-*b*]carbazole as donor moiety into sensitizers for DSCs is very promising.

Recently, ladder-type D-π-A sensitizers with pentaphenylene structures were reported by our group.[205] These three ladder-type pentaphenylene-containing dyes **100**−**102** (Chart 22) possess the same acceptor/anchor group (2-cyanoacrylic acid) and the same π-spacer (ladder-type pentaphenylene) but different donor functionalities (diphenylamino **100**, phenothiazinyl **101**, and bis(*N*,*N*-4-dimethylaminophenyl)-amino **102**). The maximum absorption peaks of the three dyes range from 442 to 457 nm with high absorption coefficients up to 75600 M^{-1} cm^{-1}. The efficiency of these dye-based solar cells, however, was only around 2.3% (corresponding to an I_{sc} of 8.57 mA cm^{-2}, a V_{oc} of 0.52 V, and a FF of 0.52) in DSCs, with the low current a result of the short wavelength absorption of the dye (mainly in the blue region) (Figure 15a). Nevertheless, compared to the absorption spectra on TiO_2, the action spectra of these dyes-sensitized solar cells exhibit much broader bands (Figure 15b). For example, the absorption onset of **100** is around 520 nm, but the corresponding device displays an IPCE onset up to 650 nm, helping compound **100** achieve a moderate PCE value. This molecular structure opens up the possibility of sensitizers based on long π-spacer bridged donors and acceptors. Future work will focus on improved absorption behavior of such dyes.

Highly efficient sensitizers such as oligophenylenevinylene **75** have been prepared using a phenylene core. One can also observe in DSCs that thiophene is an important building unit for highly efficient devices. By using thiophenes or oligothiophenes as π-spacers, the sensitizers typically exhibit better photovoltaic performance than those sensitizers which do not include thiophene units. Therefore, in the 1D polyphenylene world, the introduction of a thiophene moiety seems advantageous in order to achieve high performance photovoltaic materials.

2.2. Two Dimensional Polyphenylenes

In two-dimensional benzene chemistry, graphene is a one-atom-thick planar sheet, composed of sp^2-carbons. Considering the hexagonal-extension of benzene, a graphene sheet can be considered as an infinitely large polycyclic aromatic hydrocarbon (PAH).[26,27,206] In the solid-state, graphenes are densely packed in a honeycomb crystal lattice, which has attracted many scientists to use them as key components in organic electronic devices.[207−214] On the other hand, tightly packed PAH molecules considered as small subunits raised interest in the investigation of their charge mobilities and suitability as donors in photovoltaics. In 1994, Haarer et al. investigated the liquid crystal property of 2,3,6,7,10-hexahexylthiotriphenylene (**103**).[215] This molecule is capable of forming discotic columnar phases resulting in hole mobilities up to 0.1 cm^2 V^{-1} s^{-1}. Since then, solution processable PAHs have become very promising candidates for achieving high performance devices. In the last two decades, our group has developed many large PAH compounds with solubilizing side groups.[216−220] Due to their outstanding solubility, hexa(alkylphenyl)-substituted hexabenzocoronene (**104**) can be mixed

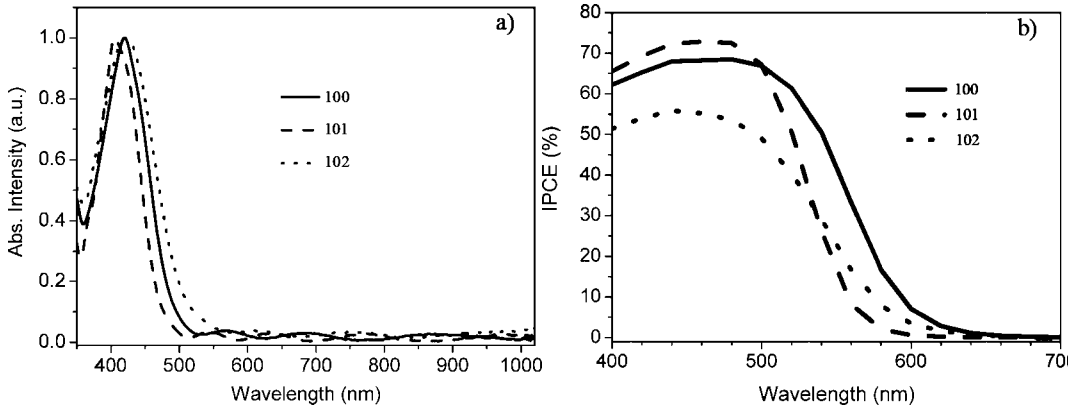

Figure 15. (a) Absorption spectra of compounds **101**−**102** on TiO_2 film; (b) IPCE spectra of **101**−**102**-sensitized solar cells.

Chart 23. Chemical Structures of 2D Polycyclic Aromatic Hydrocarbon-Based Compounds 103−108

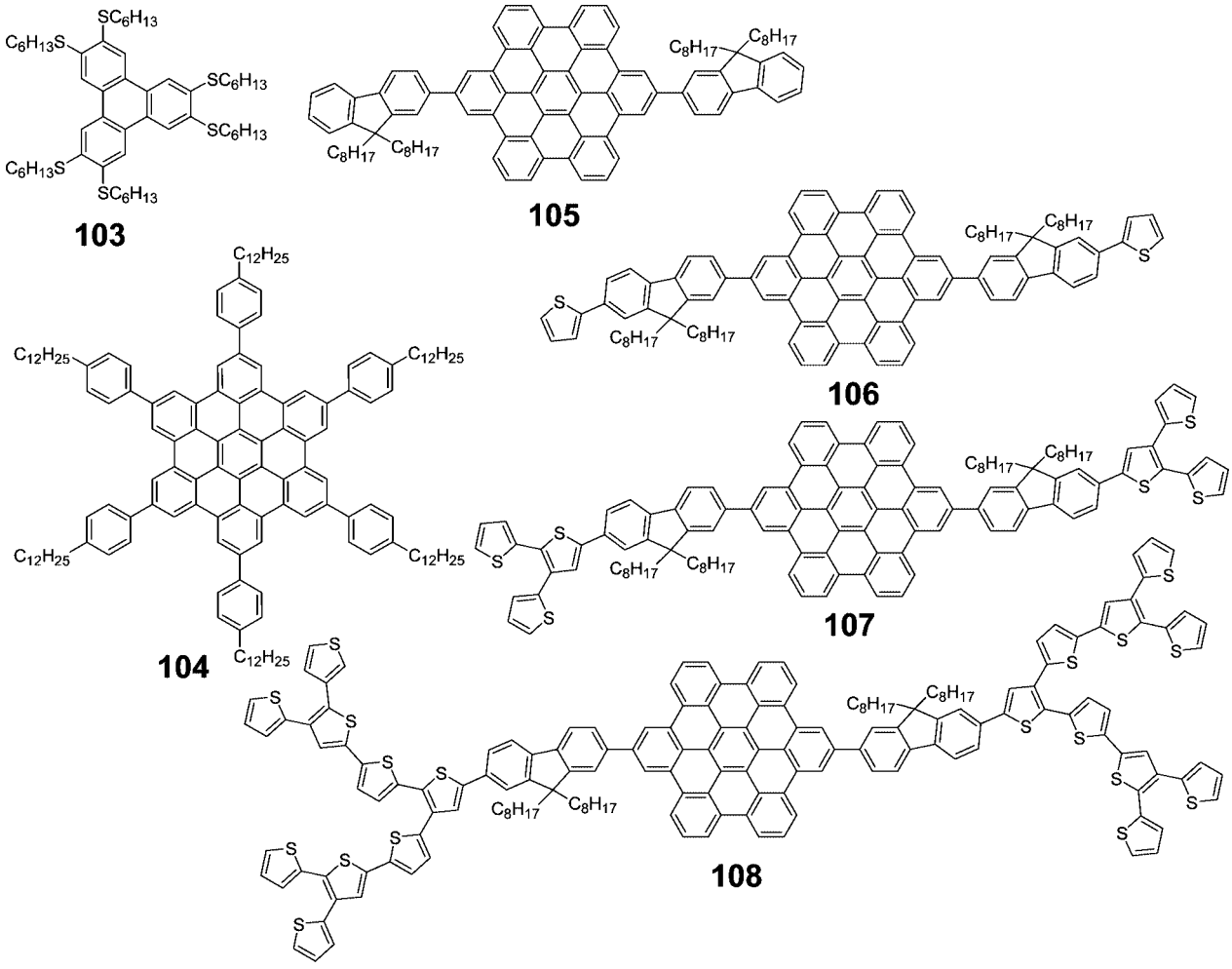

with (*N*,*N*′-bis(1-ethylpropyl)-3,4:9,10-perylenediimide) (**41**) in chloroform.[18] Blends of **104** and **41** (with a weight distribution ratio of 40:60) were spin-coated on ITO substrates and produced thin films with vertically segregated domains with a large interfacial surface area. When using Al as counter electrodes, the sandwiched **104**:**41** photodiodes exhibited an IPCE of 34% at 490 nm. This result demonstrated that efficient exciton generation and dissociation was achieved using these components. Under monochromatic illumination at 490 nm (0.47 mW cm^{-2}), the solar cell containing **104**:**40** exhibited a power conversion efficiency of 1.95% with a short circuit current of 33.5 μA cm^{-2}, an open circuit voltage of 0.69 V, and a fill factor of 40%. The photovoltaic performance of these devices under standard solar irradiation, however, was limited by the weak absorption in the visible and NIR region of **104**.

In order to achieve higher photocurrents and power conversion efficiencies from polycyclic aromatic hydrocarbons, fluorene and thiophene units were attached to the periphery of hexabenzocoronenes.[221] The resulting compounds **105**−**108** (Chart 23) exhibited greatly improved absorption into the visible range (Figure 16). Among these dyes, **108**-based solar cells have shown the most promising photovoltaic performance with a PCE of 1.5% in [60]PCBM contained solar cells and a PCE of 2.5% with devices using [70]PCBM as acceptor.

Another two-dimensional extension of benzene is represented in rylene chromophores. Rylenes are based on naphthalene units linked in the *peri*-position (Chart 24) and can also be called poly(*peri*-naphthalene) (PPN), regarding the repeating naphthalene units as a polymer. These oligonaphthalenes have distinct names: perylene ($n = 2$), terrlyene ($n = 3$), quaterrylene ($n = 4$), pentarylene ($n = 5$), and hexarylene ($n = 6$).[222,223] The nomenclature is described in Chart 24. Since rylenes are active in the *peri* positions, it was found that they can be further stabilized and achieve red-shifted absorption by transformation into their diimide derivatives. In this class of dyes, the most important representatives are the perylene-3,4:9,10-tetracarboxydimides (PDIs). These are highly fluorescent and widely used dyes and pigments, showing very promising properties in a variety of applications due to their outstanding chemical, thermal,

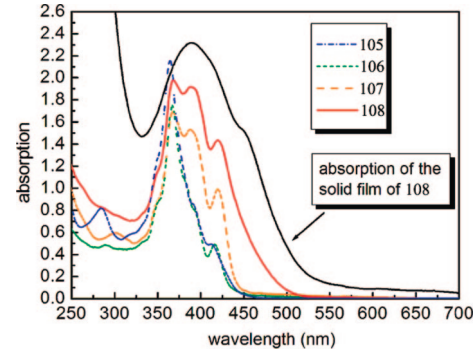

Figure 16. UV−vis absorption spectra of compounds **105**−**108** in dichloromethane and the UV−vis absorption spectrum of a solid film of **108**. Adapted with permission from ref 221. Copyright 2009 American Chemical Society.

Chart 24. Poly(*peri*-naphthalene), Perylene, and Rylenediimides

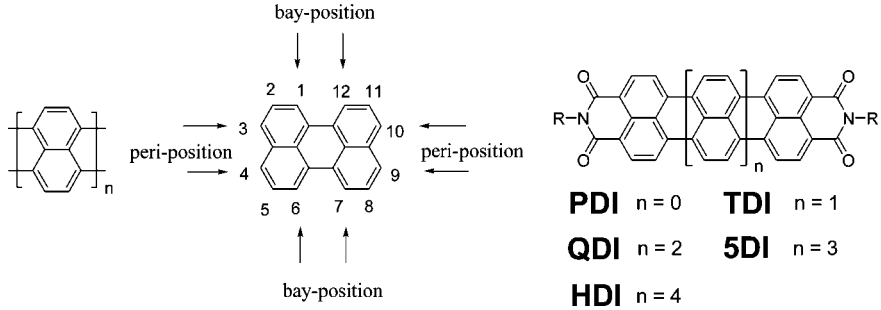

and photochemical stability.[224−226] They are applied technically in the fields of paints and lacquers, particularly in the car industry. Furthermore, they can be used as key chromophores for high-tech applications such as reprographic processes,[227] fluorescent solar collectors,[228] optical switches,[229] and dye lasers.[230] Since PDI derivatives also possess high electron mobilities,[231] Friend[18] and Gregg[232] have fabricated high-efficiency organic photovoltaic devices, using blends of electron-accepting PDIs and hole-accepting small molecules or polymer-PDI blends, respectively.

Extending the framework of rylenediimides via an additional naphthalene moiety along the molecular long axis does not only lead to a bathochromic shift but also increases the absorption coefficients, which is very important for highly efficient light absorption (Figure 17).[233] Extending the PDI via one naphthalene unit results in terrylenediimide (TDI).[234,235] The next higher homologue in the series of rylenediimides is the quaterrylenediimide (QDI).[236−238] Furthermore, our group developed a synthesis for the higher derivatives, pentarylenediimide (5DI), hexarylenediimide (HDI), heptarylenediimide (7DI), and octarylenediimide (8DI) and their derivatives.[239−243] PDI has a brilliant red color (abs. max. 550 nm), while 8DI is completely colorless in solution and exhibits an absorption maximum at 1066 nm.[240] Such high absorption coefficients are unprecedented for organic NIR-dyes, thus qualifying rylene dyes as excellent candidates for solar cell applications.

2.2.1. Rylene Dyes for Flat-Heterojunction Solar Cells

In the rylene family, the exploitation of perylene dyes for organic solar cells can be traced back to the first efficient organic photovoltaic cell fabricated by Tang, where phthalocyanine and perylenedibenzimidazole (**109**; Chart 25) were applied as active materials with a reasonable power conversion efficiency of up to 1%.[13] Their tunable solubilities and

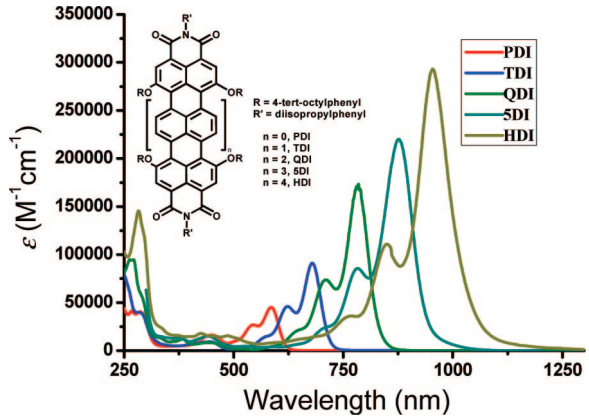

Figure 17. Absorption spectra of rylenediimide dyes.

Chart 25. Chemical Structures of Perylene Derivatives in Flat-Heterojunction Solar Cells

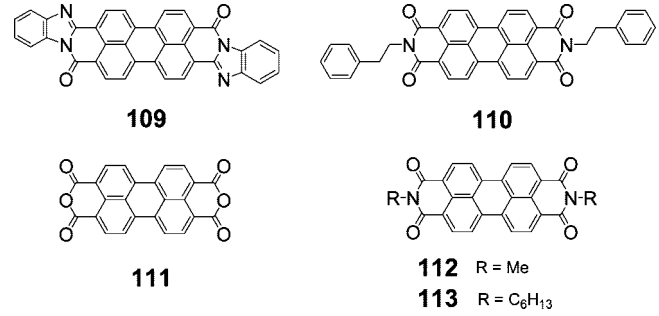

optical and electrochemical properties make perylene dyes available for all kinds of organic solar cells. Because of their outstanding π-conjugated planar structure with two imide or amidine groups, perylene compounds have high electron affinities and can thus accept electrons from most donor compounds. As mentioned before, soluble perylene dyes have been widely used in solution processable polymer solar cells, while perylene pigments can be employed in flat-heterojunction solar cells via sublimation. A vast number of studies have been devoted to improving photovoltaic performance by introducing different derivatives of perylenes (**109**−**113**) as electron acceptors and metal phthalocyanines or conjugated polymers as electron donors.[244−253] However, the highest efficiency reported so far for this kind of cell is 2.7%,[38] which is, yet, too low for practical applications.

Most perylene dyes (for example **109**−**113**) used in BHJ solar cells have no substituents in the *bay* positions of perylene. Interestingly, Sharma and Mikroyannidis et al. developed diphenoxylated PDI acceptors for organic solar cells.[254−256] A blend of **114** (Chart 26) with small molecule **115** or polymer **116** exhibited power conversion efficiencies up to 2.85% with a short circuit current of 6.8 mA cm^{-2}, an open circuit voltage of 0.88 V, and a fill factor of 0.47.[254,255] Additionally, the incorporation of a thin annealed ZnO layer between the BHJ of **117** and **118** and the top Al electrode resulted in a PCE of 3.17%.[256] These results opened a new design of perylene-based bichromophores as acceptors in BHJs. The pyrene or anthracene groups in **114** and **117** enable additional intramolecular energy transfer to perylenediimide, on one hand improving the light-harvesting ability of the dye and on the other hand enhancing the communication between the perylene acceptor and the donor compounds in devices.

2.2.2. Rylene Dyes for Bulk-Heterojunction Solar Cells

In bulk-heterojunction solar cells with a donor−acceptor mixture, the charge transport and collection in a disordered nanoscale blend may be hindered by phase boundaries and

Chart 26. Chemical Structures of Perylene Derivatives in Flat-Heterojunction Solar Cells

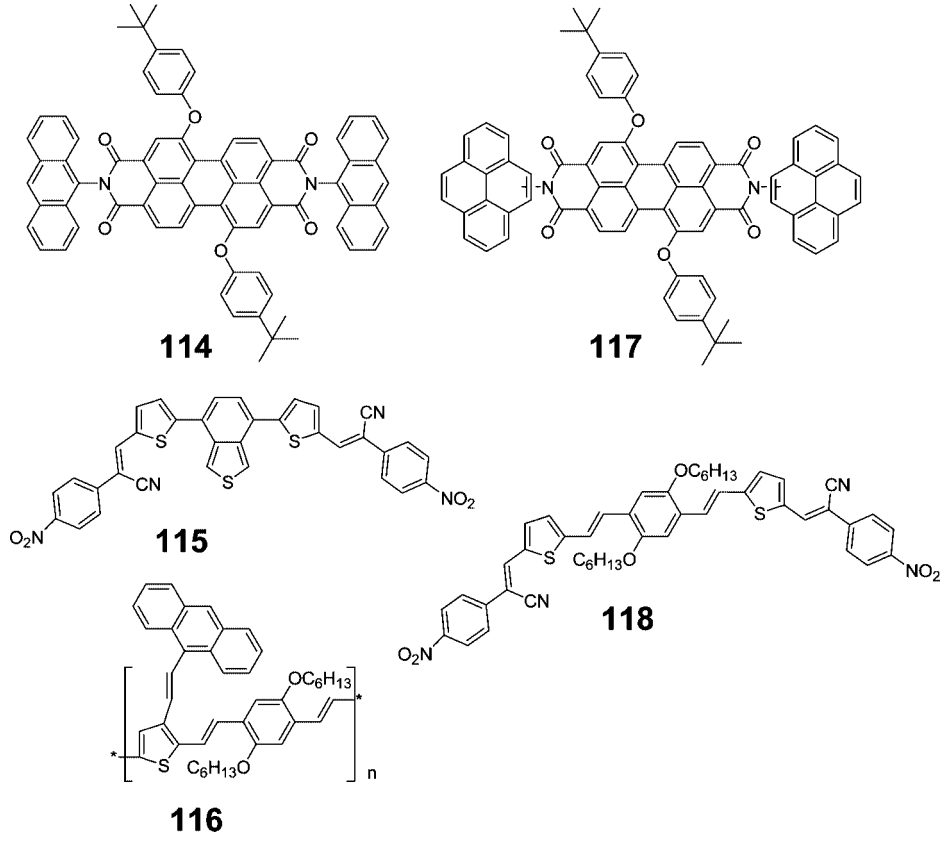

discontinuities. Covalent connection of donor and acceptor in a single polymer or oligomer chain can overcome these drawbacks. Perylene dyes have therefore been linked to other electron-donating groups to form donor−acceptor oligomers or polymers for photovoltaic applications. The intramolecular donor−acceptor combination can enhance the photoinduced energy and electron transfer between donor and acceptor moieties. Therefore, many perylene copolymers have been developed.[257,258] There are three types of covalently linked donor−acceptor polymers: (1) semiconducting polymers as a donor with pendant acceptor groups; (2) alternative (random or regular) donor−acceptor copolymers; and (3) extended donor and acceptor units arranged in diblock copolymers. Because of the strong inter- and intramolecular interactions between donor and acceptor moieties, the latter two strategies may have important advantages. The intrinsic tendency of each segment in block copolymers to aggregate in an individual phase provides a means to create a well-ordered nanoscale morphology.

Bäuerle et al. were the first to report the combination of perylene dyes with structurally defined oligothiophenes.[259−261] They designed and synthesized a series of *N*-(2,6-diisopropylphenyl)perylene-3,4-dicarboximides (perylenemonoimide (PMI), as acceptor) substituted by oligo(3-hexylthiophenes) (as donors) in the 9-position of the perylene core (compounds **119**−**130**; Chart 27). This type of π-donor π-acceptor dyad molecule was to preserve the typical charge transport and self-assembling properties of oligiothiophene in the solid state, whereas the perylene unit should provide high absorptivity in the visible region as well as electron-accepting properties. With increasing oligothiophene length, the intensity of the emission bands and the quantum yields progressively decreased due to the increased intramolecular charge transfer. Excitation at wavelengths corresponding to the oligothiophene absorption resulted in complete fluorescence quenching in the oligothiophene part, and the fluorescent spectra only showed the emission of the perylene compounds. These aspects indicate an energy transfer from the oligothiophene to the perlyene moiety. HOMO/LUMO energies were determined via CV in dichloromethane. It was clearly observed that the HOMO−LUMO band gap decreases with increasing chain length of the oligothiophene unit, which is mainly due to the constant rise of the HOMO energy level as the LUMO level remains more or less unchanged. With the device structure of ITO/PEDOT:PSS/perylene-oligothiophene:PCBM/LiF/Al, these compounds were tested for in solar cells. In the donor−acceptor series, **124** gave the best photovoltaic performance with a V_{oc} of 0.94 V and a power conversion efficiency of 0.48%. With the acceptor−donor−acceptor structure, the solar cells based on **125** exhibited a V_{oc} of 0.68 V and a PCE of 0.2%. The perylene−oligothiophene compound **129** showed a V_{oc} of 0.60 V and a PCE of 0.25% in a solar cell device. From these results it can be concluded that the structural tuning greatly affects the device performance. The compounds showed completely different behaviors with the same perylene and oligothiophene moieties in different combinations. To further improve the structure of the compounds for better photovoltaic performance, more focus should be placed on the perylene moiety, e.g. changing from an isopropylphenyl imide substituent to an alkyl imide in order to enhance the self-organization ability of the whole molecule. As shown here, the best photovoltaic performance of these three structural classes came from the donor−acceptor structure, where the oligothiophenes play a very important role in the film formation, producing the best photovoltaic result. A detailed investigation of the morphology of the devices should help in improving such systems.

Chart 27. Chemical Structures of Thiophene-Containing Perylenemonoimide 119−130

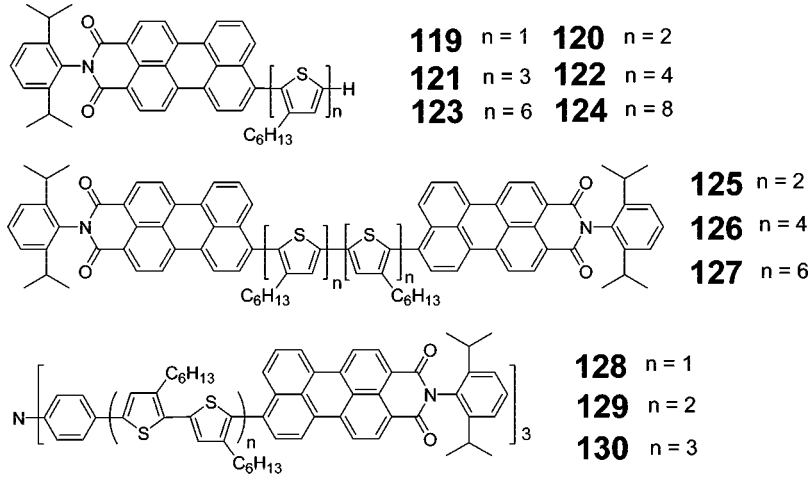

Chart 28. Chemical Structures of Oligophenylenevinylene-Perylenediimide Copolymers 131−132

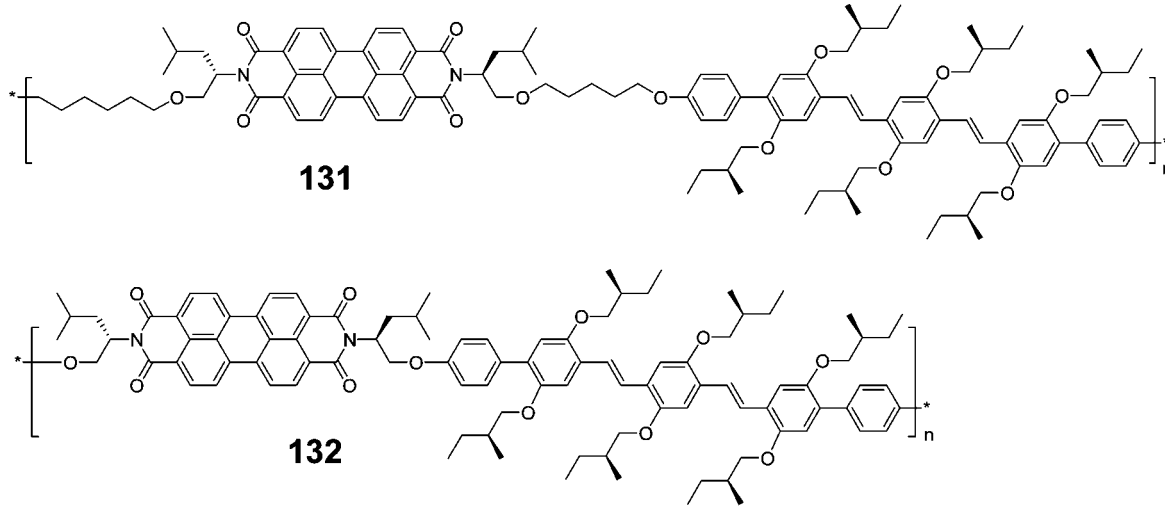

Janssen and his co-workers first reported copolymers based on oligophenylenevinylene and perylenediimide.[257] Photovoltaic devices were prepared by spin-coating a solution of **131** and **132** (Chart 28) in chloroform on ITO glass covered with a layer of PEDOT:PSS. A LiF/Al top electrode was deposited by vacuum. With an ITO/PEDOT:PSS/polymer/LiF/Al structure, the devices exhibited high V_{oc} values (1−1.2 V); however, the short circuit current densities were extremely low (0.008−0.012 mA cm^{-2}). The fast geminate recombination (more than 80% recombination within 1 ns) and poor transport characteristics led to the low current due to face-to-face orientations of the perylenediimide and oligophenylenevinylene segments in alternating stacks in the polymer films (Figure 18). These results showed that, in order to overcome the intrinsic tendency of donor and acceptor segments giving alternating stacks, stronger antagonistic interactions directing the microscopic morphology should be introduced.

Besides the combination of perylene compounds as acceptor moieties with electron rich donor oligomers or polymers via the *peri* positions of the perylene core, many perylene copolymers, where the polymerization occurs at the perylene *bay* positions, have been investigated.[262−265] The synthesis of these compounds is much easier than for the *peri* polymerized perylenes. In 2005, the first example of such polymers was reported by Zhu et al.[262] The introduction of donor moieties with different properties in the *bay* positions of perylene produced final polymers with good solubility due to the strong twist of the perylene core.[266,267] In comparison to pure 1,7-diphenoxyperylenediimide, which shows an absorption maximum at 526 nm, the absorption maxima of **133** and **134** (Chart 29) are red-shifted by 10 and 13 nm, respectively. The solar cell devices based on **133** and **134** were fabricated under the structure of ITO/PEDOT:PSS/polymer/Ca/Al. A solar cell with polymer **133** had a short circuit current of 0.45 mA cm^{-2}, an open circuit voltage of 0.3 V, and a fill factor of 36%. However, the solar cell with **134** gave a much lower I_{sc} of 0.0167 mA cm^{-2}, a higher V_{oc} of 0.42 V, and a lower FF of 28%. The authors claimed that the higher I_{sc} of the **133** cell was due to the much higher content of perylene in **133** than that in **134**. The absorber in the two copolymers should mainly be the perylene units, since the stilbene or triphenylamine is almost transparent in the visible region. The content of perylene units in the copolymers, therefore, played an important role in the photovoltaic performance.

Due to the outstanding photovoltaic performance of thiophene derivatives, many perylene copolymers with thiophene derivative moieties have been developed.[263,268] Via the Stille coupling, compound **135** was synthesized with a dithienothiophene scaffold.[263−265] This polymer is well soluble in most organic solvents and exhibits charge carrier mobilities of up to 1.3 × 10^{-2} cm^2 V^{-1} s^{-1} characterized in an OFET geometry under nitrogen atmosphere. To investi-

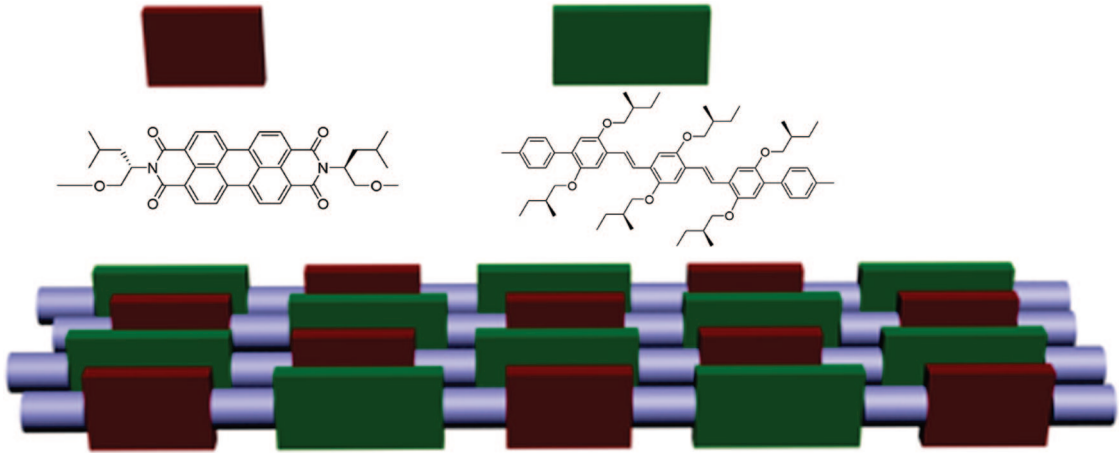

Figure 18. Illustration of polymers **131** and **132** in the solid-state: for both **131** and **132**, the polymers showed face-to-face interchain interactions.

Chart 29. Chemical Structures of *bay*-Functionalized Perylenediimide Copolymers 133−135 and Donorlike Thiophene-Containing Polymers 136

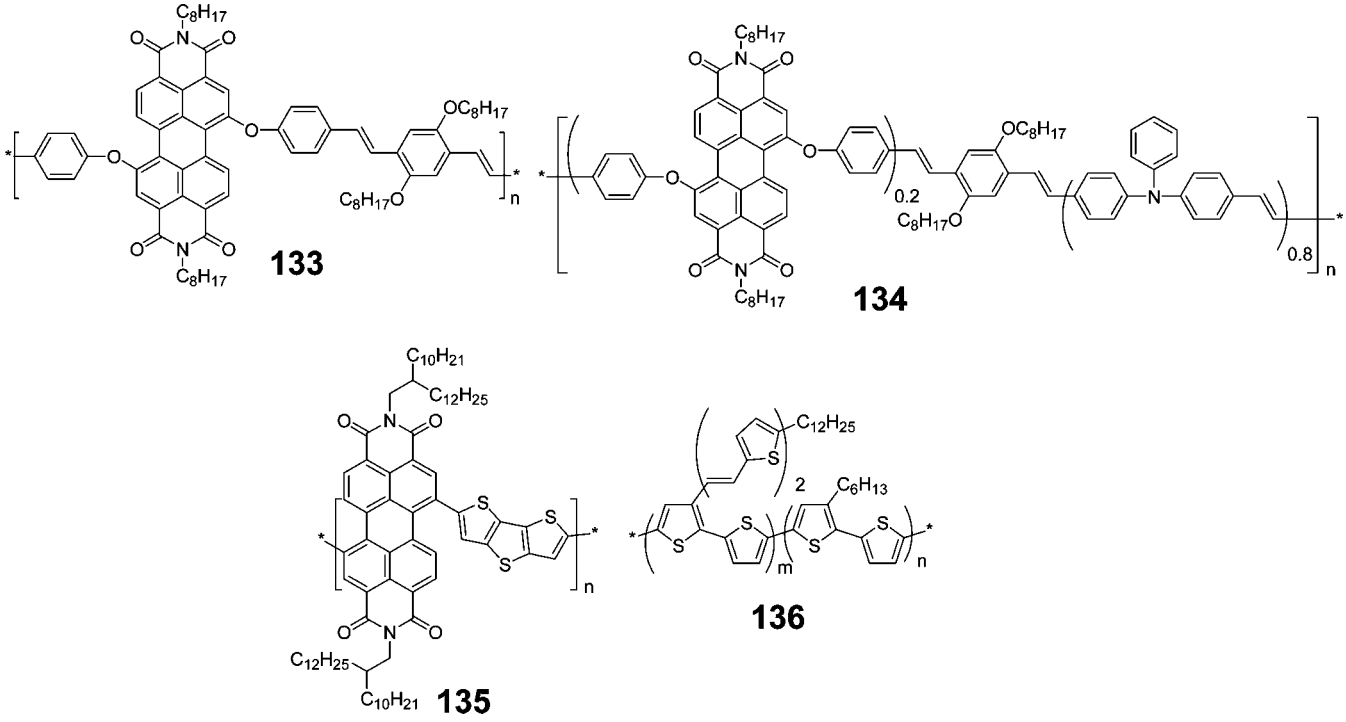

gate the potential of **135** for photovoltaic applications, an all-polymer solar cell was fabricated, where **135** acted as the electron acceptor and **136** was used as the electron donor. With the device structure ITO/PEDOT:PSS/**135**:**136**(1:1)/Al, a V_{oc} of 0.63 V, a I_{sc} of 4.2 mA cm^{-2}, and a FF of 0.39 resulted in a power conversion efficiency of 1.5%. Like other low-band-gap polymers, polymer **135** was also designed using the donor−acceptor construction to lower the polymer band gap. Therefore, it shows a broad absorption band over the whole visible region and into the near-infrared (Figure 19). Within the given donor−acceptor structure, the donor part in the polymer main chain can be easily varied, as the perylene moiety is left unchanged. In this way, the energy gap of such polymers can be well controlled.

Another method to introduce perylenes into polymers, where the perylene moiety is not directly in the polymer backbone, was first realized by Tian et al., who synthesized a highly soluble polymer based on polyphenylenevinylene, triphenylamine, and tetraphenoxy perylenediimide.[269] The photovoltaic performance observed for ITO/PEDOT:PSS/polymer **137**/Ba/Al solar cells presented that the PCE reached only values of 0.0005%. According to the authors, the cell's poor performance was due to the majority of the absorbed

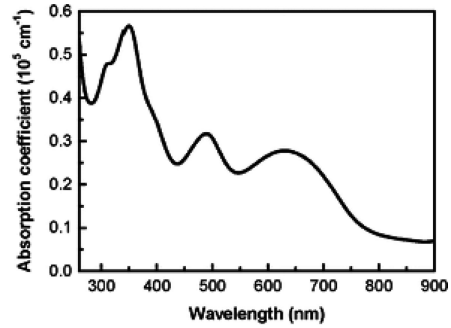

Figure 19. UV−vis absorption spectra of compound **135** in a film spin-coated from chlorobenzene. Adapted with permission from ref 262. Copyright 2007 American Chemical Society.

Chart 30. Chemical Structures of Perylenediimide-Containing Copolymer 137

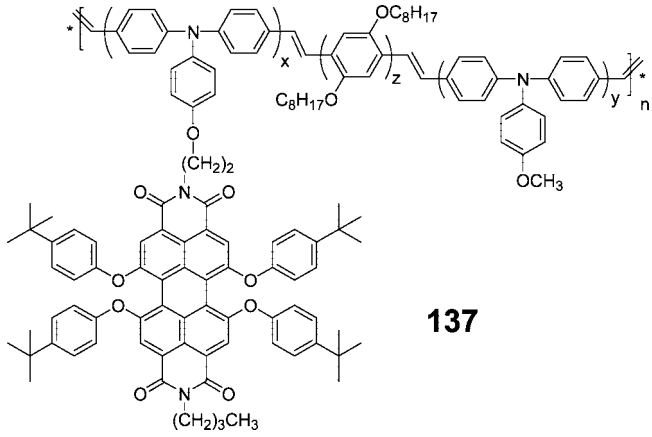

energy by the polyphenylenevinylene backbone being promptly conveyed to the perylene's lowest singlet excited state, leaving only a very small portion of absorbed light to contribute effectively to the photocurrent. Additionally, the fluorescence quantum yield of polymer **137** (Chart 30) is only around 0.1, which is much lower than that of perylenediimide (~1). Therefore, the unexpected low fluorescence indicated strong photoinduced electron transfer instead of energy transfer from the triphenylamine moiety to perylenediimide in the polymers.

To further optimize the nanostructured bulk-heterojuctions, Thelakkat and his co-workers reported a diblock copolymer bearing perylenediimide.[270−272] These block copolymers **138**−**140** (Chart 31) can self-assemble into a nanostructure, which provides charge-separation interfaces on the nanometer scale. With an ITO/PEDOT:PSS/polymer/Al configuration, the cells based on these polymers demonstrated a much better photovoltaic performance than the device based on the monomer blend. A top PCE of 0.3% with an I_{sc} of 1.14 mA cm^{-2}, a V_{oc} of 0.69 V, and a FF of 0.32 could be achieved by using **139** as a single-active layer. Based on these results, the use of a block copolymer with suitable electronic properties appears to be an elegant and promising solution for overcoming the short exciton diffusion length in organic semiconductors.

In heterojunction solar cells, perylenes can be used as electron acceptors, they can be copolymerized with electron rich units, resulting in materials functioning as donors, or they can be used alone as D−A systems for single-system devices. Due to their outstanding photo- and thermostability as well as their broad absorption in the visible region, perylenes are seemingly desirable acceptor compounds or moieties for heterojunction solar cells.

2.2.3. Rylene Dyes for Dye-Sensitized Solar Cells

Complementary to their use in flat-hetero- and bulk-heterojunction solar cells, rylene dyes have also been applied as sensitizers in dye-sensitized solar cells, since they can be easily functionalized with carboxylic acid or anhydride groups which serve as anchor groups for attachment onto

Chart 31. Chemical Structures of Perylenediimide-Triphenylamine-Containing Copolymer 138−140

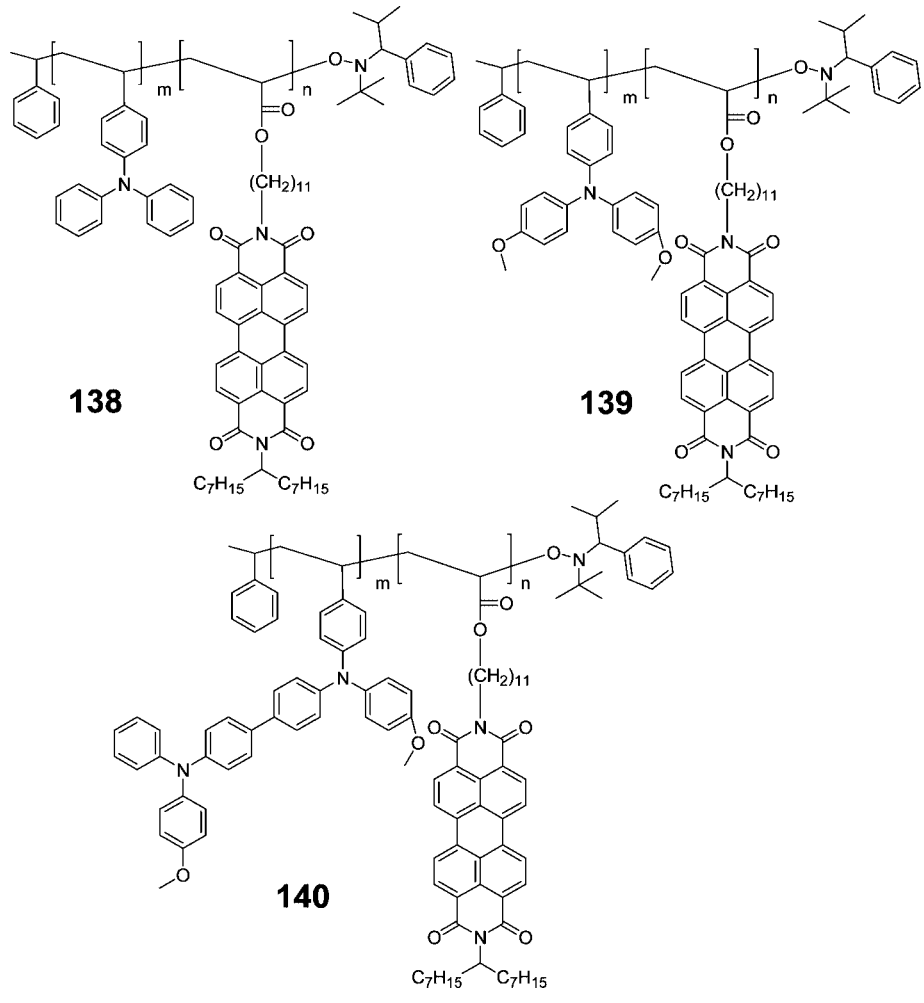

Chart 32. Chemical Structures of Perylene Sensitizers 141−149

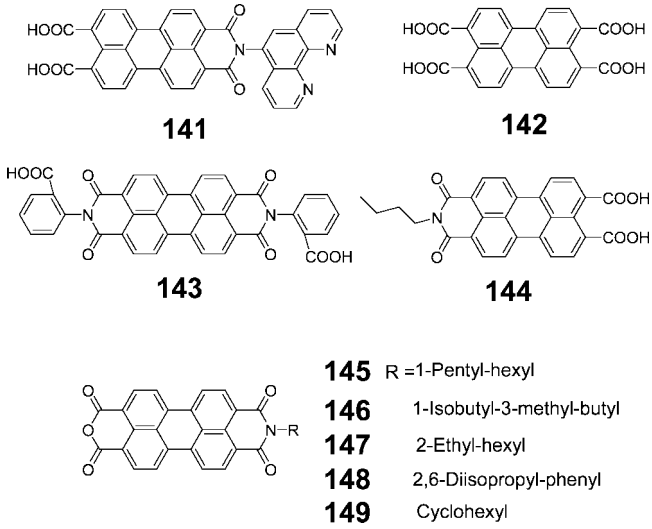

Chart 33. Chemical Structures of *bay*-Functionalized Perylene-3,4:9,10-tetracarboxy-Containing Sensitizers 150−153

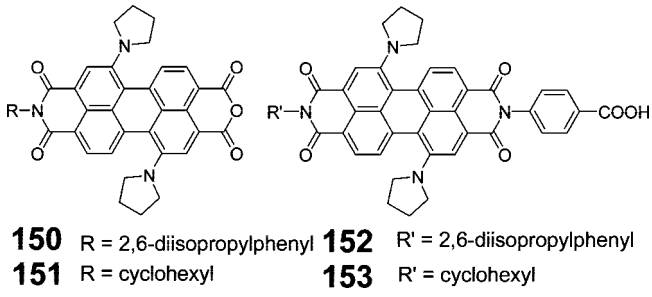

inorganic semiconductor surfaces. Research into rylene sensitizers started in 1996, when Willig reported an electron injection rate of 190 fs for 2,5-bis(*tert*-butyl)-9-methylphosphonic acid perylene adsorbed on nanocrystalline TiO_2.[273]

2.2.3.1. Derivatives of Perylenediimides. The application of rylene dyes as sensitizers began in 1997, when Gregg et al. introduced a sensitizing dye-semiconductor system comprising perylene **141**−**143** (Chart 32) with a carboxylic acid groups on SnO_2.[274] These perylenes are highly emissive, facilitating time-correlated emission experiments employed to measure charge injection rates. The cells had a 2.5 μm thick nanoporous SnO_2 film on FTO glass and contained an electrolyte solution of 0.5 M LiBr, 0.05 M Br_2, and 0.2 M 4-*tert*-butylpyridine in 80:20 (v:v) ethylene carbonate:propylene carbonate. The counter electrode was a platinum-coated F-SnO_2 glass substrate. With such a device structure, the maximum IPCE value of the cell based on **143** was approximately 30% for the wavelength region 458−488 nm, and an overall power conversion efficiency of 0.89% was achieved.

Li et al. reported TiO_2 nanocrystalline films sensitized by perylene **142** and **144** in 2002.[275] The maximum IPCE of the perylene dye **142** was improved up to 40% for the wavelength region from 440 to 530 nm via bromine-doping of a TiO_2 nanocrystalline film.

Since the anhydride group reacts chemically with inorganic semiconductors, such as TiO_2, many perylene sensitizers have been developed using such anchoring groups.[276] Icli et al. studied the influence of the substituents in the imide groups of perylene monoimide monoanhydride on the photovoltaic performance in DSCs.[276] It was found that the dyes with longer and branched alkyl chains exhibited higher efficiencies in devices. The highest efficiency in this series of dyes was 1.61% under AM 1.5 solar light with **145**.

Chart 34. Chemical Structures of Perylene Sensitizers 154−161

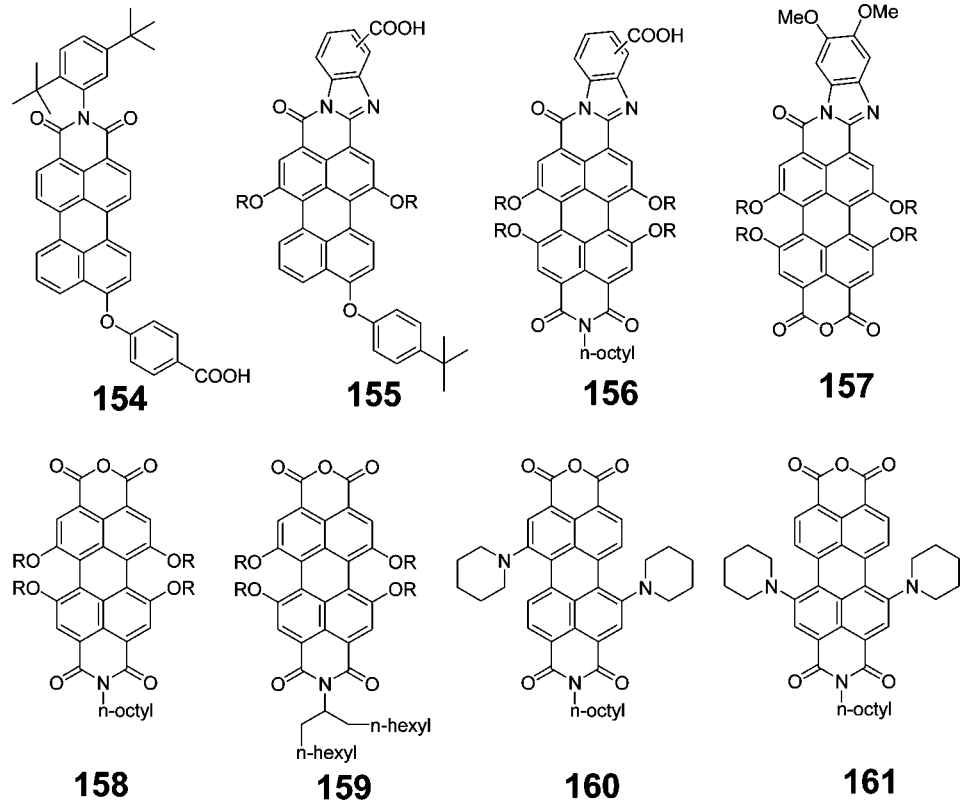

Table 4. Absorption Maxima and Device Performance of Dyes 154−161 Sensitized Solar Cells under AM 1.5G Illumination

dye	λ_{max} (nm)	electrolyte[a]	I_{sc} (mA cm^{-2})	V_{oc} (V)	FF	PCE (%)
154	517	A	2.6	0.42	0.66	0.72
		B	0.6	0.44	0.83	0.22
155	560	A	0.9	0.34	0.71	0.21
		B	0.13	0.37	0.79	0.04
156	602	A	1.0	0.43	0.60	0.26
		B	0.3	0.46	0.81	0.11
157	626	A	2.9	0.40	0.65	0.76
		B	2.9	0.46	0.71	0.96
158	578	A	5.3	0.44	0.63	1.47
		B	4.1	0.52	0.76	1.64
159	581	A	6.8	0.49	0.62	2.09
		B	6.2	0.55	0.67	2.29
160	692	A	5.9	0.38	0.48	1.08
		B	4.9	0.45	0.64	1.42
161	648	A	7.6	0.41	0.62	1.96
		B	3.2	0.43	0.69	0.96

[a] Electrolyte A: 0.6 M 1-methyl-3-*n*-propyl imidazolium iodide, 0.1 M LiI, 0.05 M I_2 in propylene carbonate. Electrolyte B: 0.6 M 1-methyl-3-*n*-propyl imidazolium iodide, 0.1 M LiI, 0.05 M I_2, and 0.1 M 4-*tert*-butylpyridine I_2 in propylene carbonate.

To further improve the efficiency of perylene sensitizers, Imahori et al. introduced pyrrolidines as electron-donating groups in the 1,6-positions of the perylene core.[277] The authors claimed that such structures have the following benefits: (1) The pyrrolidine groups exhibit strong electron donation at the perylene core and shift the first oxidation potential considerably in the negative direction. Therefore, a more exothermic electron injection from the excited singlet state to the conduction band of the TiO_2 electrode could be expected. Such substitution could also improve the light-harvesting ability in the red-to-NIR region. (2) Further, the *bay*-substituents suppress the dye aggregation on the TiO_2 surface and thus lower the intermolecular charge recombination. The cells were built under typical procedures using 13 μm TiO_2 and I^-/I_3^- electrolyte. The highest efficiency of 2.6% was obtained using **150** (Chart 33) as the sensitizer.

Similar to the research of Imahori, Odobel et al. reported the effect of (1) the nature of electron-donating substituents (phenoxy or piperidine) on the perylene core, (2) the position of the anchoring groups, and (3) the presence of a fused benzimidazole moiety on the performance of DSCs.[278] The efficiency of these dyes **154−161** (Chart 34) ranged from 0.2% to 2.3% (Table 4). From the results of photovoltaic devices, it was noted that the position of the anchoring groups can control the electron injection efficiency. The presence of the four phenoxy groups in the perylene *bay* position led to effects similar to those of the two piperidine groups, but with a lower propensity to aggregation and a slightly higher photovoltaic performance. The functionalization of perylene with a benzimidazole moiety is an effective strategy to extend the absorption spectrum into the red, but owing to its rather electron-rich nature, it should be placed at the opposite side of the anchoring group.

Moving one step further with respect to piperidine-substituted perylene sensitizers, Sastre-Santos and Fernández-Lázaro et al. presented the perylene sensitizer **162** (Chart 35), which contains a complexing unit, capable of selectively binding lithium ions in DSCs.[279] Compared to the **163**-sensitized solar cells, the devices of **162** yielded higher voltages but lower photocurrents under simulated sunlight (Figure 20). This indicated a shift in the TiO_2 conduction band edge due to the complexation of Li with the azacrown ether, which may induce the formation of a dipole at the nanoparticle surface.

Chart 35. Chemical Structures of Azacrown Ether-Containing Perylene Sensitizer 162 and Dye 163

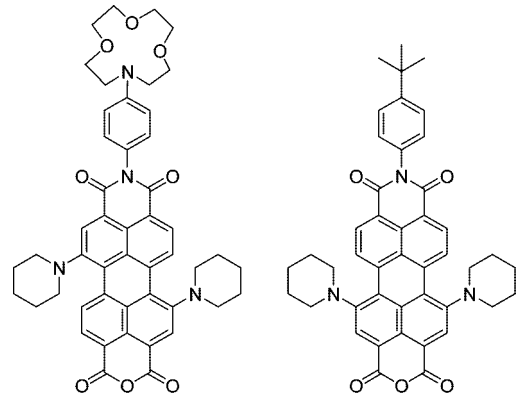

2.2.3.2. Derivatives of Perylenemonoimides. In 2001, Ferrere and Gregg developed push−pull-type perylenes **164−168** (Chart 36).[280,281] The device efficiency was improved through exposure to ultraviolet (UV) light.[282] The short circuit photocurrent improvements ranged from 3- to more than 100-fold. The primary mechanism appears to be a positive shift of the conduction band of TiO_2.[282] The cells were constructed using 6−7 μm thick TiO_2 layers and an electrolyte which contained 0.5 M tetra-*n*-butylammonium iodide, 0.05 M I_2, and 0.2 M 4-*tert*-butylpyridine in 3-methoxyproprionitrile solution. The highest power efficiency of 1.92% was obtained by perylene **165** after UV treatment, while cells sensitized by the **N3** ruthenium complex (*cis*-di(thiocyanato)bis(2,2′-bipyridyl-4,4′-dicarboxylate)ruthenium(II)) showed an efficiency of 4.4% under the same conditions.[280]

Based on the research of Ferrere and Gregg, Matsui et al. reported a series of 9-substituted perlyene monoanhydrides **169−174** (Chart 37) for dye-sensitized ZnO solar cells.[283] Of these compounds, the 9-bromoperylene monoanhydride **170** showed the highest overall power efficiency of 0.52%, with no improvement compared to previous examples. Obviously, the poor photovoltaic performance of these dyes

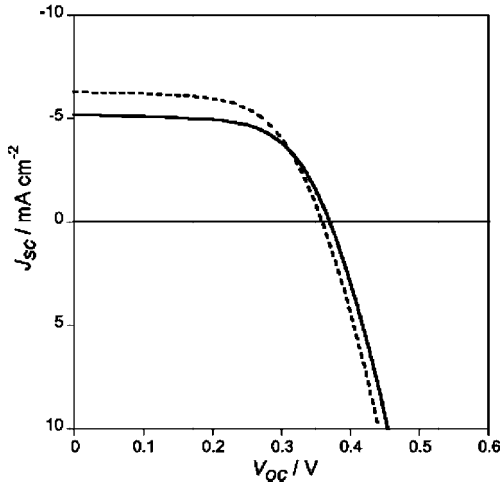

Figure 20. Current vs voltage ($I-V$ curve) for the **162** (straight line) and **163** (dashed line) DSC devices. Adapted with permission from ref 278. Copyright 2009. Reproduced by permission of The Royal Society of Chemistry.

Chart 36. Chemical Structures of Perylene Sensitizers 164−168

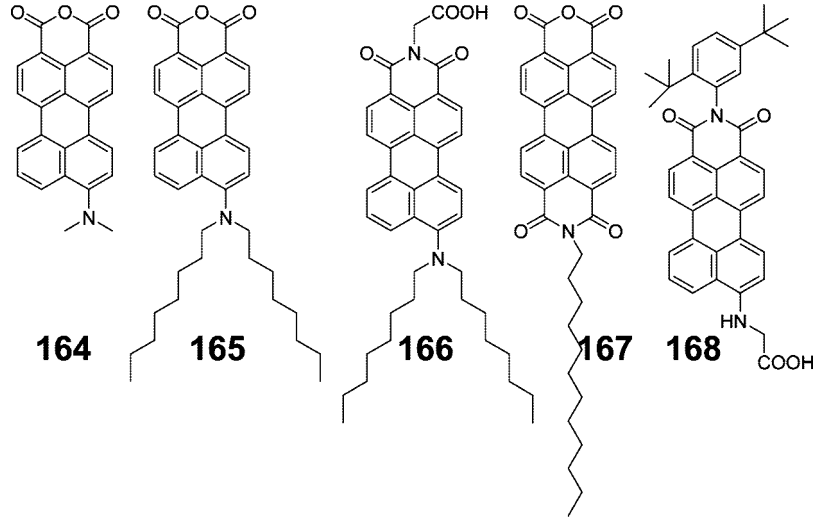

Chart 37. Chemical Structures of Perylenemonoanhydrides 169−174

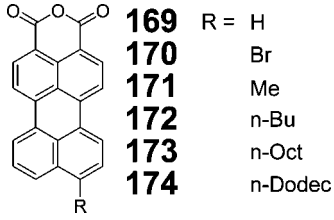

is due to the lack of strong donor substituents in the 9-position (see Chart 24 for definitions of the positions) of perylene.

In the field of dye-sensitized solar cells, most organic metal-free sensitizers have push−pull structures with donor−acceptor functionalization.[193] With this molecular design principle, our group constructed a family of perylene dyes covering the entire visible region (Figure 21). Their optical and electrochemical properties were thereby tunable via the introduction of electron-donating or electron-withdrawing groups in the 1,6-positions (see Charts 24 and 38) of perylenemonoimide and additional electron-donating groups in the 9-position of perylenemonoimide to form push−pull structures with controllable properties.[284] The simple synthesis and facile tuning of the optical and electrochemical properties of these perylenes created push−pull-type perylenes **175**−**179**, displaying a rainbow of colors and absorption maxima modifiable throughout the whole visible region. Moreover, due to the strong electron-donating groups in the 9-position, intramolecular charge

Chart 38. Chemical Structures of Rainbow Perylenemonoimides 175−179 (Twisted Charge Transfer Excited States)

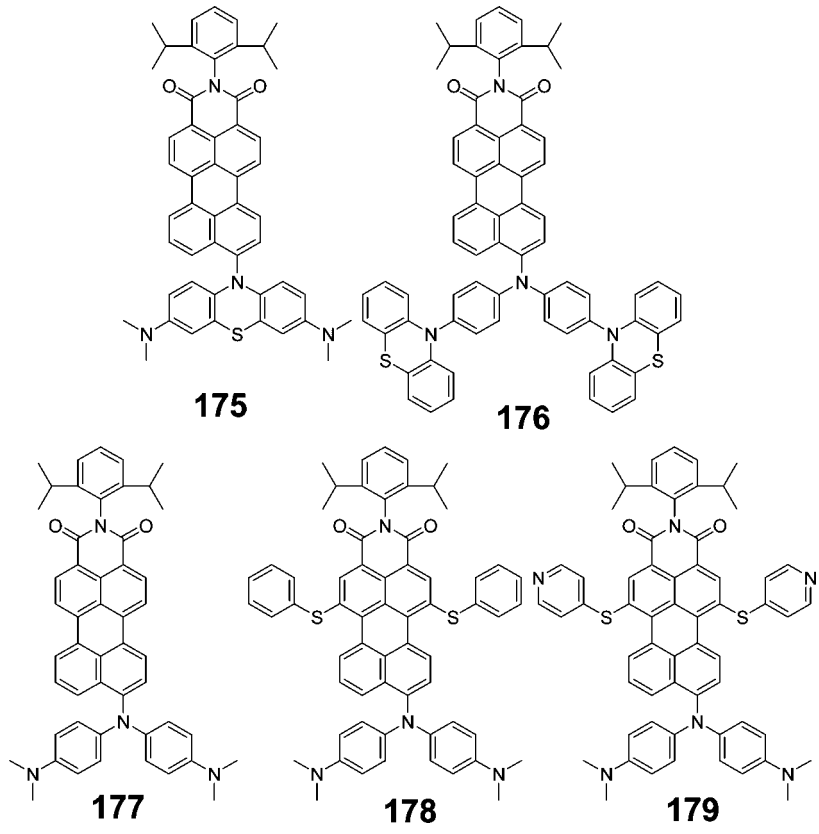

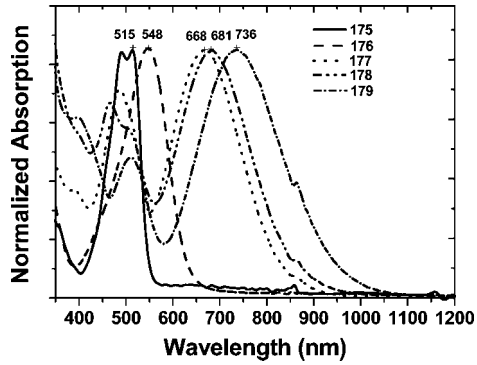

Figure 21. Absorption spectra of compounds **175**−**179** in dichloromethane.

transfer and favorable orbital partitioning (which occurs when on the donor part of the molecule the HOMO coefficients are high, while on the acceptor part of the same molecule the coefficients of the LUMO are high), necessary for DSC, are achieved.

Taking advantage of these properties, many perylene sensitizers have been synthesized.[285−287] Going from perylene **180** to **183** (Chart 39), a monotonic increase of the absorption maximum in dichloromethane was observed due to increasing donor strength, which also induced a dipole moment increase of the compounds as well as an improvement of the intramolecular charge transfer. Consequently, the power efficiencies of perylene **180**−**183** sensitized TiO_2 improved from 1.4% to 2.0% to 2.4% to 3.2%, which corresponded to the trend of the intramolecular charge transfer values.[285]

To investigate the relationship between the photovoltaic performance and the size of the sensitizers, three push−pull-type perylene sensitizers **184**−**186** with different molecular sizes, but similar spectroscopic and electrochemical properties, were made via the introduction of different substituents into the 1,6-positions of the perylene core.[287] It was found that sensitizers with a smaller size show better performance at low light intensities. At higher light intensities, however, the efficiencies for the cells with larger dyes approached those of the smaller dyes, despite much less adsorption on TiO_2. The results suggest that dye morphology plays an important role in device performance, with specific regard to aggregation and recombination.

A breakthrough in perylene sensitizers was the discovery that the introduction of two phenylthio groups in the 1,6-position of perylene core could tune the HOMO and LUMO energies as well as the absorption wavelength of the dyes (especially on TiO_2).[286] As a result, compound **187** exhibited an unprecedented IPCE of 87% and yielded an efficiency of 6.8% under standard AM 1.5 solar conditions. Moreover,

Chart 39. Chemical Structures of Perylene 180 and Perylene Sensitizers 181−188 with Strong Dipole Moments

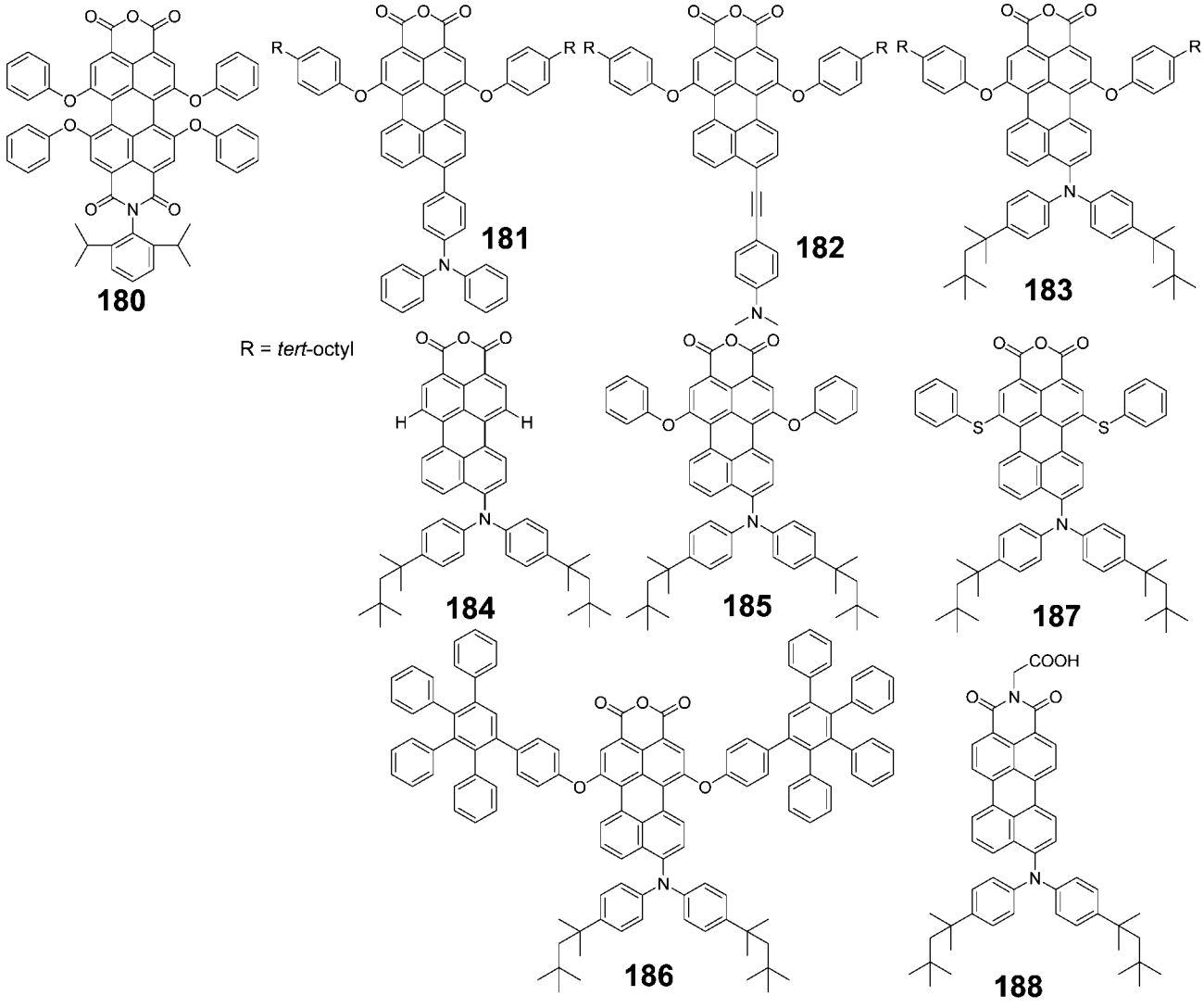

Chart 40. Chemical Structures of Perylene Sentitizers 189−193 for p-Type DSCs

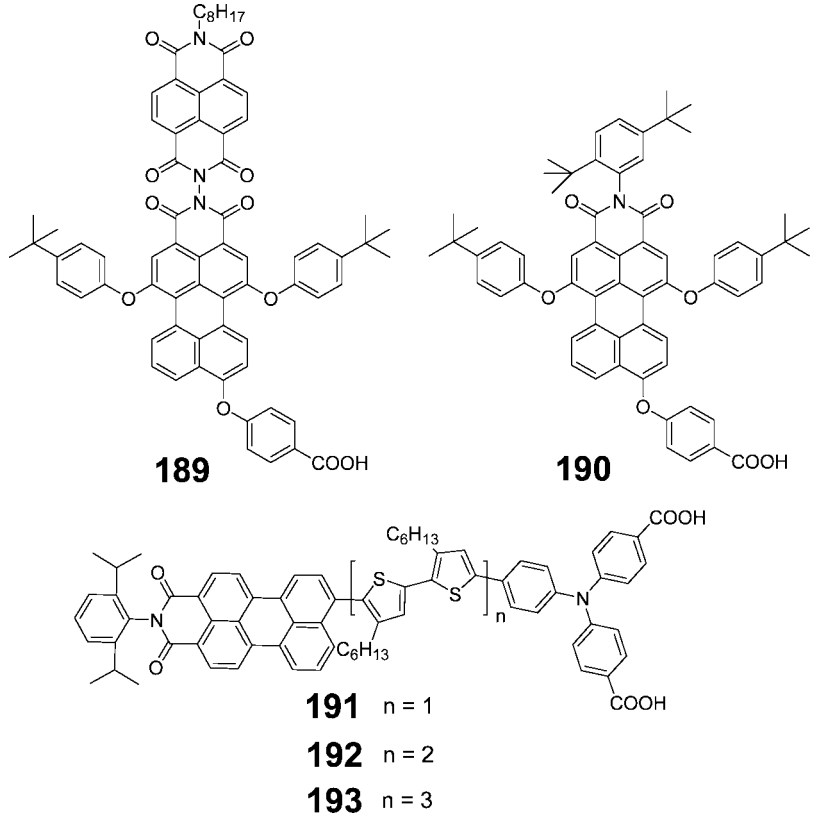

this sensitizer showed a 1.8% power conversion efficiency in solid-state dye-sensitized solar cells where the electrolyte was replaced by spiro-MeOTAD.

Based on the structure of compound **184**, Hagfeldt et al. reported a perylene **188**-sensitized solid state solar cell, where the hole conductor is spiro-MeOTAD.[288] The device exhibited a power conversion efficiency of 3.2% with a short circuit current of 8.7 mA cm^{-2}, an open circuit voltage of 0.64 V, and a fill factor of 0.57. Interestingly, **188** showed poor efficiency (PCE 1.2%) in a liquid-electrolyte-based solar cell, much lower than **184** (3.9%). This result demonstrates that dyes which have not been successfully applied in

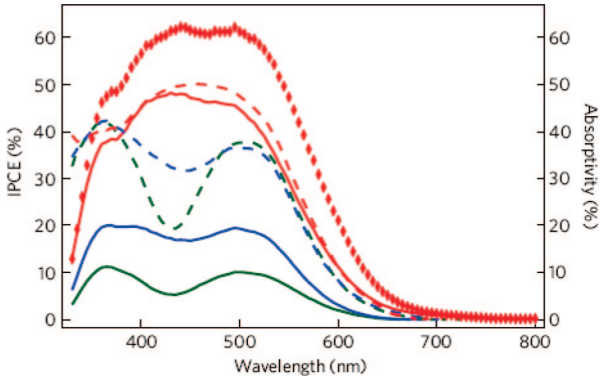

Figure 22. IPCE spectra of p-DSCs assembled from mesoporous 1.25-μm-thick NiO electrodes (solid lines), sensitized with dyes **191** (green), **192** (blue), and **193** (red) as well as the percentage of incident photons that are absorbed by the dye inside the p-DSC (absorptivity, dashed lines). The red diamonds indicate the IPCE of a mesoporous 2.3 μm thick NiO electrode sensitized with **193**. Platinum-coated conducting glass (fluorine-doped tin oxide) was used as a counter electrode. Adapted with permission from ref 290. Reprinted by permission from Macmillan Publishers Ltd.: Nature Materials, Copyright 2010.

Table 5. Photovoltaic Performance of a Tandem Solar Cell as Well as a p-Type DSC and n-Type DSC under AM 1.5G Illumination[a]

	I_{sc} (mA cm^{-2})	V_{oc} (V)	FF	PCE (%)
p	4.64	0.19	0.35	0.3
n	2.74	0.91	0.72	1.79
pn	2.40	1.08	0.74	1.91

[a] Identical NiO and TiO_2 films were used for the construction of the tandem and p- and n-DSC. The photocathodes consisted of a 3.3 μm thick NiO layer sensitized with **193**. The photoanodes consisted of a 0.8 μm thick TiO_2 layer, sensitized with 4′-carboxy-2,2′-bipyridine-4-carboxylate (**N719**). The tandem pn-DSC and n-DSCs were illuminated through the n-side; the p-DSC, through the p-side.

electrolyte DSCs can still be candidates for solid-state DSCs, as different injection and regeneration mechanisms may apply.

Besides their application in n-type DSCs, where the photoactive electrodes are typically SnO_2, TiO_2, or ZnO, perylene monoimides can also be used as sensitizers for p-type DSCs where the semiconductor electrode is NiO. Pioneering research in that field was reported by Hagfeldt, Hammarström, and Odobel et al.[289] The photovoltaic performance of perylene **189** and **190** sensitized p-type solar cells, however, is quite low with an IPCE maximum of 4.0 for **189** and 1.3% for **190** (Chart 40). The authors ascribe the low efficiencies of devices to poor dye loading, which leads to insufficient light absorption.

Bäuerle and Bach et al. further improved the efficiencies of perylene-sensitized p-type solar cells by enhancement of the push−pull effect of the molecules.[290] Compounds **191−193** contain perylene monoimide as acceptor moieties, oligothiophenes as π-spacers, and triphenylamines as donor substituents. The anchoring groups were introduced on the triphenylamine side in order to achieve better electron

Chart 41. Chemical Structures of Perylene-Containing Multichromophores 194−197

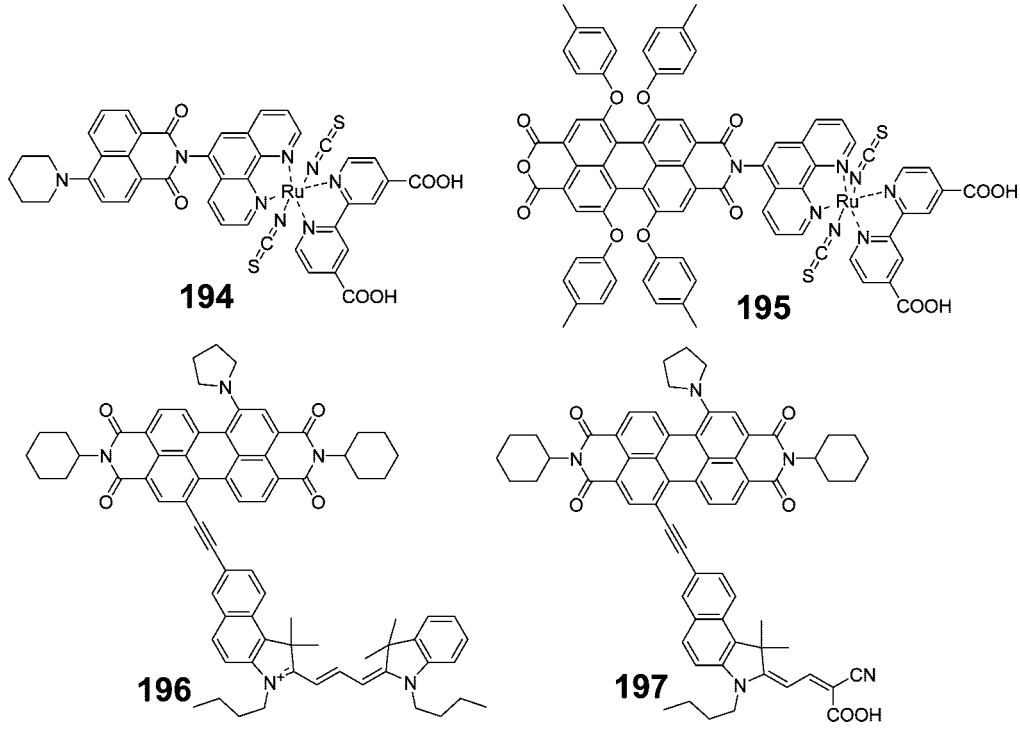

collection from the NiO. The IPCE results (Figure 22) indicated that the increase in efficiency with increasing length of the oligothiophene bridge resulted primarily from reduced charge recombination on the recorded 100 ns to 100 μs time scale. Compound **193** gave the best performance in p-DSCs (0.3%) and pn-tandem DSCs (1.91%) (Table 5). This result indicated that tandem pn-DSCs can be constructed which exceed the efficiency of their individual components.

2.2.3.3. Perylene-Containing Multichromophores. Aiming to improve the absorption properties of ruthenium complexes, Tian et al. introduced naphthalene or perylene moieties into the ligand of ruthenium compounds.[291] However, the strong electron-withdrawing nature of the imide groups affects the intramolecular charge transfer properties, resulting in low efficiencies of these dyes in DSCs. The highest efficiency of 3.08% was achieved by using **194** (Chart 41) as the sensitizer.

Meng et al. designed and synthesized another kind of bichromophore which contained perylene and benzo[e]indole units.[292] These dyes showed wide absorption bands with high molar absorption coefficients over the entire visible spectrum (Figure 23). However, both compounds **196** and **197** showed low efficiencies, 0.34% and 1.38%, respectively, under irradiation with 75 mW cm^{-2} light illumination. The authors ascribed these lower conversion efficiencies to the imide group. The strong electron-withdrawing nature of the imide group influences the polarity of the whole molecule, resulted in the unfavorable transfer direction of photogenerated electrons, which decreased the overall photocurrent performance.

2.2.3.4. Terrylene Sensitizers. Quite recently, Hagfeldt et al. reported the photovoltaic performance of the next higher homologue of perylene in rylene family: terrylene monoimide monoanhydride with four phenoxy groups.[293] Compound **198** (Chart 42) showed a strong absorption band at 680 nm with a molar absorption coefficient of 178,000 M^{-1} cm^{-1} in dichloromethane. For the best terrylene-sensitized (8 μm TiO_2) solar cell, a PCE of 2.4% was obtained under AM 1.5 solar light by using 0.5 M LiI and 0.05 M I_2 in acetonitrile as electrolyte. This terylene delivers a remarkable current (9.4 mA cm^{-2}), arising from absorption between 400 and

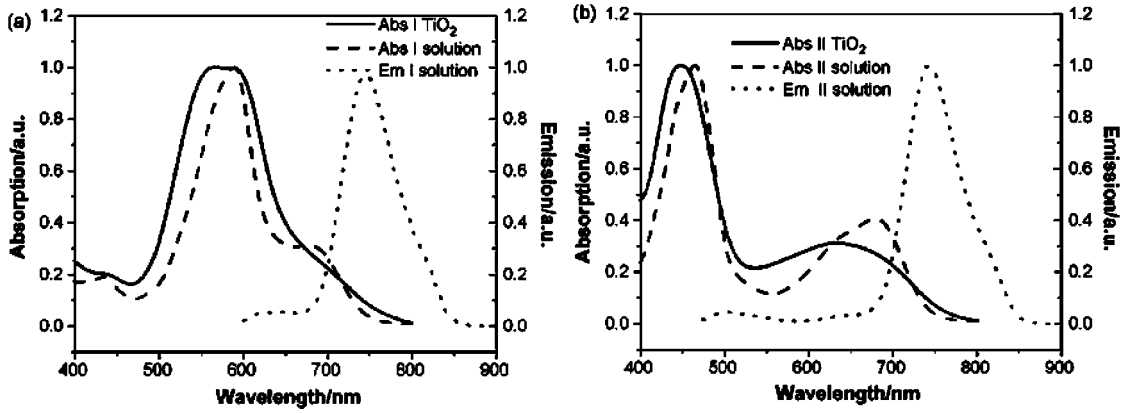

Figure 23. Normalized absorption and emission spectra of (a) **196** and (b) **197** in an acetonitrile and ethanol mixture solution (volume ratio 1:1) compared to the absorption spectra of the dye attached to TiO_2. Adapted with permission from ref 291. Copyright 2008 Elsevier.

Chart 42. Chemical Structures of Terrylene Sensitizer **198**

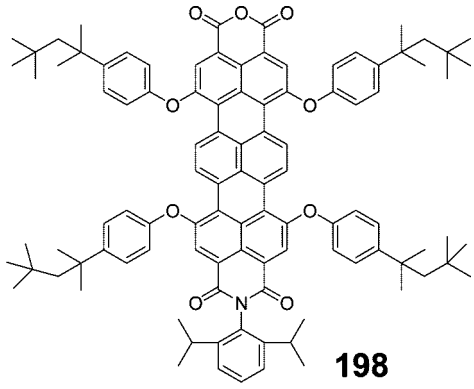

800 nm (the IPCE spectrum of a **198**-sensitized solar cell exhibits a broad band which is corresponding to the absorption of **198** and much broader than that of **N719**-based solar cells; see Figure 24). Lower voltages, however, partially resulting from the dye's incompatiblity with additives such as 4-*tert*-butylpyridine, have limited this dye's application in DSCs until now. The higher rylene homologues such as quaterrylene, pentarylene, etc. are still under investigation.

In view of all the rylene sensitizers, the donor−acceptor concept has proven to be quite successful in the design of highly efficient dyes for DSCs. The push−pull effect not only improves the light-harvesting ability of dyes but further induces intramolecular charge transfer, thus improving the performance of the solar cell devices.

2.3. Polyphenylene Dendrimers

In the three-dimensional world of benzene, our group has developed polyphenylene-containing mutichromophors in the past decade.[294,295] The introduction of a terrylenediimide chromophore into the center of a polyphenylene dendrimer produced efficient spatial isolation of naphthalenemonoimide (NMI), perylenemonoimide (PMI), and terrylenediimide (TDI) (Chart 43). Additionally, the presence of the dendrimer branches suppresses the aggregation of the chromophores. Figure 25 shows the absorption and emission spectra of the

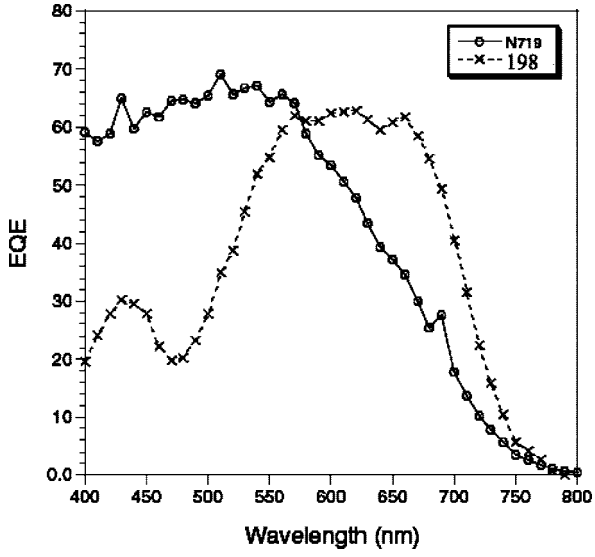

Figure 24. Photocurrent action spectra of compound **198-** and **N719**-sensitized solar cells with an electrolyte consisting of 0.5 M LiI and 0.05 M I_2 in acetonitrile. Adapted with permission from ref 293. Copyright 2009 Elsevier.

individual rylene chromophores. There are large spectral overlaps between the NMI emission and the PMI absorption and between the PMI emission and the TDI absorption. However, between the NMI emission and the TDI absorption, there is no overlap, which suggests a very difficult energy transfer from the NMI directly to the TDI. Therefore, this triad dendrimer covers the entire visible region and shows a stepwise energy transfer over a distance of 30 Å from the periphery via the scaffold toward the center of the dendrimer. The emission spectra of the dendrimer, excited at 370 nm, confirm an efficient energy transfer, which can be explained by the large Förster interaction radius ($R_0 = 6$ nm), as well as the favorable absorption and emission properties of these three chromophores. Evidently, under solar irradiation, the energy is transferred from NMI to PMI and finally concentrates on the core, e.g. the TDI. If the TDI core can be monofunctionalized with carboxy groups, the entire multichromophore molecule could be attached onto the surface of semiconductors, such as TiO_2. In this way, the energy transfer and light-harvesting ability of the molecule can be well controlled. The light-harvesting enhancement has been developed via different pathways. By using dye-cocktails, different sensitizers are coadsorbed onto TiO_2, thus the absorption spectrum of the device is enhanced. However, the reproducibility is not high due to the different adsorption abilities of the sensitizers. Recently, McGehee and his coworkers reported a 26% increase in power conversion efficiency when using an energy relay dye (1,6,7,12-tetra(4-*tert*-butylphenoxy)-*N*,*N*′-bis(2,6-diisopropylphenyl)perylenediimide) with an organic sensitizing dye (zinc phthalocyanine).[296] In these devices, the perylene dyes absorb the higher energy photons and the resulting energy undergoes Förster energy transfer to the phthalocyanine sensitizers. In this case, the unfixed perylene molecules in the electrolyte have a common problem, namely negative intermolecular interactions, such as aggregation and dye self-quenching, which will limit the energy transfer efficiency. Therefore, compared to these two methods (cosensitizers and energy relay dyes) for improved light-harvesting enhancement, using multichromophore dendrimers to improve the efficiency of photoabsorption provides an alternative method. The multichromophore dendrimers create the possibility to build reproducible solar cell devices with highly efficient energy transfer and light-harvesting.

3. Conclusion and Outlook

In the research on renewable energies, due to the oil crisis and the requirements of environment protection, solar energy technology is the most important solution for securing sustainable global energy. Benzene, as the basic accessory in organic compounds, provides a wonderful platform for developing small molecules, polymers, and dendrimers. In this review, we have described their performance in organic solar cells starting with linear conjugated phenylene polymers and oligomers and rylene dye molecules and concluding with multichromophores. In the one-dimensional conjugated polyphenes, copolymers containing carbazole showed a new record power conversion efficiency of 6% under AM 1.5 sunlight irradiation (certified by NREL). Introducing donor−acceptor groups at the ends of the oligophenylene results in compounds well-suited for dye-sensitized solar cells. Using phenylenevinylene as a π-spacer and functionalizing this with triphenyl amine (donor) and cyano acetic acid (acceptor), benzene-based materials as sensitizers achieved power

Chart 43. Chemical Structure of Multichromphore **199**

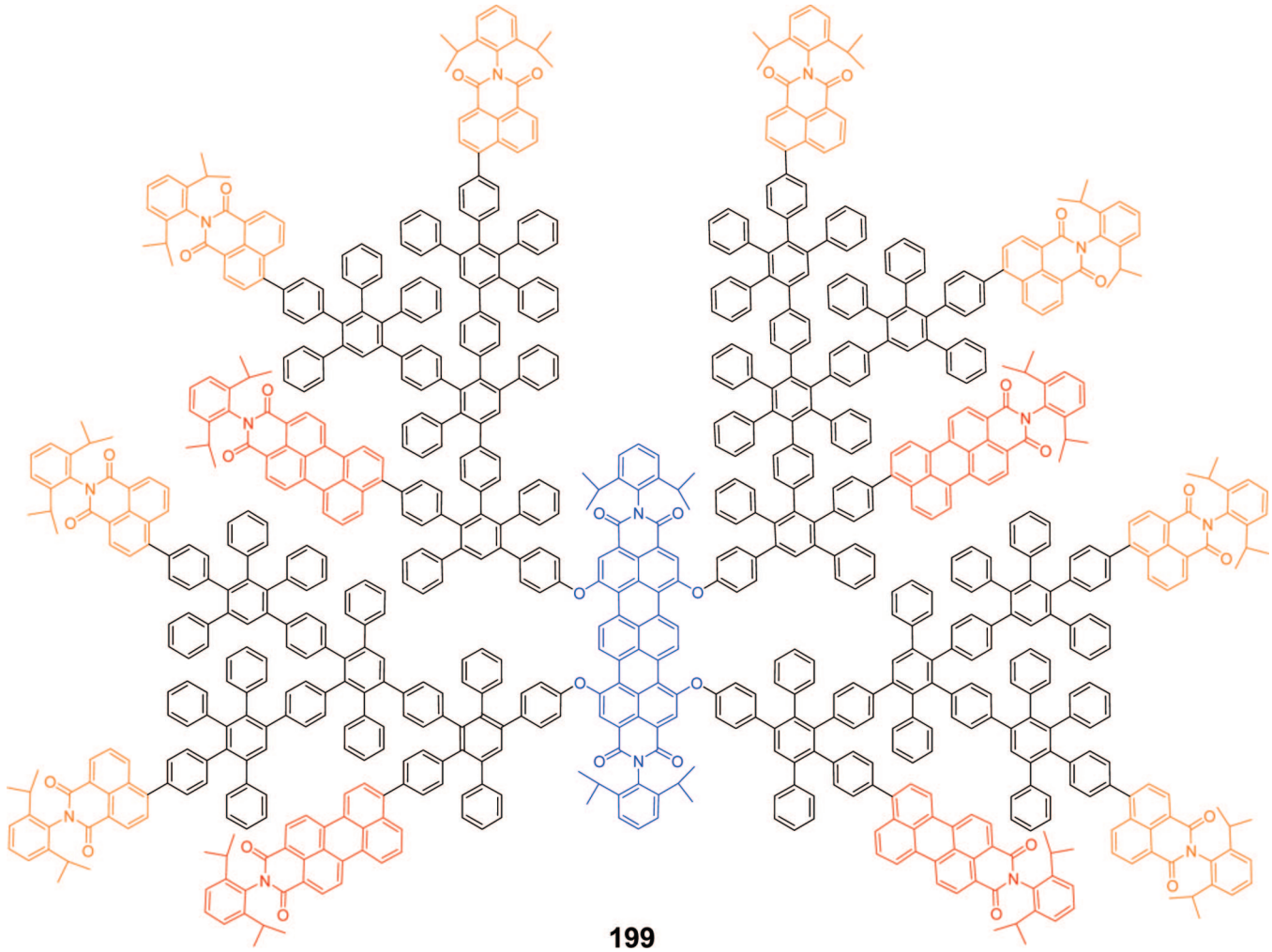

conversion efficiencies of up to 8% in DSCs. Polyphenylene-based materials may also prove to be interesting as hole-conductors, i.e. in solid state DSCs.

In the two-dimensional world, rylene compounds, functionalized with electron-withdrawing groups such as imides, show impressive photostability, thermostability, and chemical stability as well as high electron affinity. With these special properties, rylenes, especially perylenes, have been used as one of the most important n-type semiconductors. Blended with donor compounds such as phthalocyanine or polycarbazole, perylene-based bulk-heterojunction solar cells exhibited a satisfactory photovoltaic performance (up to 2.7%). With unsymmetrical structure using electron-donating groups such as diphenylamine, perylene dyes have also been used in dye-sensitized solar cells and yielded high power efficiencies of up to 7%.

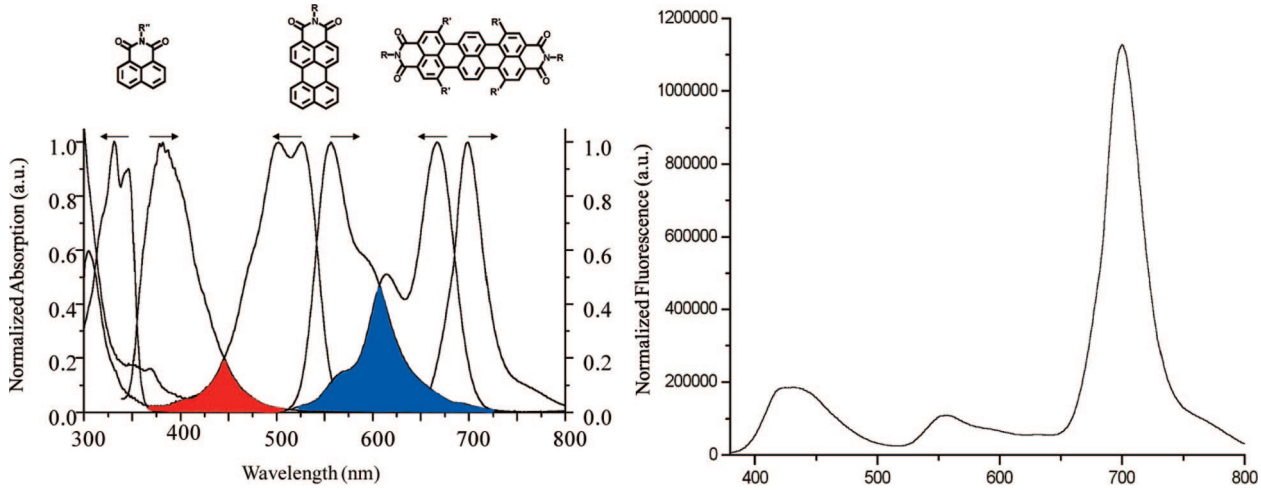

Figure 25. Absorption and fluorescence spectra of NMI, PMI, and TDI (left), and fluorescence spectrum of compound **200** (right, excited at 370 nm).

Polyphenylene dendrimers with their three-dimensional structures provided a 3D-functional ability to harvest light as efficiently as possible and will be good candidates for dye-sensitized solar cells.

Finally, it is worth noting that the polyphenylene compounds can be built into full organic metal-free solar cells and tandem solar cells, where the pyrolyzed 2D polycyclic aromatic hydrocarbon can be applied as the electrodes and the functionalized polyphenylene conjugated polympers or oligophenylenes as active materials.[297−299] We believe that further functionalization of polyphenylene-based materials will render these materials an even greater potential in the solar cell field.

4. Acknowledgments

We acknowledge the financial support of the Deutsche Forschungsgemeinschaft (DFG) priority program (SPP 1355) Elementary Processes of Organic Photovoltaics, the BMBF (Bundesministerium für Bildung and Forschung), and BASF SE.

5. Note Added after ASAP Publication

This paper was published on the Web on June 29, 2010, with errors that inadvertently had not been corrected at the proof stage. The corrected version was posted on July 1, 2010.

6. References

(1) Lior, N. *Energy* **2008**, *33*, 842.
(2) Penner, S. S.; Haraden, J.; Mates, S. *Energy* **1992**, *17*, 883.
(3) http://en.wikipedia.org/wiki/Renewable_energy.
(4) Goswami, D. Y. *Advances in Solar Energy: An Annual Review of Research and Development*; 2003; Vol. 15.
(5) *Organic Photovoltaics: Materials, Device Physics, and Manufacturing Technologies*; Brabec, C., Scherf, U., Dyakonov, V., Eds.; Wiley-VCH: 2008.
(6) *High-Efficient Low-Cost Photovoltaics*; Petrova-Koch, V., Hezel, R., Goetzberger, A., Eds.; Springer Series in Optical Sciences; 2009.
(7) *Organic Photovoltaics: Mechanisms, Materials, and Devices*; Sun, S.-S., Sariciftci, N. S., Eds.; Marcel Dekker Inc.: 2005.
(8) Smee, A. *Elements of Electro-Biology*; Longman, Brown, Green, and Longmans: London, 1849.
(9) Becquerel, A. E. *Comptes Rendus* **1839**, *9*, 561.
(10) http://en.wikipedia.org/wiki/Charles_Fritts.
(11) Ohl, R. S.; Silver, L. U.S. Patent 2402662, 1946.
(12) Chapin, D. M.; Fuller, C. S.; Pearson, G. L. *J. Appl. Phys.* **1954**, *25*, 676.
(13) Tang, C. W. *Appl. Phys. Lett.* **1986**, *48*, 183.
(14) Peumans, P.; Uchida, S.; Forrest, S. R. *Nature* **2003**, *425*, 158.
(15) Yu, G.; Gao, J.; Hummelen, J. C.; Wudl, F.; Heeger, A. J. *Science* **1995**, *270*, 1789–91.
(16) O'Regan, B.; Grätzel, M. *Nature* **1991**, *353*, 737.
(17) Bach, U.; Lupo, D.; Comte, P.; Moser, J. E.; Weissortel, F.; Salbeck, J.; Spreitzer, H.; Grätzel, M. *Nature* **1998**, *395*, 583.
(18) Schmidt-Mende, L.; Fechtenkotter, A.; Müllen, K.; Moons, E.; Friend, R. H.; MacKenzie, J. D. *Science* **2001**, *293*, 1119.
(19) Lee, M. R.; Eckert, R. D.; Forberich, K.; Dennler, G.; Brabec, C. J.; Gaudiana, R. A. *Science* **2009**, *324*, 232.
(20) van Hal, P. A.; Wienk, M. M.; Kroon, J. M.; Verhees, W. J. H.; Slooff, L. H.; van Gennip, W. J. H.; Jonkheijm, P.; Janssen, R. A. J. *Adv. Mater.* **2003**, *15*, 118.
(21) Rocke, A. J. *Ann. Sci.* **1985**, *42*, 355.
(22) Grimsdale, A. C.; Müllen, K. *Chem. Rec.* **2001**, *1*, 243.
(23) Schmaltz, B.; Weil, T.; Müllen, K. *Adv. Mater.* **2009**, *21*, 1067.
(24) Berresheim, A. J.; Müller, M.; Müllen, K. *Chem. Rev.* **1999**, *99*, 1747.
(25) Gross, M.; Müller, D. C.; Nothofer, H.-G.; Scherf, U.; Neher, D.; Brächle, C.; Merrholz, K. *Nature* **2000**, *405*, 661.
(26) Watson, M. D.; Fechtenkoetter, A.; Müllen, K. *Chem. Rev.* **2001**, *101*, 1267.
(27) Wu, J.; Pisula, W.; Müllen, K. *Chem. Rev.* **2007**, *107*, 718.
(28) Müllen, K.; Rabe, J. P. *Acc. Chem. Res.* **2008**, *41*, 511.
(29) Bauer, R. E.; Bernhardt, S.; Mihov, G.; Oesterling, I.; Scheppelmann, I.; Müllen, K. *PMSE Prepr.* **2004**, *91*, 51.
(30) Cotlet, M.; Vosch, T.; Habuchi, S.; Weil, T.; Müllen, K.; Hofkens, J.; De Schryver, F. *J. Am. Chem. Soc.* **2005**, *127*, 9760.
(31) Oesterling, I.; Müllen, K. *J. Am. Chem. Soc.* **2007**, *129*, 4595.
(32) *Organic Photovoltaics: Concepts and Realization*; Brabec, C. J., Dyakonov, V., Parisi, J., Sariciftci, N. S., Eds.; Springer: Berlin, 2003.
(33) Ameri, T.; Dennler, G.; Waldauf, C.; Denk, P.; Forberich, K.; Scharber, M. C.; Brabec, C. J.; Hingerl, K. *J. Appl. Phys.* **2008**, *103*, 084506.
(34) Pagliaro, M.; Ciriminna, R.; Palmisano, G. *ChemSusChem* **2008**, *1*, 880.
(35) Hiramoto, M.; Fujiwara, H.; Yokoyama, M. *J. Appl. Phys.* **1992**, *72*, 3781.
(36) Taima, T.; Chikamatsu, M.; Yoshida, Y.; Saito, K.; Yase, K. *Appl. Phys. Lett.* **2004**, *85*, 6412.
(37) Forrest, S. R. *MRS Bull.* **2005**, *30*, 28.
(38) Peumans, P.; Bulovic, V.; Forrest, S. R. *Appl. Phys. Lett.* **2000**, *76*, 2650.
(39) Xue, J.; Rand, B. P.; Uchida, S.; Forrest, S. R. *J. Appl. Phys.* **2005**, *98*, 124903/1.
(40) http://www.heliatek.com/en/page/index.php.
(41) Sariciftci, N. S.; Braun, D.; Zhang, C.; Srdanov, V. I.; Heeger, A. J.; Stucky, G.; Wudl, F. *Appl. Phys. Lett.* **1993**, *62*, 585.
(42) Sariciftci, N. S.; Smilowitz, L.; Zhang, C.; Srdanov, V. I.; Heeger, A. J.; Wudl, F. *Proc. SPIE—Int. Soc. Opt. Eng.* **1993**, *1852*, 297.
(43) Morita, S.; Lee, S. B.; Zakhidov, A. A.; Yoshino, K. *Mol. Cryst. Liq. Cryst. Sci. Technol., Sect. A* **1994**, *256*, 839.
(44) Sariciftci, N. S.; Heeger, A. J. *Int. J. Mod. Phys. B* **1994**, *8*, 237.
(45) Yu, G.; Pakbaz, K.; Zhang, C.; Heeger, A. J. *Mol. Cryst. Liq. Cryst. Sci. Technol., Sect. A* **1994**, *256*, 543.
(46) Lee, S. B.; Khabibullaev, P. K.; Zakhidov, A. A.; Morita, S.; Yoshino, K. *Synth. Met.* **1995**, *71*, 2247.
(47) Tada, K.; Morita, S.; Kawai, T.; Onoda, M.; Yoshino, K.; Zakhidov, A. A. *Synth. Met.* **1995**, *70*, 1347.
(48) Yu, G.; Heeger, A. J. *J. Appl. Phys.* **1995**, *78*, 4510.
(49) Park, S. H.; Roy, A.; Beaupre, S.; Cho, S.; Coates, N.; Moon, J. S.; Moses, D.; Leclerc, M.; Lee, K.; Heeger, A. J. *Nat. Photonics* **2009**, *3*, 297.
(50) Liang, Y.; Feng, D.; Wu, Y.; Tsai, S.-T.; Li, G.; Ray, C.; Yu, L. *J. Am. Chem. Soc.* **2009**, *131*, 7792.
(51) Chen, H.-Y.; Hou, J.; Zhang, S.; Liang, Y.; Yang, G.; Yang, Y.; Yu, L.; Wu, Y.; Li, G. *Nat. Photonics* **2009**, *3*, 649.
(52) http://www.solarmer.com/newsevents.php.
(53) Cao, Y.; Yu, G.; Zhang, C.; Menon, R.; Heeger, A. J. *Synth. Met.* **1997**, *87*, 171.
(54) Heywang, G.; Jonas, F. *Adv. Mater.* **1992**, *4*, 116.
(55) Chen, L.-M.; Hong, Z.; Li, G.; Yang, Y. *Adv. Mater.* **2009**, *21*, 1434.
(56) Long, Y. *Appl. Phys. Lett.* **2009**, *95*, 193301/1.
(57) Ng, T. W.; Lo, M. F.; Liu, Z. T.; Wong, F. L.; Lai, S. L.; Fung, M. K.; Lee, C. S.; Lee, S. T. *J. Appl. Phys.* **2009**, *106*, 114501/1.
(58) Niggemann, M.; Gombert, A. *Org. Photovoltaics* **2008**, 441.
(59) Xu, Z.; Chen, L.-M.; Yang, G.; Huang, C.-H.; Hou, J.; Wu, Y.; Li, G.; Hsu, C.-S.; Yang, Y. *Adv. Funct. Mater.* **2009**, *19*, 1227.
(60) Zhao, D. W.; Liu, P.; Sun, X. W.; Tan, S. T.; Ke, L.; Kyaw, A. K. K. *Appl. Phys. Lett.* **2009**, *95*, 153304/1.
(61) Hagfeldt, A.; Grätzel, M. *Chem. Rev.* **1995**, *95*, 49.
(62) Grätzel, M. *MRS Bull.* **2005**, *30*, 23.
(63) Chiba, Y.; Islam, A.; Watanabe, Y.; Komiya, R.; Koide, N.; Han, L. *Jpn. J. Appl. Phys., Part 2* **2006**, *45*, 638.
(64) Nazeeruddin, M. K.; De Angelis, F.; Fantacci, S.; Selloni, A.; Viscardi, G.; Liska, P.; Ito, S.; Takeru, B.; Grätzel, M. *J. Am. Chem. Soc.* **2005**, *127*, 16835.
(65) Yum, J.-H.; Chen, P.; Grätzel, M.; Nazeruddin, M. K. *ChemSusChem* **2008**, *1*, 699–707.
(66) Snaith, H. J.; Schmidt-Mende, L. *Adv. Mater.* **2007**, *19*, 3187.
(67) Yanagida, S.; Yu, Y.; Manseki, K. *Acc. Chem. Res.* **2009**, *42*, 1827.
(68) Snaith, H. J.; Moule, A. J.; Klein, C.; Meerholz, K.; Friend, R. H.; Grätzel, M. *Nano Lett.* **2007**, *7*, 3372.
(69) Bandara, J.; Weerasinghe, H. *Sol. Energy Mater. Sol. Cells* **2005**, *85*, 385.
(70) He, J.; Lindstroem, H.; Hagfeldt, A.; Lindquist, S.-E. *J. Phys. Chem. B* **1999**, *103*, 8940.
(71) He, J.; Lindstrom, H.; Hagfeldt, A.; Lindquist, S. E. *Sol. Energy Mater. Sol. Cells* **2000**, *62*, 265.
(72) Bandara, J.; Divarathne, C. M.; Nanayakkara, S. D. *Sol. Energy Mater. Sol. Cells* **2004**, *81*, 429.
(73) Gibson, E. A.; Smeigh, A. L.; Le Pleux, L.; Fortage, J.; Boschloo, G.; Blart, E.; Pellegrin, Y.; Odobel, F.; Hagfeldt, A.; Hammarstrom, L. *Angew. Chem., Int. Ed.* **2009**, *48*, 4402.
(74) Nakasa, A.; Usami, H.; Sumikura, S.; Hasegawa, S.; Koyama, T.; Suzuki, E. *Chem. Lett.* **2005**, *34*, 500.

(75) Qin, P.; Zhu, H.; Edvinsson, T.; Boschloo, G.; Hagfeldt, A.; Sun, L. *J. Am. Chem. Soc.* **2008**, *130*, 8570.
(76) Reguig, B. A.; Regragui, M.; Morsli, M.; Khelil, A.; Addou, M.; Bernede, J. C. *Sol. Energy Mater. Sol. Cells* **2006**, *90*, 1381.
(77) Vera, F.; Schrebler, R.; Munoz, E.; Suarez, C.; Cury, P.; Gomez, H.; Cordova, R.; Marotti, R. E.; Dalchiele, E. A. *Thin Solid Films* **2005**, *490*, 182.
(78) Zhu, H.; Hagfeldt, A.; Boschloo, G. *J. Phys. Chem. C* **2007**, *111*, 17455.
(79) Qin, P.; Linder, M.; Brinck, T.; Boschloo, G.; Hagfeldt, A.; Sun, L. *Adv. Mater.* **2009**, *21*, 2993.
(80) Scharber, M. C.; Muehlbacher, D.; Koppe, M.; Denk, P.; Waldauf, C.; Heeger, A. J.; Brabec, C. J. *Adv. Mater.* **2006**, *18*, 789.
(81) Gurnee, E. F. *J. Chem. Educ.* **1969**, *46*, 80.
(82) Mott, N. F. *Philos. Mag. B* **1988**, *58*, 369.
(83) Vayenas, C. G.; Tsiplakides, D. *Surf. Sci.* **2000**, *467*, 23.
(84) Grätzel, M. *Nature* **2001**, *414*, 338.
(85) Grätzel, M. *Inorg. Chem.* **2005**, *44*, 6841.
(86) Grätzel, M. *Prog. Photovoltaics* **2006**, *14*, 429.
(87) Avlasevich, Y.; Li, C.; Müllen, K. *J. Mater. Chem.* **2010**, *20*, 3814.
(88) Mainthia, S. B.; Kronick, P. L.; Ur, H.; Chapman, E. F.; Labes, M. M. *Polym. Prepr.* **1963**, *4*, 208.
(89) Akiyama, M.; Iwakura, Y.; Shiraishi, S.; Imai, Y. *J. Polym. Sci., Part B: Polym. Lett.* **1966**, *4*, 305.
(90) Kovacic, P.; Oziomek, J. *Macromol. Synth.* **1966**, *2*, 23.
(91) Leung, L. M. *Plast. Eng.* **1997**, *41*, 817.
(92) Grimsdale, A. C.; Müllen, K. *Adv. Polym. Sci.* **2006**, *199*, 1.
(93) Grimsdale, A. C.; Müllen, K. *Adv. Polym. Sci.* **2008**, *212*, 1.
(94) Wong, W. W. H.; Holmes, A. B. *Adv. Polym. Sci.* **2008**, *212*, 85.
(95) Becker, K.; Lupton, J. M. *J. Am. Chem. Soc.* **2006**, *128*, 6468.
(96) Becker, K.; Lupton, J. M.; Feldmann, J.; Setayesh, S.; Grimsdale, A. C.; Müllen, K. *J. Am. Chem. Soc.* **2006**, *128*, 680.
(97) Hennebicq, E.; Pourtois, G.; Scholes, G. D.; Herz, L. M.; Russell, D. M.; Silva, C.; Setayesh, S.; Grimsdale, A. C.; Müllen, K.; Bredas, J.-L.; Beljonne, D. *J. Am. Chem. Soc.* **2005**, *127*, 4744.
(98) Usta, H.; Facchetti, A.; Marks, T. J. *J. Am. Chem. Soc.* **2008**, *130*, 8580.
(99) Usta, H.; Risko, C.; Wang, Z.; Huang, H.; Deliomeroglu, M. K.; Zhukhovitskiy, A.; Facchetti, A.; Marks, T. J. *J. Am. Chem. Soc.* **2009**, *131*, 5586.
(100) Scherf, U.; Müllen, K. *Makromol. Chem., Rapid Commun.* **1991**, *12*, 489.
(101) Scherf, U.; Müllen, K. *Macromolecules* **1992**, *25*, 3546.
(102) Dierschke, F.; Grimsdale, A. C.; Müllen, K. *Macromol. Chem. Phys.* **2004**, *205*, 1147.
(103) Grimsdale, A. C.; Müllen, K. *Macromol. Rapid Commun.* **2007**, *28*, 1676.
(104) Guenes, S.; Neugebauer, H.; Sariciftci, N. S. *Chem. Rev.* **2007**, *107*, 1324.
(105) Sariciftci, N. S.; Smilowitz, L.; Heeger, A. J.; Wudl, F. *Science* **1992**, *258*, 1474.
(106) Sariciftci, N. S.; Smilowitz, L.; Braun, D.; Srdanov, G.; Srdanov, V.; Wudl, F.; Heeger, A. J. *Synth. Met.* **1993**, *56*, 3125.
(107) Liu, J.; Hains, A. W.; Servaites, J. D.; Ratner, M. A.; Marks, T. J. *Chem. Mater.* **2009**, *21*, 5258.
(108) Maturova, K.; van Bavel, S. S.; Wienk, M. M.; Janssen, R. A. J.; Kemerink, M. *Nano Lett.* **2009**, *9*, 3032.
(109) Mens, R.; Adriaensens, P.; Lutsen, L.; Swinnen, A.; Bertho, S.; Ruttens, B.; D'Haen, J.; Manca, J.; Cleij, T.; Vanderzande, D.; Gelan, J. *J. Polym. Sci., Part A: Polym. Chem.* **2007**, *46*, 138.
(110) Moet, D. J. D.; Koster, L. J. A.; de Boer, B.; Blom, P. W. M. *Chem. Mater.* **2007**, *19*, 5856.
(111) Park, L. Y.; Munro, A. M.; Ginger, D. S. *J. Am. Chem. Soc.* **2008**, *130*, 15916.
(112) Tajima, K.; Suzuki, Y.; Hashimoto, K. *J. Phys. Chem. C* **2008**, *112*, 8507.
(113) Tuladhar, S. M.; Sims, M.; Choulis, S. A.; Nielsen, C. B.; George, W. N.; Steinke, J. H. G.; Bradley, D. D. C.; Nelson, J. *Org. Electron.* **2009**, *10*, 562.
(114) Aernouts, T.; Geens, W.; Poortmans, J.; Heremans, P.; Borghs, S.; Mertens, R. *Thin Solid Films* **2002**, *403*−*404*, 297.
(115) Manca, J. V.; Munters, T.; Martens, T.; Beelen, Z.; Goris, L.; D'Haen, J.; D'Olieslaeger, M.; Lutsen, L.; Vanderzande, D.; De Schepper, L.; Haenen, K.; Nesladek, M.; Geens, W.; Poortmans, J.; Andriessen, R. *Proc. SPIE*−*Int. Soc. Opt. Eng.* **2003**, *4801*, 15.
(116) Greenham, N. C.; Moratti, S. C.; Bradley, D. D. C.; Friend, R. H.; Holmes, A. B. *Nature* **1993**, *365*, 628.
(117) Granström, M.; Petritsch, K.; Arias, A. C.; Lux, A.; Andersson, M. R.; Friend, R. H. *Nature* **1998**, *395*, 257.
(118) Andersson, M. R.; Berggren, M.; Inganaes, O.; Gustafsson, G.; Gustafsson-Carlberg, J. C.; Selse, D.; Hjertberg, T.; Wennerstroem, O. *Macromolecules* **1995**, *28*, 7525.
(119) Andersson, M. R.; Selse, D.; Berggren, M.; Jaervinen, H.; Hjertberg, T.; Inganaes, O.; Wennerstroem, O.; Oesterholm, J. E. *Macromolecules* **1994**, *27*, 6503.
(120) Halls, J. J. M.; Arias, A. C.; MacKenzie, J. D.; Wu, W.; Inbasekaran, M.; Woo, E. P.; Friend, R. H. *Adv. Mater.* **2000**, *12*, 498.
(121) Arias, A. C.; MacKenzie, J. D.; Stevenson, R.; Halls, J. J. M.; Inbasekaran, M.; Woo, E. P.; Richards, D.; Friend, R. H. *Macromolecules* **2001**, *34*, 6005.
(122) Snaith, H. J.; Arias, A. C.; Morteani, A. C.; Silva, C.; Friend, R. H. *Nano Lett.* **2002**, *2*, 1353.
(123) Xia, Y.; Friend, R. H. *Macromolecules* **2005**, *38*, 6466.
(124) McNeill, C. R.; Abrusci, A.; Zaumseil, J.; Wilson, R.; McKiernan, M. J.; Burroughes, J. H.; Halls, J. J. M.; Greenham, N. C.; Friend, R. H. *Appl. Phys. Lett.* **2007**, *90*, 193506/1.
(125) Huang, Y.-s.; Westenhoff, S.; Avilov, I.; Sreearunothai, P.; Hodgkiss, J. M.; Deleener, C.; Friend, R. H.; Beljonne, D. *Nat. Mater.* **2008**, *7*, 483.
(126) Westenhoff, S.; Howard, I. A.; Hodgkiss, J. M.; Kirov, K. R.; Bronstein, H. A.; Williams, C. K.; Greenham, N. C.; Friend, R. H. *J. Am. Chem. Soc.* **2008**, *130*, 13653.
(127) Yim, K.-H.; Zheng, Z.; Liang, Z.; Friend, R. H.; Huck, W. T. S.; Kim, J.-S. *Adv. Funct. Mater.* **2008**, *18*, 1012.
(128) Foster, S.; Finlayson, C. E.; Keivanidis, P. E.; Huang, Y.-S.; Hwang, I.; Friend, R. H.; Otten, M. B. J.; Lu, L.-P.; Schwartz, E.; Nolte, R. J. M.; Rowan, A. E. *Macromolecules* **2009**, *42*, 2023.
(129) Svensson, M.; Zhang, F.; Inganas, O.; Andersson, M. R. *Synth. Met.* **2003**, *135*−*136*, 137.
(130) Svensson, M.; Zhang, F.; Veenstra, S. C.; Verhees, W. J. H.; Hummelen, J. C.; Kroon, J. M.; Inganaes, O.; Andersson, M. R. *Adv. Mater.* **2003**, *15*, 988.
(131) Inganaes, O.; Svensson, M.; Zhang, F.; Gadisa, A.; Persson, N. K.; Wang, X.; Andersson, M. R. *Appl. Phys. A: Mater. Sci. Process.* **2004**, *79*, 31.
(132) Zhang, F. L.; Gadisa, A.; Inganas, O.; Svensson, M.; Andersson, M. R. *Appl. Phys. Lett.* **2004**, *84*, 3906.
(133) Gadisa, A.; Zhang, F.; Sharma, D.; Svensson, M.; Andersson, M. R.; Inganaes, O. *Thin Solid Films* **2007**, *515*, 3126.
(134) Yohannes, T.; Zhang, F.; Svensson, M.; Hummelen, J. C.; Andersson, M. R.; Inganas, O. *Thin Solid Films* **2004**, *449*, 152.
(135) Zhang, F.; Perzon, E.; Wang, X.; Mammo, W.; Andersson, M. R.; Inganaes, O. *Adv. Funct. Mater.* **2005**, *15*, 745.
(136) Perzon, E.; Wang, X.; Zhang, F.; Mammo, W.; Delgado, J. L.; de la Cruz, P.; Inganaes, O.; Langa, F.; Andersson, M. R. *Synth. Met.* **2005**, *154*, 53.
(137) Perzon, E.; Wang, X.; Admassie, S.; Inganaes, O.; Andersson, M. R. *Polymer* **2006**, *47*, 4261.
(138) Wang, X.; Perzon, E.; Mammo, W.; Oswald, F.; Admassie, S.; Persson, N.-K.; Langa, F.; Andersson, M. R.; Inganaes, O. *Thin Solid Films* **2006**, *511*−*512*, 576.
(139) Zhang, F.; Mammo, W.; Andersson, L. M.; Admassie, S.; Andersson, M. R.; Inganaes, O. *Adv. Mater.* **2006**, *18*, 2169.
(140) Gadisa, A.; Mammo, W.; Andersson, L. M.; Admassie, S.; Zhang, F.; Andersson, M. R.; Inganaes, O. *Adv. Funct. Mater.* **2007**, *17*, 3836.
(141) Mammo, W.; Admassie, S.; Gadisa, A.; Zhang, F.; Inganaes, O.; Andersson, M. R. *Sol. Energy Mater. Sol. Cells* **2007**, *91*, 1010.
(142) Zhang, F.; Bijleveld, J.; Perzon, E.; Tvingstedt, K.; Barrau, S.; Inganaes, O.; Andersson, M. R. *J. Mater. Chem.* **2008**, *18*, 5468.
(143) Zhang, F.; Jespersen, K. G.; Bjoerstroem, C.; Svensson, M.; Andersson, M. R.; Sundstroem, V.; Magnusson, K.; Moons, E.; Yartsev, A.; Inganaes, O. *Adv. Funct. Mater.* **2006**, *16*, 667.
(144) Zhou, Q.; Hou, Q.; Zheng, L.; Deng, X.; Yu, G.; Cao, Y. *Appl. Phys. Lett.* **2004**, *84*, 1653.
(145) Wang, F.; Luo, J.; Yang, K.; Chen, J.; Huang, F.; Cao, Y. *Macromolecules* **2005**, *38*, 2253.
(146) Wang, F.; Luo, J.; Chen, J.; Huang, F.; Cao, Y. *Polymer* **2005**, *46*, 8422.
(147) Yang, R.; Tian, R.; Yan, J.; Zhang, Y.; Yang, J.; Hou, Q.; Yang, W.; Zhang, C.; Cao, Y. *Macromolecules* **2005**, *38*, 244.
(148) Xia, Y.; Luo, J.; Deng, X.; Li, X.; Li, D.; Zhu, X.; Yang, W.; Cao, Y. *Macromol. Chem. Phys.* **2006**, *207*, 511.
(149) Becerril, H. A.; Miyaki, N.; Tang, M. L.; Mondal, R.; Sun, Y.-S.; Mayer, A. C.; Parmer, J. E.; McGehee, M. D.; Bao, Z. *J. Mater. Chem.* **2009**, *19*, 591.
(150) Okamoto, T.; Jiang, Y.; Qu, F.; Mayer, A. C.; Parmer, J. E.; McGehee, M. D.; Bao, Z. *Macromolecules* **2008**, *41*, 6977.
(151) Liu, L.; Ho, C.-L.; Wong, W.-Y.; Cheung, K.-Y.; Fung, M.-K.; Lam, W.-T.; Djurišić, A. B.; Chan, W.-K. *Adv. Funct. Mater.* **2008**, *18*, 2824.
(152) Wong, W.-Y.; Wang, X.-Z.; He, Z.; Chan, K.-K.; Djurišić, A. B.; Cheung, K.-Y.; Yip, C.-T.; Ng, A. M.-C.; Xi, Y. Y.; Mak, C. S. K.; Chan, W.-K. *J. Am. Chem. Soc.* **2007**, *129*, 14372.

(153) Wong, W.-Y.; Wang, X.-Z.; He, Z.; Djurišić, A. B.; Yip, C.-T.; Cheung, K.-Y.; Wang, H.; Mak, C. S. K.; Chan, W.-K. *Nat. Mater.* **2007**, *6*, 521.
(154) Wong, W.-Y. *Macromol. Chem. Phys.* **2008**, *209*, 14.
(155) Ameri, T.; Dennler, G.; Lungenschmied, C.; Brabec, C. J. *Energy Environ. Sci.* **2009**, *2*, 347.
(156) Dennler, G.; Forberich, K.; Ameri, T.; Waldauf, C.; Denk, P.; Brabec, C. J.; Hingerl, K.; Heeger, A. J. *J. Appl. Phys.* **2007**, *102*, 123109/1.
(157) Ambrose, J. F.; Nelson, R. F. *J. Electrochem. Soc.* **1968**, *115*, 1159.
(158) Siove, A.; Ades, D. *Polymer* **2004**, *45*, 4045.
(159) Brihaye, O.; Legrand, C.; Chapoton, A.; Chevrot, C.; Siove, A. *Synth. Met.* **1993**, *57*, 5075.
(160) Dierschke, F.; Grimsdale, A. C.; Müllen, K. *Synthesis* **2003**, 2470.
(161) Pisula, W.; Mishra, A. K.; Li, J.; Baumgarten, M.; Müllen, K. *Org. Photovoltaics* **2008**, 93.
(162) Li, J.; Dierschke, F.; Wu, J.; Grimsdale, A. C.; Müllen, K. *J. Mater. Chem.* **2006**, *16*, 96.
(163) Li, J. Ph.D. Thesis, Johannes Gutenberg-University, 2006.
(164) Langhals, H.; Demmig, S.; Potrawa, T. *J. Prakt. Chem.* **1991**, *333*, 733.
(165) Langhals, H.; Ismael, R.; Yuruk, O. *Tetrahedron* **2000**, *56*, 5435.
(166) Pisula, W.; Dierschke, F.; Müllen, K. *J. Mater. Chem.* **2006**, *16*, 4058.
(167) Pisula, W.; Kastler, M.; Wasserfallen, D.; Pakula, T.; Müllen, K. *J. Am. Chem. Soc.* **2004**, *126*, 8074.
(168) Pisula, W.; Tomovic, Z.; El Hamaoui, B.; Watson, M. D.; Pakula, T.; Müllen, K. *Adv. Funct. Mater.* **2005**, *15*, 893.
(169) Dittmer, J. J.; Marseglia, E. A.; Friend, R. H. *Adv. Mater.* **2000**, *12*, 1270.
(170) Ooi, Z. E.; Tam, T. L.; Shin, R. Y. C.; Chen, Z. K.; Kietzke, T.; Sellinger, A.; Baumgarten, M.; Müllen, K.; de Mello, J. C. *J. Mater. Chem.* **2008**, *18*, 4619.
(171) Leclerc, N.; Michaud, A.; Sirois, K.; Morin, J.-F.; Leclerc, M. *Adv. Funct. Mater.* **2006**, *16*, 1694.
(172) Blouin, N.; Michaud, A.; Gendron, D.; Wakim, S.; Blair, E.; Neagu-Plesu, R.; Belletete, M.; Durocher, G.; Tao, Y.; Leclerc, M. *J. Am. Chem. Soc.* **2008**, *130*, 732.
(173) Blouin, N.; Michaud, A.; Leclerc, M. *Adv. Mater.* **2007**, *19*, 2295.
(174) Wakim, S.; Aich, B.-R.; Tao, Y.; Leclerc, M. *Polym. Rev.* **2008**, *48*, 432.
(175) Wakim, S.; Beaupre, S.; Blouin, N.; Aich, B.-R.; Rodman, S.; Gaudiana, R.; Tao, Y.; Leclerc, M. *J. Mater. Chem.* **2009**, *19*, 5351.
(176) Kim, J. Y.; Lee, K.; Coates, N. E.; Moses, D.; Nguyen, T.-Q.; Dante, M.; Heeger, A. J. *Science* **2007**, *317*, 222.
(177) Yi, H.; Johnson, R. G.; Iraqi, A.; Mohamad, D.; Royce, R.; Lidzey, D. G. *Macromol. Rapid Commun.* **2008**, *29*, 1804.
(178) Jost, M.; Iqbal, A.; Rochat, A. C. (Ciba-Geigy A.-G., Switz.), Patent EP133156, 1985.
(179) Cassar, L.; Iqbal, A.; Rochat, A. C. (Ciba-Geigy A.-G., Switz.), Patent EP98808, 1984.
(180) Burgi, L.; Turbiez, M.; Pfeiffer, R.; Bienewald, F.; Kirner, H.-J.; Winnewisser, C. *Adv. Mater.* **2008**, *20*, 2217.
(181) Wienk, M. M.; Turbiez, M.; Gilot, J.; Janssen, R. A. J. *Adv. Mater.* **2008**, *20*, 2556.
(182) Zou, Y.; Gendron, D.; Badrou-Aich, R.; Najari, A.; Tao, Y.; Leclerc, M. *Macromolecules* **2009**, *42*, 2891.
(183) Zhou, E.; Yamakawa, S.; Tajima, K.; Yang, C.; Hashimoto, K. *Chem. Mater.* **2009**, *21*, 4055.
(184) Boudreault, P.-L. T.; Michaud, A.; Leclerc, M. *Macromol. Rapid Commun.* **2007**, *28*, 2176.
(185) Wang, E.; Wang, L.; Lan, L.; Luo, C.; Zhuang, W.; Peng, J.; Cao, Y. *Appl. Phys. Lett.* **2008**, *92*, 033307/1.
(186) Chmil, K.; Scherf, U. *Makromol. Chem., Rapid Commun.* **1993**, *14*, 217.
(187) Grimsdale, A. C., Müllen, K., Eds. *Polyphenylene-type Emissive Materials: Poly(para-phenylene)s, Polyfluorenes, and Ladder Polymers*; 2006.
(188) Hertel, D.; Setayesh, S.; Nothofer, H.-G.; Scherf, U.; Müllen, K.; Bassler, H. *Adv. Mater.* **2001**, *13*, 65.
(189) Wakim, S.; Leclerc, M. *Synlett* **2005**, 1223.
(190) Zenz, C.; Graupner, W.; Tasch, S.; Leising, G.; Müllen, K.; Scherf, U. *Appl. Phys. Lett.* **1997**, *71*, 2566.
(191) Lu, J.; Liang, F.; Drolet, N.; Ding, J.; Tao, Y.; Movileanu, R. *Chem. Commun.* **2008**, 5315.
(192) Tsai, J.-H.; Chueh, C.-C.; Lai, M.-H.; Wang, C.-F.; Chen, W.-C.; Ko, B.-T.; Ting, C. *Macromolecules* **2009**, *42*, 1897.
(193) Mishra, A.; Fischer, M. K. R.; Baüerle, P. *Angew. Chem., Int. Ed.* **2009**, *48*, 2474.
(194) Ooyama, Y.; Harima, Y. *Eur. J. Org. Chem.* **2009**, 2903.
(195) Ning, Z.; Tian, H. *Chem. Commun.* **2009**, 5483.
(196) Grätzel, M. *Acc. Chem. Res.* **2009**, *42*, 1788.
(197) Kim, C.; Choi, H.; Kim, S.; Baik, C.; Song, K.; Kang, M.-S.; Kang, S. O.; Ko, J. *J. Org. Chem.* **2008**, *73*, 7072.
(198) Thomas, K. R. J.; Lin, J. T.; Hsu, Y.-C.; Ho, K.-C. *Chem. Commun.* **2005**, 4098.
(199) Wang, Z.-S.; Koumura, N.; Cui, Y.; Takahashi, M.; Sekiguchi, H.; Mori, A.; Kubo, T.; Furube, A.; Hara, K. *Chem. Mater.* **2008**, *20*, 3993.
(200) Teng, C.; Yang, X.; Yuan, C.; Li, C.; Chen, R.; Tian, H.; Li, S.; Hagfeldt, A.; Sun, L. *Org. Lett.* **2009**, *11*, 5542.
(201) Koumura, N.; Wang, Z.-S.; Mori, S.; Miyashita, M.; Suzuki, E.; Hara, K. *J. Am. Chem. Soc.* **2006**, *128*, 14256.
(202) Koumura, N.; Wang, Z.-S.; Miyashita, M.; Uemura, Y.; Sekiguchi, H.; Cui, Y.; Mori, A.; Mori, S.; Hara, K. *J. Mater. Chem.* **2009**, *19*, 4829.
(203) Kim, D.; Lee, J. K.; Kang, S. O.; Ko, J. *Tetrahedron* **2007**, *63*, 1913.
(204) Zhang, X.-H.; Wang, Z.-S.; Cui, Y.; Koumura, N.; Furube, A.; Hara, K. *J. Phys. Chem. C* **2009**, *113*, 13409.
(205) Zhou, G.; Pschirer, N.; Schoeneboom, J. C.; Eickemeyer, F.; Baumgarten, M.; Müllen, K. *Chem. Mater.* **2008**, *20*, 1808.
(206) Iyer, V. S.; Wehmeier, M.; Brand, J. D.; Keegstra, M. A.; Müllen, K. *Angew. Chem., Int. Ed. Engl.* **1997**, *36*, 1604.
(207) Feng, X.; Liu, M.; Pisula, W.; Takase, M.; Li, J.; Müllen, K. *Adv. Mater.* **2008**, *20*, 2684.
(208) Li, J.; Kastler, M.; Pisula, W.; Robertson, J. W. F.; Wasserfallen, D.; Grimsdale, A. C.; Wu, J.; Müllen, K. *Adv. Funct. Mater.* **2007**, *17*, 2528.
(209) Yamamoto, Y.; Fukushima, T.; Suna, Y.; Ishii, N.; Saeki, A.; Seki, S.; Tagawa, S.; Taniguchi, M.; Kawai, T.; Aida, T. *Science* **2006**, *314*, 1761.
(210) Pisula, W.; Menon, A.; Stepputat, M.; Lieberwirth, I.; Kolb, U.; Tracz, A.; Sirringhaus, H.; Pakula, T.; Müllen, K. *Adv. Mater.* **2005**, *17*, 684.
(211) Pisula, W.; Kastler, M.; Wasserfallen, D.; Mondeshki, M.; Piris, J.; Schnell, I.; Müllen, K. *Chem. Mater.* **2006**, *18*, 3634.
(212) Kastler, M.; Pisula, W.; Laquai, F.; Kumar, A.; Davies, R. J.; Baluschev, S.; Garcia-Gutierrez, M.-C.; Wasserfallen, D.; Butt, H.-J.; Riekel, C.; Wegner, G.; Müllen, K. *Adv. Mater.* **2006**, *18*, 2255.
(213) Kastler, M.; Laquai, F.; Müllen, K.; Wegner, G. *Appl. Phys. Lett.* **2006**, *89*, 252103/1.
(214) Feng, X.; Marcon, V.; Pisula, W.; Hansen, M. R.; Kirkpatrick, J.; Grozema, F.; Andrienko, D.; Kremer, K.; Müllen, K. *Nat. Mater.* **2009**, *8*, 421.
(215) Adam, D.; Schuhmacher, P.; Simmerer, J.; Haeussling, L.; Siemensmeyer, K.; Etzbach, K. H.; Ringsdorf, H.; Haarer, D. *Nature* **1994**, *371*, 141.
(216) Elmahdy, M. M.; Dou, X.; Mondeshki, M.; Floudas, G.; Butt, H.-J.; Spiess, H. W.; Müllen, K. *J. Am. Chem. Soc.* **2008**, *130*, 5311.
(217) Feng, X.; Pisula, W.; Müllen, K. *J. Am. Chem. Soc.* **2007**, *129*, 14116.
(218) Feng, X.; Wu, J.; Ai, M.; Pisula, W.; Zhi, L.; Rabe, J. P.; Müllen, K. *Angew. Chem., Int. Ed.* **2007**, *46*, 3033.
(219) Feng, X.; Wu, J.; Enkelmann, V.; Müllen, K. *Org. Lett.* **2006**, *8*, 1145.
(220) Iyer, V. S.; Yoshimura, K.; Enkelmann, V.; Epsch, R.; Rabe, J. P.; Müllen, K. *Angew. Chem., Int. Ed.* **1998**, *37*, 2696.
(221) Wong, W. W. H.; Ma, C.-Q.; Pisula, W.; Yan, C.; Feng, X.; Jones, D. J.; Müllen, K.; Janssen, R. A. J.; Bauerle, P.; Holmes, A. B. *Chem. Mater.* **2010**, *22*, 457.
(222) Baumgarten, M.; Koch, K. H.; Müllen, K. *J. Am. Chem. Soc.* **1994**, *116*, 7341.
(223) Bohnen, A.; Koch, K. H.; Luettke, W.; Müllen, K. *Angew. Chem.* **1990**, *102*, 548.
(224) *Color Chemistry*; Zollinger, H., Ed.; VCH: Weinheim, 2003.
(225) Rademacher, A.; Maerkle, S.; Langhals, H. *Chem. Ber.* **1982**, *115*, 2927.
(226) Nagao, Y.; Misono, T. *Dyes Pigm.* **1984**, *5*, 171.
(227) Loutfy, R. O.; Hor, A. M.; Kazmaier, P.; Tam, M. *J. Imaging Sci.* **1989**, *33*, 151.
(228) Langhals, H. *Nachr. Chem., Tech. Lab.* **1980**, *28*, 716.
(229) O'Neil, M. P.; Niemczyk, M. P.; Svec, W. A.; Gosztola, D.; Gaines, G. L. I.; Wasielewski, M. R. *Science* **1992**, *257*, 63.
(230) Sadrai, M.; Hadel, L.; Sauers, R. R.; Husain, S.; Krogh-Jespersen, K.; Westbrook, J. D.; Bird, G. R. *J. Phys. Chem.* **1992**, *96*, 7988.
(231) Struijk, C. W.; Sieval, A. B.; Dakhorst, J. E. J.; van Dijk, M.; Kimkes, P.; Koehorst, R. B. M.; Donker, H.; Schaafsma, T. J.; Picken, S. J.; van de Craats, A. M.; Warman, J. M.; Zuilhof, H.; Sudholter, E. J. R. *J. Am. Chem. Soc.* **2000**, *122*, 11057.
(232) Breeze, A. J.; Salomon, A.; Ginley, D. S.; Gregg, B. A.; Tillmann, H.; Horhold, H.-H. *Appl. Phys. Lett.* **2002**, *81*, 3085.
(233) Herrmann, A.; Müllen, K. *Chem. Lett.* **2006**, *35*, 978.
(234) Holtrup, F. O.; Mueller, G. R. J.; Quante, H.; De Feyter, S.; De Schryver, F. C.; Müllen, K. *Chem.—Eur. J.* **1997**, *3*, 219.
(235) Nagao, Y.; Iwawaki, H.; Kozawa, K. *Heterocycles* **2002**, *56*, 331.
(236) Adachi, M.; Nagao, Y. *Chem. Mater.* **2001**, *13*, 662.
(237) Langhals, H.; Schoenmann, G.; Feiler, L. *Tetrahedron Lett.* **1995**, *36*, 6423.

(238) Quante, H.; Müllen, K. *Angew. Chem., Int. Ed. Engl.* **1995**, *34*, 1323.
(239) Pschirer, N. G.; Kohl, C.; Nolde, F.; Qu, J.; Müllen, K. *Angew. Chem., Int. Ed.* **2006**, *45*, 1401.
(240) Qu, J.; Pschirer, N. G.; Koenemann, M.; Müllen, K.; Avlasevic, Y. WO2008052927, 2008.
(241) Avlasevich, Y.; Mueller, S.; Erk, P.; Müllen, K. *Chem.—Eur. J.* **2007**, *13*, 6555.
(242) Kohl, C.; Becker, S.; Müllen, K. *Chem. Commun.* **2002**, 2778.
(243) Liu, Z.; Li, C.; Wagner, M.; Avlasevich, Y.; Herrmann, A.; Müllen, K. *Chem. Commun.* **2008**, 5028.
(244) Al-Mohamad, A.; Soukieh, M. *Thin Solid Films* **1995**, *271*, 132.
(245) Derouiche, H.; Bernede, J. C.; L'Hyver, J. *Dyes Pigm.* **2004**, *63*, 277.
(246) Dittmer, J. J.; Petritsch, K.; Marseglia, E. A.; Friend, R. H.; Rost, H.; Holmes, A. B. *Synth. Met.* **1999**, *102*, 879.
(247) Gregg, B. A. *Chem. Phys. Lett.* **1996**, *258*, 376.
(248) Haensel, H.; Zettl, H.; Krausch, G.; Kisselev, R.; Thelakkat, M.; Schmidt, H.-w. *Adv. Mater.* **2003**, *15*, 2056.
(249) Halls, J. J. M.; Friend, R. H. *Synth. Met.* **1997**, *85*, 1307.
(250) Hiramoto, M.; Fujiwara, H.; Yokoyama, M. *Appl. Phys. Lett.* **1991**, *58*, 1062.
(251) Kim, I.; Haverinen, H. M.; Wang, Z.; Madakuni, S.; Li, J.; Jabbour, G. E. *Appl. Phys. Lett.* **2009**, *95*, 023305/1.
(252) Rim, S.-B.; Fink, R. F.; Schoneboom, J. C.; Erk, P.; Peumans, P. *Appl. Phys. Lett.* **2007**, *91*, 173504/1.
(253) Sylvester-Hvid, K. O. *J. Phys. Chem. B* **2006**, *110*, 2618.
(254) Mikroyannidis, J. A.; Stylianakis, M. M.; Suresh, P.; Sharma, G. D. *Sol. Energy Mater. Sol. Cells* **2009**, *93*, 1792.
(255) Sharma, G. D.; Balraju, P.; Mikroyannidis, J. A.; Stylianakis, M. M. *Sol. Energy Mater. Sol. Cells* **2009**, *93*, 2025.
(256) Sharma, G. D.; Suresh, P.; Mikroyannidis, J. A.; Stylianakis, M. M. *J. Mater. Chem.* **2010**, *20*, 561.
(257) Neuteboom, E. E.; Meskers, S. C. J.; Van Hal, P. A.; Van Duren, J. K. J.; Meijer, E. W.; Janssen, R. A. J.; Dupin, H.; Pourtois, G.; Cornil, J.; Lazzaroni, R.; Bredas, J.-L.; Beljonne, D. *J. Am. Chem. Soc.* **2003**, *125*, 8625.
(258) Li, C.; Pan, X.; Hua, C.; Su, J.; Tian, H. *Eur. Polym. J.* **2003**, *39*, 1091.
(259) Cremer, J.; Baeuerle, P. *Eur. J. Org. Chem.* **2005**, 3715.
(260) Cremer, J.; Baeuerle, P. *J. Mater. Chem.* **2006**, *16*, 874.
(261) Cremer, J.; Mena-Osteritz, E.; Pschierer, N. G.; Müllen, K.; Baeuerle, P. *Org. Biomol. Chem.* **2005**, *3*, 985.
(262) Liu, Y.; Yang, C.; Li, Y.; Li, Y.; Wang, S.; Zhuang, J.; Liu, H.; Wang, N.; He, X.; Li, Y.; Zhu, D. *Macromolecules* **2005**, *38*, 716.
(263) Zhan, X.; Tan, Z. a.; Domercq, B.; An, Z.; Zhang, X.; Barlow, S.; Li, Y.; Zhu, D.; Kippelen, B.; Marder, S. R. *J. Am. Chem. Soc.* **2007**, *129*, 7246.
(264) Tan, Z. a.; Zhou, E.; Zhan, X.; Wang, X.; Li, Y.; Barlow, S.; Marder, S. R. *Appl. Phys. Lett.* **2008**, *93*, 073309/1.
(265) Zhan, X.; Tan, Z. a.; Zhou, E.; Li, Y.; Misra, R.; Grant, A.; Domercq, B.; Zhang, X.-H.; An, Z.; Zhang, X.; Barlow, S.; Kippelen, B.; Marder, S. R. *J. Mater. Chem.* **2009**, *19*, 5794.
(266) Wuerthner, F. *Pure Appl. Chem.* **2006**, *78*, 2341.
(267) Chen, Z.; Baumeister, U.; Tschierske, C.; Wuerthner, F. *Chem.—Eur. J.* **2007**, *13*, 450.
(268) Huo, L.; Zhou, Y.; Li, Y. *Macromol. Rapid Commun.* **2008**, *29*, 1444.
(269) Hua, J.; Meng, F.; Li, J.; Ding, F.; Fan, X.; Tian, H. *Eur. Polym. J.* **2006**, *42*, 2686.
(270) Sommer, M.; Lindner, S. M.; Thelakkat, M. *Adv. Funct. Mater.* **2007**, *17*, 1493.
(271) Sommer, M.; Thelakkat, M. *Eur. Phys. J.: Appl. Phys.* **2006**, *36*, 245.
(272) Lindner, S. M.; Huettner, S.; Chiche, A.; Thelakkat, M.; Krausch, G. *Angew. Chem., Int. Ed.* **2006**, *45*, 3364.
(273) Burfeindt, B.; Hannappel, T.; Storck, W.; Willig, F. *J. Phys. Chem.* **1996**, *100*, 16463.
(274) Ferrere, S.; Zaban, A.; Gregg, B. A. *J. Phys. Chem. B* **1997**, *101*, 4490.
(275) Wang, S.; Li, Y.; Du, C.; Shi, Z.; Xiao, S.; Zhu, D.; Gao, E.; Cai, S. *Synth. Met.* **2002**, *128*, 299.
(276) Zafer, C.; Kus, M.; Turkmen, G.; Dincalp, H.; Demic, S.; Kuban, B.; Teoman, Y.; Icli, S. *Sol. Energy Mater. Sol. Cells* **2007**, *91*, 427.
(277) Shibano, Y.; Umeyama, T.; Matano, Y.; Imahori, H. *Org. Lett.* **2007**, *9*, 1971.
(278) Fortage, J.; Severac, M.; Houarner-Rassin, C.; Pellegrin, Y.; Blart, E.; Odobel, F. *J. Photochem. Photobiol., A* **2008**, *197*, 156.
(279) Planells, M.; Cespedes-Guirao, F. J.; Goncalves, L.; Sastre-Santos, A.; Fernandez-Lazaro, F.; Palomares, E. *J. Mater. Chem.* **2009**, *19*, 5818.
(280) Ferrere, S.; Gregg, B. A. *Proc. Electrochem. Soc.* **2001**, *2001−10*, 161.
(281) Ferrere, S.; Gregg, B. A. *New J. Chem.* **2002**, *26*, 1155.
(282) Ferrere, S.; Gregg, B. A. *J. Phys. Chem. B* **2001**, *105*, 7602.
(283) Osasa, T.; Matsui, Y.; Matsumura, T.; Matsumura, M. *Sol. Energy Mater. Sol. Cells* **2006**, *90*, 3136.
(284) Li, C.; Schoeneboom, J.; Liu, Z.; Pschirer, N. G.; Erk, P.; Herrmann, A.; Müllen, K. *Chem.—Eur. J.* **2009**, *15*, 878.
(285) Edvinsson, T.; Li, C.; Pschirer, N.; Schoeneboom, J.; Eickemeyer, F.; Sens, R.; Boschloo, G.; Herrmann, A.; Müllen, K.; Hagfeldt, A. *J. Phys. Chem. C* **2007**, *111*, 15137.
(286) Li, C.; Yum, J.-H.; Moon, S.-J.; Herrmann, A.; Eickemeyer, F.; Pschirer, N. G.; Erk, P.; Schoeneboom, J.; Müllen, K.; Grätzel, M.; Nazeeruddin, M. K. *ChemSusChem* **2008**, *1*, 615.
(287) Li, C.; Liu, Z.; Schoeneboom, J.; Eickemeyer, F.; Pschirer, N. G.; Erk, P.; Herrmann, A.; Müllen, K. *J. Mater. Chem.* **2009**, *19*, 5405.
(288) Cappel, U. B.; Karlsson, M. H.; Pschirer, N. G.; Eickemeyer, F.; Schoneboom, J.; Erk, P.; Boschloo, G.; Hagfeldt, A. *J. Phys. Chem. C* **2009**, *113*, 14595.
(289) Morandeira, A.; Fortage, J.; Edvinsson, T.; Le Pleux, L.; Blart, E.; Boschloo, G.; Hagfeldt, A.; Hammarstroem, L.; Odobel, F. *J. Phys. Chem. C* **2008**, *112*, 1721.
(290) Nattestad, A.; Mozer, A. J.; Fischer, M. K. R.; Cheng, Y. B.; Mishra, A.; Baeuerle, P.; Bach, U. Nat. Mater. **2010**, *9*, 31.
(291) Liu, B.; Zhu, W.; Wu, W.; Ri, K. M.; Tian, H. *J. Photochem. Photobiol., A* **2008**, *194*, 268.
(292) Jin, Y.; Hua, J.; Wu, W.; Ma, X.; Meng, F. *Synth. Met.* **2008**, *158*, 64.
(293) Edvinsson, T.; Pschirer, N.; Schoeneboom, J.; Eickemeyer, F.; Boschloo, G.; Hagfeldt, A. *Chem. Phys.* **2009**, *357*, 124.
(294) Weil, T.; Reuther, E.; Beer, C.; Müllen, K. *Chem.—Eur. J.* **2004**, *10*, 1398.
(295) Figueira-Duarte, T. M.; Simon, S. C.; Wagner, M.; Druzhinin, S. I.; Zachariasse, K. A.; Müllen, K. *Angew. Chem., Int. Ed.* **2008**, *47*, 10175.
(296) Hardin, B. E.; Hoke, E. T.; Armstrong, P. B.; Yum, J.-H.; Comte, P.; Torres, T.; Frechet, J. M. J.; Nazeeruddin, M. K.; Grätzel, M.; McGehee, M. D. *Nat. Photonics* **2009**, *3*, 406.
(297) Wang, X.; Zhi, L.; Tsao, N.; Tomovic, Z.; Li, J.; Müllen, K. *Angew. Chem., Int. Ed.* **2008**, *47*, 2990.
(298) Wang, X.; Zhi, L.; Müllen, K. *Nano Lett.* **2008**, *8*, 323.
(299) Zhi, L.; Müllen, K. *J. Mater. Chem.* **2008**, *18*, 1472.

CR100052Z